

**PHYSICAL PROPERTIES OF POLY (LACTIC ACID)/  
POLY (BUTYLENE ADIPATE-CO-TEREPHTHALATE)  
BLENDS AND THEIR COMPOSITES**

**Arpaporn Teamsinsungvon**

**A Thesis Submitted in Partial Fulfillment of the Requirements for the  
Degree of Master of Engineering in Polymer Engineering**

**Suranaree University of Technology**

**Academic Year 2011**

สมบัติทางกายภาพของพอลิเมอร์ผสมระหว่างพอลิแลคติก แอซิดกับพอลิบีวที  
ดินอะดิเพรตเทอแรพธาเรตและพอลิเมอร์คอมโพสิตของพอลิเมอร์ผสม

นางสาวอาภาภรณ์ เทียมสินสังวร

วิทยานิพนธ์นี้เป็นส่วนหนึ่งของการศึกษาตามหลักสูตรปริญญาวิศวกรรมศาสตรมหาบัณฑิต  
สาขาวิชาวิศวกรรมพอลิเมอร์  
มหาวิทยาลัยเทคโนโลยีสุรนารี  
ปีการศึกษา 2554

**PHYSICAL PROPERTIES OF POLY (LACTIC ACID)/ POLY  
(BUTYLENE ADIPATE-CO-TEREPHTHALATE)  
BLENDS AND THEIR COMPOSITES**

Suranaree University of Technology has approved this thesis submitted in partial fulfillments of the requirements for a Master's Degree.

Thesis Examining Committee

Nitinat Suppakarn  
(Asst. Prof. Dr. Nitinat Suppakarn)

Chairperson

Kasama Jarukumjorn  
(Asst. Prof. Dr. Kasama Jarukumjorn)

Member (Thesis Advisor)

Yupaporn Ruksakulpiwat  
(Asst. Prof. Dr. Yupaporn Ruksakulpiwat)

Member

Pranee Chumsamrong  
(Asst. Prof. Dr. Pranee Chumsamrong)

Member

Visit Vao-soongnern  
(Asst. Prof. Dr. Visit Vao-soongnern)

Member

Kontorn Chamniprasart  
(Assoc. Prof. Flt. Lt. Dr. Kontorn Chamniprasart)

Sukit Limpijumnong  
(Prof. Dr. Sukit Limpijumnong)

Vice Rector for Academic Affairs

Dean of Institute of Engineering

อาการณ์ เทียมลินสังวร : สมบัติทางกายภาพของพอลิเมอร์ผสมระหว่างพอลิแลคติก  
แอซิดกับพอลิบิวทีลีนอะดิเพรตเทอเรพธาเรตและพอลิเมอร์คอมโพสิทของพอลิเมอร์ผสม  
(PHYSICAL PROPERTIES OF POLY (LACTIC ACID)/POLY (BUTYLENE  
ADIPATE-CO-TEREPHTHALATE) BLENDS AND THEIR COMPOSITES)  
อาจารย์ที่ปรึกษา : ผู้ช่วยศาสตราจารย์ ดร.กษมา จารุกัจจร, 136 หน้า.

ในการศึกษานี้พอลิเมอร์ผสมระหว่างพอลิแลคติกแอซิดกับพอลิบิวทีลีนอะดิเพรตเทอเรพธาเรตที่อัตราส่วน 100/0 90/10 80/20 และ 70/30 เปอร์เซ็นต์โดยน้ำหนักถูกเตรียมโดยเครื่องอัดรีดชนิดแกนคู่หมุนในทิศทางเดียวกัน สมบัติทางกล สมบัติทางสัณฐานวิทยา สมบัติทางความร้อนและสมบัติทางกระแสวิทยาของพอลิเมอร์ผสมระหว่างพอลิแลคติกแอซิดกับพอลิบิวทีลีนอะดิเพรตเทอเรพธาเรตถูกตรวจสอบ พอลิเมอร์ผสมระหว่างพอลิแลคติกแอซิดกับพอลิบิวทีลีนอะดิเพรตเทอเรพธาเรตแสดงค่าการยืดตัวสูงสุด ณ จุดขาดและค่าความต้านทานต่อแรงกระแทกสูงกว่าพอลิแลคติกแอซิดแต่ค่าการทนต่อแรงดึงและค่ามอดูลัสของยังก็ต่ำกว่า ผลของการทดสอบทางสัณฐานวิทยาแสดงว่าพอลิแลคติกแอซิดไม่เข้ากันกับพอลิบิวทีลีนอะดิเพรตเทอเรพธาเรต นอกจากนี้ผลการศึกษาทางกระแสวิทยาพบว่าความหนืดของพอลิเมอร์ผสมเพิ่มขึ้นเมื่อเพิ่มปริมาณของพอลิบิวทีลีนอะดิเพรตเทอเรพธาเรต

พอลิแลคติกแอซิดกราฟท์มาลิกแอนไฮไดรด์ถูกใช้เป็นสารช่วยให้เข้ากันเพื่อปรับปรุงความเข้ากันได้ของพอลิเมอร์ผสมระหว่างพอลิแลคติกแอซิดกับพอลิบิวทีลีนอะดิเพรตเทอเรพธาเรต พอลิแลคติกแอซิดกราฟท์มาลิกแอนไฮไดรด์ถูกเตรียมโดยเครื่องบดผสมภายใน อินฟราเรด-สเปกโตรสโคปีถูกนำมาใช้ยืนยันการกราฟท์ของมาลิกแอนไฮไดรด์บนพอลิแลคติกแอซิดและการไทเทรตถูกนำมาใช้เพื่อวิเคราะห์ปริมาณการกราฟท์ของมาลิกแอนไฮไดรด์บนโมเลกุลของพอลิแลคติกแอซิด ปริมาณการกราฟท์ของพอลิแลคติกแอซิดกราฟท์มาลิกแอนไฮไดรด์ที่สูงที่สุดถูกเตรียมโดยใช้มาลิกแอนไฮไดรด์ 5 เปอร์เซ็นต์โดยน้ำหนักและ 2, 5-บิวทิลเพอร์ออกไซด์-2, 5 ไดเมทิลเฮกเซน 1 เปอร์เซ็นต์โดยน้ำหนัก ปริมาณพอลิแลคติกแอซิดกราฟท์มาลิกแอนไฮไดรด์คือ 2 4 6 8 และ 10 ส่วนในร้อยส่วนของพอลิเมอร์ผสม พอลิแลคติกแอซิดกราฟท์มาลิกแอนไฮไดรด์เพิ่มการยึดติดที่พื้นผิวระหว่างพอลิแลคติกแอซิดกับพอลิบิวทีลีนอะดิเพรตเทอเรพธาเรตซึ่งนำไปสู่การปรับปรุงสมบัติทางกล ความเสถียรทางความร้อนของพอลิเมอร์ผสมถูกปรับปรุงเมื่อเติมพอลิแลคติกแอซิดกราฟท์มาลิกแอนไฮไดรด์ พอลิเมอร์ผสมระหว่างพอลิแลคติกแอซิดกับพอลิบิวทีลีนอะดิเพรตเทอเรพธาเรตที่ถูกปรับปรุงความเข้ากันได้ด้วยพอลิแลคติกแอซิดกราฟท์มาลิกแอนไฮไดรด์ที่ปริมาณ 2 และ 4 ส่วนในร้อยส่วนของพอลิเมอร์ผสมแสดงค่าความหนืดสูงกว่าพอลิ

เมอร์ผสมระหว่างพอลิแลคติกแอซิดกับพอลิบิวทีลีนอะดิเพรตเทอเรพทาเรตที่ไม่ถูกปรับปรุงความเข้ากันได้

พอลิเมอร์คอมโพลิทระหว่างพอลิแลคติกแอซิด พอลิบิวทีลีนอะดิเพรตเทอเรพทาเรตและแคลเซียมคาร์บอเนตแสดงสมบัติทางกลที่ต่ำกว่าเมื่อเปรียบเทียบกับพอลิเมอร์ผสมระหว่างพอลิแลคติกแอซิดกับพอลิบิวทีลีนอะดิเพรตเทอเรพทาเรตที่มีการปรับปรุงความเข้ากันได้ เมื่อเพิ่มปริมาณแคลเซียมคาร์บอเนตค่าการทนต่อแรงดึงและค่าการยืดตัวสูงสุด ณ จุดขาดของพอลิเมอร์คอมโพลิทลดลงเนื่องจากการรวมตัวกันของแคลเซียมคาร์บอเนต โดยเฉพาะที่มีปริมาณแคลเซียมคาร์บอเนตที่สูง ความเสถียรทางความร้อนและความหนืดของพอลิเมอร์ผสมระหว่างพอลิแลคติกแอซิดกับพอลิบิวทีลีนอะดิเพรตเทอเรพทาเรตที่ถูกปรับปรุงความเข้ากันได้ลดลงเมื่อเติมแคลเซียมคาร์บอเนต

ฟิล์มชนิดเป่าของพอลิเมอร์ผสมระหว่างพอลิแลคติกแอซิดกับพอลิบิวทีลีนอะดิเพรตเทอเรพทาเรต พอลิเมอร์ผสมระหว่างพอลิแลคติกแอซิดกับพอลิบิวทีลีนอะดิเพรตเทอเรพทาเรตที่ถูกปรับปรุงความเข้ากันได้และพอลิเมอร์คอมโพลิทระหว่างพอลิแลคติกแอซิด พอลิบิวทีลีนอะดิเพรตเทอเรพทาเรตและแคลเซียมคาร์บอเนตสามารถถูกเตรียมโดยเครื่องเป่าฟิล์มในเชิงพาณิชย์ ฟิล์มของพอลิเมอร์ผสมระหว่างพอลิแลคติกแอซิดกับพอลิบิวทีลีนอะดิเพรตเทอเรพทาเรตที่ไม่ถูกและถูกปรับปรุงความเข้ากันได้แสดงความโปร่งใสมากกว่าฟิล์มของพอลิเมอร์คอมโพลิทของพอลิแลคติกแอซิด พอลิบิวทีลีนอะดิเพรตเทอเรพทาเรตและแคลเซียมคาร์บอเนต การเติมพอลิแลคติกแอซิดกราฟท์มาลิกแอนไฮไดรด์ปรับปรุงค่าการทนต่อแรงดึง ค่ามอดูลัสของยังก์และค่าการยืดตัวสูงสุด ณ จุดขาดของฟิล์มที่เตรียมได้จากพอลิเมอร์ผสมระหว่างพอลิแลคติกแอซิดกับพอลิบิวทีลีนอะดิเพรตเทอเรพทาเรต การเติมแคลเซียมคาร์บอเนตส่งผลต่อการปรับปรุงค่าการทนต่อแรงดึงและค่ามอดูลัสของยังก์ของฟิล์ม

สาขาวิชา วิศวกรรมพอลิเมอร์

ปีการศึกษา 2554

ลายมือชื่อนักศึกษา ชานภรณ์ เกียรติอินทร์

ลายมือชื่ออาจารย์ที่ปรึกษา กนกมา ชูวงศ์

ลายมือชื่ออาจารย์ที่ปรึกษาร่วม [ลายมือ]

ARPAPORN TEAMSINSUNGVON : PHYSICAL PROPERTIES OF POLY (LACTIC ACID)/ POLY (BUTYLENE ADIPATE-*CO*-TEREPHTHALATE) BLENDS AND THEIR COMPOSITES. THESIS ADVISOR : ASST. PROF. KASAMA JARUKUMJORN, Ph.D., 136 PP.

POLY (LACTIC ACID)/POLY (BUTYLENE ADIPATE-*CO*-TEREPHTHALATE)/  
PLA GRAFTED WITH MALEIC ANHYDRIDE/CALCIUM CARBONATE

In this study, blends of PLA/PBAT with various ratios of 100/0, 90/10, 80/20 and 70/30 wt% were prepared using a co-rotating intermeshing twin screw extruder. Mechanical, morphological, thermal, and rheological properties of PLA/PBAT blends were investigated. PLA/PBAT blend exhibited higher elongation at break and impact strength than PLA but lower tensile strength and Young's modulus. SEM results showed that PLA was immiscible with PBAT. Furthermore, rheological results revealed that viscosity of the blends increased with increasing PBAT content.

PLA grafted with maleic anhydride (PLA-*g*-MA) was used as a compatibilizer to improve the compatibility of the PLA/PBAT blends. PLA-*g*-MA was prepared using an internal mixer. Fourier transform infrared spectroscopy (FTIR) was used to confirm the MA grafted onto PLA and a titration method was used to determine the content of MA grafted onto the PLA molecule. The highest graft content (%G) of PLA-*g*-MA was obtained with MA content of 5.0 wt% and 2,5-bis(*tert*-butylperoxy)-2,5 dimethylhexane content of 1.0 wt%. PLA-*g*-MA contents were 2, 4, 6, 8, and 10 phr. PLA-*g*-MA enhanced the interfacial adhesion between PLA and PBAT leading to the improvement of the mechanical properties. Thermal

stability of the blend was enhanced with addition of PLA-g-MA. Compatibilized PLA/PBAT blends with 2 and 4 phr of PLA-g-MA exhibited higher viscosity than uncompatibilized PLA/PBAT blend.

PLA/PBAT/CaCO<sub>3</sub> composites exhibited lower mechanical properties when compared to compatibilized PLA/PBAT blend. With increasing CaCO<sub>3</sub> content, tensile strength and elongation at break of the composites decreased due to the agglomeration of CaCO<sub>3</sub>, especially at high CaCO<sub>3</sub> content. Thermal stability and viscosity of the compatibilized PLA/PBAT blend decreased with the presence of CaCO<sub>3</sub>.

Blown films of PLA/PBAT blend, compatibilized PLA/PBAT blend, and PLA/PBAT/CaCO<sub>3</sub> composites can be prepared using a commercial blown film extruder. The films of uncompatibilized and compatibilized PLA/PBAT blend showed higher transparency than the film of PLA/PBAT/CaCO<sub>3</sub> composite. The addition of PLA-g-MA improved tensile strength, Young's modulus, and elongation at break of the film prepared from PLA/PBAT blend. Incorporating CaCO<sub>3</sub> resulted in the improvement of the tensile strength and Young's modulus of the films.

School of Polymer Engineering

Academic Year 2011

Student's Signature Arpaporn Teamsinsungvon.

Advisor's Signature Wasama Jarukumjorn

Co-advisor's Signature Arpaporn Chit

## **ACKNOWLEDGEMENTS**

I gratefully acknowledge the financial supports from Suranaree University of Technology, Center of Excellence on Petrochemical and Materials Technology, and National Innovation Agency (NIA)

First and foremost, I am deeply grateful to my thesis advisor, Asst. Prof. Dr. Kasama Jarukumjorn, for her valuable supervision, inspiring guidance, support, and kindness throughout the period of the study. Sincere appreciation is also extended to the thesis co-advisor, Asst. Prof. Dr. Yupaporn Ruksakulpiwat, for her valuable suggestions. In addition, I wish to express my gratitude to Asst. Prof. Dr. Nitinat Suppakarn, Asst. Prof. Dr. Pranee Chumsamrong, and Asst. Prof. Dr. Visit Vao-soongnern for their valuable suggestions and guidance given as committee members.

My appreciation also goes to Dr. Wanwisa Pattanasiriwisawa for her excellent descriptions in the details of FTIR testing. Special thanks are extended to Synchrotron Light Research Institute (SLRI) for the facilities in the use of FTIR spectrometer and Bags and Gloves Company Limited for supporting blown film preparation. Furthermore, I am deeply indebted to lecturers, staff members, and all friends of School of Polymer Engineering for their helps, supports, and encouragement.

Finally, my graduation would not be achieved without best wish from my parents, Mr. Boontom and Mrs. Banyen Teamsinsungvon, and my sisters, Miss Kullakarn and Miss Aemorn Teamsinsungvon, who give me a valuable life with their endless love, support, and encouragement throughout my life.

Arpaporn Teamsinsungvon

# TABLE OF CONTENTS

	<b>Page</b>
ABSTRACT (THAI) .....	I
ABSTRACT (ENGLISH).....	III
ACKNOWLEDGEMENTS .....	V
TABLE OF CONTENTS.....	VI
LIST OF TABLES.....	X
LIST OF FIGURES .....	XII
SYMBOLS AND ABBREVIATIONS.....	XVIII
<b>CHAPTER</b>	
<b>I INTRODUCTION .....</b>	<b>1</b>
1.1 Background.....	1
1.2 Research objectives.....	3
1.3 Scope and limitation of the study.....	4
<b>II LITERATURE REVIEW .....</b>	<b>6</b>
2.1 Poly (lactic acid) .....	6
2.2 The toughness improvement of PLA .....	6
2.2.1 PLA plasticization .....	7
2.2.2 Copolymerization of PLA .....	10
2.2.3 Blending of PLA with flexible polymers .....	11
2.3 The study of compatibilization of PLA blends.....	16

## TABLE OF CONTENTS (Continued)

	<b>Page</b>
2.4 The effect of filler on properties of PLA blends.....	20
<b>III EXPERIMENTAL</b> .....	<b>26</b>
3.1 Materials .....	26
3.2 Experimental.....	26
3.2.1 Synthesis of poly (lactic acid) grafted with maleic anhydride .....	26
3.2.2 Characterization of poly (lactic acid) grafted with maleic anhydride.....	26
3.2.2.1 Determination of maleic anhydride content ..	26
3.2.2.2 Fourier transform infrared spectroscopy .....	27
3.2.2.3 Gel permeation chromatography .....	27
3.2.3 Preparation of PLA/PBAT blends .....	28
3.2.4 Preparation of PLA/PBAT/CaCO <sub>3</sub> composites .....	29
3.2.5 Preparation of blown films from PLA/PBAT blends and PLA/PBAT/CaCO <sub>3</sub> composite .....	29
3.2.6 Characterization of PLA, PBAT, PLA/PBAT blends, and PLA/PBAT/CaCO <sub>3</sub> composites .....	30
3.2.6.1 Mechanical properties .....	30
3.2.6.2 Morphological properties .....	30
3.2.6.3 Thermal properties.....	30

## TABLE OF CONTENTS (Continued)

	<b>Page</b>
3.2.6.4 Rheological properties.....	31
3.2.7 Properties of blown films prepared from PLA/PBAT blends and PLA/PBAT/CaCO <sub>3</sub> composite.....	32
<b>IV RESULTS AND DISSCUSSION.....</b>	<b>33</b>
4.1 The effects of initiator and monomer content on graft content of PLA-g-MA .....	33
4.1.1 Identification of PLA-g-MA .....	33
4.1.2 Determination of graft content.....	36
4.1.2.1 Effect of monomer content.....	36
4.1.2.2 Effect of initiator content.....	39
4.2 The effect of blend composition on properties of PLA/PBAT blends .....	42
4.2.1 Mechanical properties.....	42
4.2.2 Morphological properties.....	48
4.2.3 Thermal properties .....	49
4.2.4 Rheological properties .....	53
4.3 The effect of compatibilizer content on properties of PLA/PBAT blends .....	55
4.3.1 Mechanical properties.....	56
4.3.2 Morphological properties.....	61

## TABLE OF CONTENTS (Continued)

	<b>Page</b>
4.3.3 Thermal properties .....	64
4.3.4 Rheological properties .....	70
4.4 The effect of CaCO <sub>3</sub> content on properties of compatibilized PLA/PBAT blends.....	72
4.4.1 Mechanical properties .....	72
4.4.2 Morphological properties.....	77
4.4.3 Thermal properties .....	79
4.4.4 Rheological properties .....	85
4.5 The properties of blown films prepared from PLA/PBAT blends and PLA/PBAT/CaCO <sub>3</sub> composite.....	87
<b>V CONCLUSIONS</b> .....	92
REFERENCES .....	95
APPENDICES	
APPENDIX A. COST CALCULATION FOR PLA/PBAT BLENDS AND PLA/PBAT/CaCO <sub>3</sub> COMPOSITES .....	105
APPENDIX B. PUBLICATIONS .....	110
BIOGRAPHY .....	136

## LIST OF TABLES

Table	Page
4.1	Graft content, the number average molecular weight ( $\overline{M}_n$ ), the weight average molecular weight ( $\overline{M}_w$ ), and the molecular weight distribution (MWD) of PLA-g-MA at various MA contents and a constant Luperox101 content of 0.5 wt% in chloroform : methanol (80:20 %v/v) solvent.....38
4.2	Graft content, the number average molecular weight ( $\overline{M}_n$ ), the weight average molecular weight ( $\overline{M}_w$ ), and the molecular weight distribution (MWD) of PLA-g-MA at various Luperox101 contents and a constant MA content of 5.0 wt% in chloroform : methanol (80:20 %v/v) solvent.....40
4.3	Mechanical properties of PLA and PLA/PBAT blends at various PBAT contents.....47
4.4	Thermal characteristics of PLA and PLA/PBAT blends at various PBAT contents (the second heating, heating rate 5°C/min). .....52
4.5	Mechanical properties of PLA/PBAT blend and compatibilized PLA/PBAT blends at various PLA-g-MA contents .....60
4.6	Thermal characteristics of PLA/PBAT blend and compatibilized PLA/PBAT blends at various PLA-g-MA contents .....66

## LIST OF TABLES (Continued)

<b>Table</b>		<b>Page</b>
4.7	Thermal degradation temperature and % char of PLA, PBAT, and PLA/PBAT blends .....	69
4.8	Mechanical properties of compatibilized PLA/PBAT blend and PLA/PBAT/CaCO <sub>3</sub> composites at various CaCO <sub>3</sub> contents.....	76
4.9	Thermal characteristics of compatibilized PLA/PBAT blend and PLA/PBAT/CaCO <sub>3</sub> composites at various CaCO <sub>3</sub> contents.....	81
4.10	Thermal degradation temperature and % char of PLA, PBAT, PLA/PBAT blends, and PLA/PBAT/CaCO <sub>3</sub> composites.....	85
4.11	Tensile properties of blown films prepared from PLA/PBAT blend, compatibilized PLA/PBAT blend, and PLA/PBAT/CaCO <sub>3</sub> composite .....	91

## LIST OF FIGURES

Figure	Page
2.1	Chemical structure of poly (lactic acid).....6
4.1	FTIR second derivative spectra of MA, PLA, and PLA-g-MA at a constant Luperox 101 content of 0.5 wt% and various contents of MA (a) PLA, (b) PLA-g-MA (1.0 wt%), (c) PLA-g-MA (2.5 wt%), (d) PLA-g-MA (5.0 wt%), and (e) PLA-g-MA (7.5 wt%) .....34
4.2	FTIR second derivative spectra of MA, PLA, and PLA-g-MA at a constant MA content of 5.0 wt% and various contents of Luperox 101 (a) PLA, (b) PLA-g-MA (0.1 wt%), (c) PLA-g-MA (0.25 wt%), (d) PLA-g-MA (0.5 wt%), (e) PLA-g-MA (1.0 wt%), and (f) PLA-g-MA (none). .....35
4.3	Proposed grafting reaction pathway for the reaction of MA on PLA.....36
4.4	Graft content and the number average molecular weight of PLA-g-MA at various MA contents and a constant Luperox101content of 0.5 wt% .....39
4.5	Graft content and the number average molecular weight of PLA-g-MA at various Luperox101contents and a constant MA content of 5.0 wt% .....41
4.6	Stress-strain curves of PLA and PLA/PBAT blends at various PBAT contents .....43

## LIST OF FIGURES (Continued)

Figure	Page
4.7	Optical photographs of tensile-fractured samples of (a) PLA, (b) PLA/PBAT 90/10 blend, (c) PLA/PBAT 80/20 blend, and (d) PLA/PBAT 70/30 blend. ....44
4.8	Tensile strength of PLA and PLA/PBAT blends at various PBAT contents .....44
4.9	Young's modulus of PLA and PLA/PBAT blends at various PBAT contents .....45
4.10	Elongation at break of PLA and PLA/PBAT blends at various PBAT contents .....45
4.11	Impact strength of PLA and PLA/PBAT blends at various PBAT contents .....46
4.12	SEM micrographs at 2000x magnification of (a) PLA, (b) PLA/PBAT 90/10 blend, (c) PLA/PBAT 80/20 blend, and (d) PLA/PBAT 70/30 blend .....49
4.13	DSC thermograms of PLA, PBAT, and PLA/PBAT blends at various PBAT contents (the second heating, heating rate 5°C/min) .....51
4.14	Shear viscosity of PLA, PBAT, and PLA/PBAT blends at various PBAT contents .....54
4.15	MFI of PLA, PBAT, and PLA/PBAT blends at various PBAT contents .....55

## LIST OF FIGURES (Continued)

Figure	Page
4.16	Tensile strength of PLA/PBAT blend and PLA/PBAT/PLA- <i>g</i> -MA blends at various PLA- <i>g</i> -MA contents .....57
4.17	Young's modulus of PLA/PBAT blend and PLA/PBAT/PLA- <i>g</i> -MA blends at various PLA- <i>g</i> -MA contents .....57
4.18	Elongation at break of PLA/PBAT blend and PLA/PBAT/PLA- <i>g</i> -MA blends at various PLA- <i>g</i> -MA contents .....58
4.19	Impact strength of PLA/PBAT blend and PLA/PBAT/PLA- <i>g</i> -MA blends at various PLA- <i>g</i> -MA contents .....59
4.20	SEM micrographs at 2000x magnification of (a) PLA, (b) PLA/PBAT 90/10 blend, (c) PLA/PBAT/PLA- <i>g</i> -MA 90/10/2 phr blend, (d) PLA/PBAT/PLA- <i>g</i> -MA 90/10/4 phr blend, (e) PLA/PBAT/PLA- <i>g</i> -MA 90/10/6 phr blend, (f) PLA/PBAT/PLA- <i>g</i> -MA 90/10/8 phr blend, and (g) PLA/PBAT/PLA- <i>g</i> -MA 90/10/10 phr blend.....62
4.21	DSC thermograms of PLA, PLA/PBAT blend, and PLA/PBAT/PLA- <i>g</i> -MA blends at various PLA- <i>g</i> -MA contents (the second heating, heating rate 5°C/min) .....65
4.22	TGA thermograms of PLA, PBAT, PLA/PBAT 90/10 blend, and PLA/PBAT/PLA- <i>g</i> -MA 90/10/2 phr blend .....68
4.23	DTG thermograms of PLA, PBAT, PLA/PBAT 90/10 blend, and PLA/PBAT/PLA- <i>g</i> -MA 90/10/2 phr blend .....69

## LIST OF FIGURES (Continued)

Figure	Page
4.24	Shear viscosity of PLA, PBAT, PLA/PBAT blend, and PLA/PBAT/PLA-g-MA blends at various PLA-g-MA contents.....71
4.25	MFI of PLA, PBAT, PLA/PBAT blend, and PLA/PBAT/PLA-g-MA blends at various PLA-g-MA contents .....72
4.26	Tensile strength of compatibilized PLA/PBAT blend and PLA/PBAT/CaCO <sub>3</sub> composites at various CaCO <sub>3</sub> contents.....74
4.27	Young's modulus of compatibilized PLA/PBAT blend and PLA/PBAT/CaCO <sub>3</sub> composites at various CaCO <sub>3</sub> contents.....74
4.28	Elongation at break of compatibilized PLA/PBAT blend and PLA/PBAT/CaCO <sub>3</sub> composites at various CaCO <sub>3</sub> contents.....75
4.29	Impact strength of compatibilized PLA/PBAT blend and PLA/PBAT/CaCO <sub>3</sub> composites at various CaCO <sub>3</sub> contents.....75
4.30	SEM micrographs at 2000x magnification of (a) PLA/PBAT/ PLA-g-MA 90/10/2 phr blend, (b) PLA/PBAT/PLA-g-MA/CaCO <sub>3</sub> 90/10/2 phr/5 composite, (c) PLA/PBAT/PLA-g-MA/CaCO <sub>3</sub> 90/10/2 phr/10 composite, (d) PLA/PBAT/PLA-g-MA/CaCO <sub>3</sub> 90/10/2 phr/15 composite, and (e) PLA/PBAT/PLA-g-MA/CaCO <sub>3</sub> 90/10/2 phr/30 composite .....78
4.31	DSC thermograms of compatibilized PLA/PBAT blend and PLA/PBAT/CaCO <sub>3</sub> composites at various CaCO <sub>3</sub> contents.....80

## LIST OF FIGURES (Continued)

Figure	Page
4.32 TGA thermograms of (a) PLA, (b) PLA/PBAT/PLA-g-MA/CaCO <sub>3</sub> 90/10/2 phr/5 composite, (c) PLA/PBAT/PLA-g-MA/CaCO <sub>3</sub> 90/10/2 phr/10 composite, (d) PLA/PBAT/PLA-g-MA/CaCO <sub>3</sub> 90/10/2 phr/15 composite, (e) PLA/PBAT/PLA-g-MA/CaCO <sub>3</sub> 90/10/2 phr/30 composite, and (f) PBAT. ....	83
4.33 DTG thermograms of (a) PLA, (b) PLA/PBAT/PLA-g-MA/CaCO <sub>3</sub> 90/10/2 phr/5 composite, (c) PLA/PBAT/PLA-g-MA/CaCO <sub>3</sub> 90/10/2 phr/10 composite, (d) PLA/PBAT/PLA-g-MA/CaCO <sub>3</sub> 90/10/2 phr/15 composite, (e) PLA/PBAT/PLA-g-MA/CaCO <sub>3</sub> 90/10/2 phr/30 composite, and (f) PBAT .....	84
4.34 Shear viscosity of compatibilized PLA/PBAT blend and PLA/PBAT/CaCO <sub>3</sub> composites at various CaCO <sub>3</sub> contents.....	86
4.35 MFI of compatibilized PLA/PBAT blend and PLA/PBAT/CaCO <sub>3</sub> composites at various CaCO <sub>3</sub> contents .....	87
4.36 Photographs of films prepared from PLA/PBAT blends and PLA/PBAT/CaCO <sub>3</sub> composite (10 μm thickness) on a graphic pattern (a) PLA/PBAT 90/10 blend, (b) PLA/PBAT/PLA-g-MA 90/10/2 phr blend, and (c) PLA/PBAT/PLA-g-MA/CaCO <sub>3</sub> 90/10/2 phr/5 composite .....	89

**LIST OF FIGURES (Continued)**

<b>Figure</b>		<b>Page</b>
4.37	Tensile properties of blown films prepared from PLA/PBAT blend, compatibilized PLA/PBAT blend, and PLA/PBAT/CaCO <sub>3</sub> composite.....	90



## SYMBOLS AND ABBREVIATIONS

PLA	=	Poly (lactic acid)
PBAT	=	Poly (butylene adipate- <i>co</i> -terephthalate)
CaCO <sub>3</sub>	=	Calcium carbonate
MA	=	Maleic anhydride
Luperox101	=	2,5-bis( <i>tert</i> -butylperoxy)-2,5 dimethylhexane
PLA- <i>g</i> -MA	=	Poly (lactic acid) grafted with maleic anhydride
%G	=	Graft content
FTIR	=	Fourier transform infrared spectroscopy
cm <sup>-1</sup>	=	Reciprocal centimeter
GPC	=	Gel permeation chromatography
SEM	=	Scanning electron microscope
DSC	=	Differential scanning calorimetry
TGA	=	Thermalgravimetric analysis
T <sub>5</sub>	=	Thermal degradation at 5 % weight loss
T <sub>50</sub>	=	Thermal degradation at 50 % weight loss
T <sub>f</sub>	=	Final degradation temperature

# CHAPTER I

## INTRODUCTION

### 1.1 Background

Nowadays, plastics obtained from petrochemical sources have caused extensive environmental problem associated with their disposal. Although recycling is an environmentally attractive solution, only a small percentage of plastic is actually recyclable and most end up in public landfills. One of the possible solutions to solve this problem is to replace the commodity synthetic polymers with biodegradable polymers which are readily sensitive to microbial action.

Poly (lactic acid) (PLA) has a number of interesting properties including biodegradability, biocompatibility, high strength, and high modulus. For these reasons, PLA has been widely used in biomedical and packaging applications. However, its high brittleness and high cost limit its application (Yeh, Huang, Chai, and Chen, 2009). Several modifications such as copolymerization, plasticization, and polymer blending have been proposed to improve the toughness of PLA. Blending PLA with other flexible and biodegradable polyesters, e.g. polycaprolactone (PCL) (Broz, VanderHart, and Washburn, 2003), poly (butylene adipate-*co*-terephthalate) (PBAT) (Jiang, Wolcott, and Zhang, 2006) or poly (butylenes succinate) (PBS) (Bhatia, Gupta, Bhattacharya, and Choi, 2007) is a practical method to improve toughness of PLA. Poly (butylene adipate-*co*-terephthalate) (PBAT) is an aliphatic-aromatic copolymer. It can be degraded within a few weeks with the aid of naturally

occurring enzymes (Gan, Kuwabara, Yamamoto, Abe, and Doi, 2004; Jiang, Wolcott, and Zhang, 2006). In view of its high toughness and biodegradability, PBAT is considered a good candidate for toughening PLA. In fact, all of the investigated PLA/PBAT blends are immiscible or only partially miscible (Jiang, Wolcott, and Zhang, 2006). The immiscible blends form a two-phase system with poor mechanical properties including tensile strength, Young's modulus, elongation at break, and impact strength due to weak adhesion at the interface (Carlson, Nie, Narayan, and Dubois, 1999). Many works have focused on enhancing the compatibility between the component polymers by adding a third component, which is miscible with both parent polymers (Chen, Kim, Kim, and Yoon, 2005). Therefore, these PLA/PBAT blends may need compatibilizers such as PLA-g-MA (Victor, Witold, Wunpen, and Betty, 2009), a reactive compatibilizer with glycidyl methacrylate (PE-GMA) (Kim, Choi, Kim, Lee, and Lee, 2004) and a random terpolymer of ethylene acrylic and glycidyl methacrylate (T-GMA) (Zhang, Wang, Ren, and Wang, 2009) to improve their compatibility.

Generally, the binary blends of PLA and flexible polymers exhibit higher elongation at break but lower tensile strength and Young's modulus than the pure PLA due to addition of a ductile phase. Thus, addition of fillers such as calcium sulfate ( $\text{CaSO}_4$ ) (Murariu, Da Silva Ferreira, Degée, Alexandre, and Dubois, 2007), montmorillonite clay (MMT), and calcium carbonate ( $\text{CaCO}_3$ ) (Bartczak, Argon, Cohen, and Weinberg, 1999; Jiang, Zhang, and Wolcott, 2007; Kim, Park, Choi, and Yoon, 2008; Zuiderduin, Westzaan, Huétink, and Gaymans, 2003), not only lead to increase Young's modulus but also reduce elongation and impact strength in most cases. Therefore, in an attempt to achieve balance overall properties, PLA ternary

composites containing both flexible polymer and rigid inorganic fillers such as multiwalled carbon nanotubes (MWNTs) (Ko, Gupta, Bhattacharya, and Choi, 2010), montmorillonite (MMT), and nanosized precipitated calcium carbonate (NPCC) (Jiang, Liu, and Zhang, 2009) are recently studied. Especially,  $\text{CaCO}_3$  is commonly used as an inorganic filler in polymers. It is available at low cost and a variety of particle sizes and treatments. Moreover, it has a moderate effect on mechanical properties of the polymers. Thus, the addition of  $\text{CaCO}_3$  into PLA/PBAT blends is one of the simplest and most cost effective ways to balance the mechanical properties of PLA/PBAT blends.

## 1.2 Research objectives

The main objectives of this research are as below:

- (i) To study the effects of initiator and monomer concentration on the grafting content and molecular weight of PLA grafted with maleic anhydride (PLA-g-MA).
- (ii) To study the mechanical, morphological, thermal, and rheological properties of PLA/PBAT blends at various compositions.
- (iii) To study the effect of PLA-g-MA and its content on the mechanical, morphological, thermal, and rheological properties of PLA/PBAT blends.
- (iv) To study the effect of  $\text{CaCO}_3$  and its content on the mechanical, morphological, thermal, and rheological properties of PLA/PBAT/ $\text{CaCO}_3$  composites.
- (v) To prepare blown films from PLA/PBAT blend, compatibilized PLA/PBAT blend and PLA/PBAT/ $\text{CaCO}_3$  composite and investigate their tensile properties.

### 1.3 Scope and limitation of the study

Poly (lactic acid) grafted with maleic anhydride (PLA-g-MA) was prepared using an internal mixer. Maleic anhydride (MA) contents were varied as 1.0, 2.5, 5.0, and 7.5 wt% and initiator (Luperox101) contents were varied as 0.1, 0.25, 0.5, and 1.0 wt%. Fourier transform infrared spectroscopy (FTIR) was used to confirm the MA grafted onto poly (lactic acid) (PLA) molecule and a titration method was used to determine the level of MA grafted onto PLA molecules.

Blends of PLA and poly (butylene adipate-co-terephthalate) (PBAT) were investigated. PBAT contents used in this study were 10, 20, and 30 wt%. All blends were prepared using a co-rotating intermeshing twin screw extruder and test specimens were made using a compression molding machine. The effect of PBAT content on the mechanical, morphological, thermal, and rheological properties of the PLA/PBAT blend was studied.

Based on the mechanical properties of the PLA/PBAT blend, the blend giving the optimum mechanical properties with low material cost was selected to further study the effect of compatibilizer content on the mechanical, morphological, thermal, and rheological properties of the PLA/PBAT blend. Compatibilizer contents were 2, 4, 6, 8, and 10 phr.

Based on the mechanical properties of the compatibilized PLA/PBAT blend, the compatibilized blend giving the optimum mechanical properties was selected to further study the effect of calcium carbonate ( $\text{CaCO}_3$ ) content on the mechanical, morphological, thermal, and rheological properties of the compatibilized PLA/PBAT blend.  $\text{CaCO}_3$  contents were 5, 10, 15, and 30 wt%.

The PLA/PBAT blend, the compatibilized PLA/PBAT blend, and the PLA/PBAT/CaCO<sub>3</sub> composite giving the optimum mechanical properties were chosen to prepare blown films and their tensile properties were investigated.



## CHAPTER II

### LITERATURE REVIEW

#### 2.1 Poly (lactic acid) (PLA)

Poly (lactic acid) (PLA), a biodegradable polymer, is prepared from renewable resources such as corn, sugar beets or rice. The chemical structure of PLA is shown in Figure 2.1. PLA degrades biologically into lactic acid. It offers a potential alternative to petrochemical plastics for many applications because of its high strength and stiffness. However, the applications of PLA are limited by several factors such as low glass transition temperature, weak thermal stability, and high brittleness. Moreover, PLA is still more expensive than many petroleum-derived commodity plastics. For extending PLA applications, the properties like impact strength or flexibility, and thermal stability must be improved.

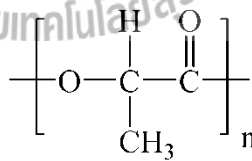


**Figure 2.1** Chemical structure of poly (lactic acid) (PLA).

#### 2.2 The toughness improvement of PLA

Toughness of PLA can be improved by using plasticizers, copolymerization of PLA, and/or blending of PLA with flexible polymers. Especially, blending of PLA with other biodegradable polymers is a useful technique to impart flexibility and

toughness to the PLA while maintains biodegradability. Various biodegradable polymers such as aliphatic polyesters and aliphatic–aromatic copolyesters have been used for blending with PLA to improve its properties.

### 2.2.1 PLA plasticization

Plasticizers are used to improve flexibility and ductility of glassy polymers. They are usually low molecular weight and form secondary bonds with polymer chains and thus increase the intermolecular distance of the polymer chains. A preferred plasticizer for PLA should have significantly lower  $T_g$  than PLA. In addition, it should be biodegradable, nonvolatile, nontoxic, and minimal leaching or migration during aging.

Recently, various monomers and oligomers have been investigated as potential plasticizers for PLA. Among them, polyethylene glycol (PEG), oligomer lactic acid (OLA), glycerol, triacetine (TAc), and citrate esters are perhaps the most common investigated plasticizers.

Martin and Averous (2001) investigated the influence of plasticizer such as polyethylene glycol (PEG), oligomer lactic acid (OLA), and glycerol on thermal properties of PLA. Plasticizers with various amounts (10 and 20 wt%) were mixed together with PLA within an internal mixer for 15 min at 90°C. In a second step, each polymer-plasticizer system was extruded with a single screw extruder, equipped with a specific high-shear zone (conical–shaped element). From DSC analysis, a significant decrease in  $T_g$  was obtained with PEG and OLA. Especially, glycerol had only limited effect on the thermal transition of PLA. It induced a  $T_g$  shift as low as 5°C at 20 wt% glycerol while the lower  $T_g$  values of 12 and 18°C were obtained with PEG and OLA, respectively. Moreover, plasticized PLA system also

showed a significant decrease in  $T_m$  and the depression of  $T_m$  did not seem to be much dependent on the plasticizer concentration. The results of the depression of  $T_g$  suggested that glycerol was clearly a non-plasticizer of PLA whereas PEG and OLA can be considered as the most efficient plasticizers of PLA.

Pillin, Montrelay, and Grohens (2006) determined thermal and mechanical properties of PLA with PEG and several other oligomeric plasticizers that were used in food packaging. The plasticizers (10, 20, and 30 wt%) were blended with PLA using an internal mixer. Blending temperature and time were 180°C and 15 min, respectively. Blade rotation speed was 30 rpm. Plasticizers lowered the  $T_g$  and modified the melting and crystallization characteristics of PLA. PEG was the most efficient plasticizer for the  $T_g$  reduction. It clearly appeared that, for compositions higher than 20 wt% of plasticizer, all the blends presented a limit of miscibility and the  $T_g$  reached a plateau value. PEG exhibited lower interaction parameters with PLA than other plasticizers. No strong differences were observed between PEG and other plasticizers on the  $T_m$  since it could be deduced from Flory Huggins equation that the interaction parameter was balanced by the enthalpy of melting. Moreover, mechanical characteristics of these materials showed a decrease in modulus and stress at break. Nevertheless, the PLA blended with PEG became very brittle with an increase in plasticizer content because of a lack of cohesion between the separate phases.

Li and Huneault (2007) studied effect of plasticization on the crystallization and rheological properties of PLA. PEG and acetyl triethyl citrate (ATC) were used as plasticizers. Mixtures of PLA at various plasticizer contents (2, 5, and 10 wt%) were prepared using a co-rotating twin screw extruder. The viscosities of PLA and PLA with 10% ATC or PEG were relatively stable over a period of 1800 s (30

min) indicating that no obvious degradation or phase separation occurred. At high plasticizer content, a leveling off the viscosity was expected if the plasticizer saturation point was reached resulting in phase separation. In non-isothermal DSC experiment, a decrease in  $T_g$  and higher nucleation density of PLA plasticized were observed. The higher nucleation density of PLA resulted in crystallization peaks that shifted to a lower temperature as the plasticizer content increased.

Coltelli, Maggiore, Bertoldo, Signori, Bronco, and Ciardelli (2008) studied the modulation of PLA properties by the addition of acetyl tributyl citrate (ATBC). ATBC contents were 10, 20, and 35 wt%. All blends were prepared in a discontinuous laboratory mixer. The effect of the plasticizer concentration on thermal, morphological, and mechanical properties of the blends was evaluated.  $T_g$  of PLA decreased with increasing amount of ATBC. From SEM analysis, the appearance of inhomogeneous system at 25 wt% ATBC revealed the probably overcoming of the solubility threshold for ATBC in the PLA phase. Moreover, the analysis of the second heating scan in the DSC thermograms of the PLA/ATBC mixtures evidenced cold crystallization peaks whose enthalpy increased with increasing ATBC content. The positive values of  $\Delta H_{mc}$ , obtained by the summation of the enthalpy of crystallization occurring during the heating step ( $\Delta H_{cc}$ ) and the melting enthalpy ( $\Delta H_m$ ), revealed that the crystallization of PLA also occurred during the rapid cooling procedure. The addition of ATBC led to a decrease in tensile modulus but an increase in strain at break due to the plasticizer effect.

Yeh, Huang, Chai, and Chen (2009) reported the plasticizing effects of triacetine (TAc) on crystallization, chain mobility, microstructure, and tensile properties of PLA. TAc contents were 5, 10, 15, 20, 25, and 30 wt%. After blending

TAc with PLA, the  $T_g$  and  $T_m$  values of  $PLA_xTAc_y$  specimens reduced significantly as TAc contents increased. However, as evidenced by WAXD analysis, significant recrystallization of  $\alpha$  form PLA crystals was found during the annealing processes of the  $PLA_xTAc_y$  series specimens. In fact, some “less perfect”  $\beta$  form PLA crystals were found as the TAc content was up to 30 wt%. Likely, the appearance of the recrystallized  $\alpha$  and  $\beta$  form PLA crystals was attributed to the expected increase in the free volume and molecular mobility of the PLA molecules as the TAc contents increased. Because the plasticized and relatively mobile PLA molecules could be recrystallized at relatively low temperatures during the heat-scanning processes. After blending TAc in PLA from 0 to 25 wt%, the tensile strength ( $\sigma_f$ ) values of  $PLA_xTAc_y$  specimens reduced from 52.6 to 30 MPa and elongation at break ( $\epsilon_f$ ) increased significantly from 2.8 to 267.2%. However, both  $\sigma_f$  and  $\epsilon_f$  values of  $PLA_xTAc_y$  specimens reduced abruptly as their TAc contents increased from 25 to 30 wt%.

### 2.2.2 Copolymerization of PLA

Copolymerization has been investigated as a powerful mean to obtain new materials with properties unattainable by homopolymers. Properties including tensile and impact performances of a copolymer can be tailored in an adaptable way by manipulating the architecture of the molecule, sequence of monomers, and composition.

Hiljanen-Vainio, Karjalainen, and Seppälä (1996) studied thermal and mechanical properties of  $\epsilon$ -caprolactone/L-lactide ( $\epsilon$ -CL/L-LA) copolymer and  $\epsilon$ -caprolactone/DL-lactide ( $\epsilon$ -CL/DL-LA) copolymer. Copolymers of  $\epsilon$ -CL/L-LA and  $\epsilon$ -CL/DL-LA were synthesized with compositions of 20, 40, and 60 wt%  $\epsilon$ -CL. The physical characteristics of resulting copolymers ranged from weak elastomers to

tough thermoplastics as a function of CL/LA ratio and type of LA monomer in the copolymerization. Compared with the PLLA or PDLA homopolymers, the copolymers exhibited larger elongation (>100% for most copolymers) but lower tensile modulus and strength. The copolymers containing L-LA had greater tensile strength than those containing D, L-LA due to the crystalline nature of the former.

Hwang, Lee, Lee, Lee, Shim, Selke, Susan, Soto-Valdez, Matuana, Rubino, and Auras (2012) evaluated the effects of maleic anhydride (MAH) and dicumyl peroxide (DCP) concentrations on thermal and mechanical properties of PLLA-g-MAH. DCP contents were 0.1 and 0.2 phr and MAH contents were 0, 0.5, 1, 2, and 3 phr. The glass transition temperature and crystallinity of PLLA-g-MAH significantly decreased with addition of MAH. The thermal decomposition of the PLLA films was affected by the MAH content while the mechanical properties were almost unchanged. With the addition of more than 0.5 phr MAH, a slight increase in molecular weight of PLLA-g-MAH was found, which could be attributed to either the MAH branching reaction or a possible crosslinking reaction between the PLLA chains. This could increase chain entanglements resulting in an increase in molecular weight and a slight decrease of MFI.

### **2.2.3 Blending of PLA with flexible polymers**

During the past decade, a large number of investigations have been performed on the blending of PLA with various flexible biodegradable polymers. Because polymer blending with biodegradable polymer is regarded as a useful and economical way to produce new materials with a wide range of properties and maintained fully biodegradability.

Lee and Lee (2005) investigated thermal, morphological, and mechanical properties of a binary blend of PLA and poly (butylene succinate adipate) (PBSA). Dried pellets of PLA and PBSA were mixed by a co-rotating twin screw extruder at a fixed rotation speed of 30 rpm. PBSA contents were 0, 10, 20, 40, 60, 80, and 100 wt%. DSC thermograms of the blends indicated that thermal properties of PLA did not change noticeably with amount of PBSA. Thermogravimetric analysis showed thermal stability of the blends was lower than that of pure PLA and PBSA. Morphology of the blends showed a typical sea and island structure of immiscible blend. In addition, tensile strength and modulus of the blends decreased with increasing PBSA content. The strain at break was nearly constant up to 60 wt% PBSA and rapidly increased at more than that composition. This may be attributed to the much more elastic characteristic of PBSA matrix phase. Interestingly, impact strength of PLA/PBAT (80/20) blend was seriously higher than the rule mixture.

Jiang, Wolcott, and Zhang (2006) prepared binary blend of PLA and PBAT in a co-rotating twin screw extruder. PBAT contents were 5, 10, 15, and 20 wt%. With increasing PBAT content, tensile strength and Young's modulus of the blends decreased but elongation and toughness dramatically increased. The failure mode changed from brittle fracture of the neat PLA to ductile fracture of the blends. The dynamic rheological properties results showed that PBAT had higher melt elasticity and viscosity than PLA. In addition, the melt elasticity and the viscosity of the blends increased with the concentration of PBAT.

Bhatia, Gupta, Bhattacharya, and Choi (2007) studied the blends of PLA and poly (butylene succinate) (PBS). PBS contents were 10, 20, 50, 80, 90, and 100 wt%. The blends were prepared using a laboratory-scale twin screw extruder at

180°C. Morphological, thermal, and mechanical properties of PLA/PBS blends were studied. SEM images showed that both the polymers were immiscible beyond 20 wt% of PBS in PLA. Modulated differential scanning calorimetry (MDSC) thermograms of the blends indicated that the  $T_g$  of PLA did not change much with the addition of PBS. However, this analysis showed that, for PLA/PBS blend up to 80/20 composition, there was partial miscibility between the two polymers. Tensile strength and Young's modulus of the blends decreased with increasing PBS content. However, tensile strength and Young's modulus values of PLA/PBS blend up to 80/20 composition nearly followed the mixture rule. Elongation at break of the blends was quite similar to that of neat PLA for compositions up to 80 wt% PBS and then increased for 10/90 PLA/PBS composition and neat PBS. This may be attributed to the more elastic characteristic of the neat PBS matrix.

Gu, Zhang, Ren, and Zhan (2008) prepared PLA/PBAT blends using a twin screw extruder. The blends contained 0, 5, 10, 15, 20, and 30 wt% PBAT. The linear and non-linear shear rheological behaviors of PLA/PBAT melts were investigated by an advanced rheology expanded system (ARES). It can be seen that slope of stress relaxation  $G(t)$  curves of the blends decreased with the introduction of PBAT. This indicated that the relaxation time increased with the incorporation of PBAT and the formation of entanglement structures in PLA/PBAT melt blends. The phase morphology of PLA/PBAT blends was observed by a scanning electron microscope (SEM). An oval cavities and enclosed round PBAT particles were visible on the fracture surfaces. These results indicated that the blend was a kind of immiscible two phase system with PBAT dispersing evenly in PLA matrix.

Xiao, Lu, and Yeh (2009) studied the crystallization behavior of fully biodegradable poly (lactic acid)/poly (butylene adipate-*co*-terephthalate) blends. PLA and PBAT were mixed together with different weight ratios of 100/0, 80/20, 60/40, 40/60, and 0/100 in an internal mixer for 3 min. The mixing rollers were maintained at 90 rpm and the temperature was set at 185°C. When compared with neat PLA, the degree of crystallinity of PLA in various blends markedly increased but the crystallization mechanism almost did not change. The equilibrium melting point of PLA initially decreased with an increase in PBAT content and then increased when PBAT content in the blends was 60 wt%.

Yeh, Tsou, Huang, Chen, Wu, and Chai (2010) studied the compatibility, crystallization, and tensile properties of PLA/PBAT blends. PBAT contents were 0, 2.5, 5, 7.5, 10, 15, 20, and 100 wt%. The dried components of PLA/PBAT blends at varying weight ratios were then melt-blended in the Plasti-Corder Mixer. The mixer was operated at 190°C and a screw speed of 250 rpm for 3 min. They found that the percentage crystallinity ( $\chi_c$ ), melting temperature ( $T_m$ ), and onset temperatures ( $T_{onset}$ ) values of PLA<sub>x</sub>PBAT<sub>y</sub> blends reduced gradually as their PBAT contents increased. Further morphological and DMA analysis showed that PBAT molecules were miscible with PLA molecules at PBAT contents equal to or less than 2.5 wt%, since no distinguished phase-separated PBAT droplets and  $\tan \delta$  transitions were found on the fracture surfaces and  $\tan \delta$  curves of PLA<sub>x</sub>PBAT<sub>y</sub> blends, respectively. In addition, PLA specimen exhibited relatively high tensile strength but low elongation at break. In contrast, PBAT specimen exhibited relatively low tensile strength but high elongation at break. After blending PBAT in PLA, the

PLA<sub>x</sub>PBAT<sub>y</sub> specimens revealed substantial reduction in tensile strength values but increased elongation at break values as their PBAT contents increased.

Zhao, Liu, Wu, and Ren (2010) studied mechanical and thermal properties of PLA/PBAT blends. The blend was prepared using a twin screw extruder, equipped with a volumetric feeder and a strand pelletizer. The extrusion temperature was independently controlled in eight zones along the extruder barrel and a strand die to achieve a temperature profile ranging from 150°C to 180°C. A 150 rpm screw speed was used for all extrusions. The weight ratios of PLA/PBAT were 95/5, 90/10, 85/15, 80/20, and 75/25. They found that PBAT could be homogeneously dispersed in PLA matrix at a low content (5–20 wt%), yielding the blends with much higher elongation at break than pure PLA. Moreover, PLA/PBAT blends showed considerably higher elongation at break than pure PLA with an acceptable loss of strength. DSC analysis showed that isothermal and nonisothermal crystallizabilities of PLA component were promoted in the presence of a small amount of PBAT. Moreover, the addition of PBAT to the PLA matrix resulted in weaker and wider crystallization peak (about 110°C), which was presented at a lower crystallization temperature than PLA. This suggested that the addition of PBAT had an influence on crystallizability of PLA.

Meng, Deng, Liu, Wu, and Yang (2012) studied the light transmission, thermal, rheological, mechanical, and morphological properties of PLA/poly (butyl acrylate) (PBA) blends. PLA/PBA blends containing different PBA contents (0, 5, 8, 11, and 15 wt%) were prepared in an internal mixer at 175°C and a mixing rotation of 50 rpm for 7 min. Dynamic rheology, SEM, and DSC results showed that the PLA was partial miscible with PBA. PBA component improved the crystallization ability

of PLA and the crystallinity of PLA increased with PBA content (<15 wt%). With an increase in PBA content, tensile strength and modulus of the blends decreased slightly while the elongation at break and toughness dramatically increased. The failure mode changed from brittle fracture of neat PLA to ductile fracture of the blend. Rheological results revealed complex viscosity and melt elasticity of the blends decreased with increasing content of PBA and phase segregation occurred at loading above 11 wt% PBA. UV–Visible light transmittance showed that transparency and transmittance of PLA/PBA blends decreased with increasing amount of PBA.

### **2.3 The study of compatibilization of PLA blends**

Generally, all most blends of PLA and flexible polymers are immiscible or only partially miscible leading to PLA blends with poor mechanical properties. To improve properties of immiscible blends, usually they need to be compatibilized. There are three aspects of compatibilization: (1) Reduction of the interfacial tension that facilitates fine dispersion, (2) Stabilization of morphology against its destructive modification during the subsequent high stress and strain process (e.g. during the injection molding), and (3) Enhancement of adhesion between phases in the solid state, facilitation the stress transfer, hence improving mechanical properties of the product (Ajjji, 2003).

The methods for improving the compatibility between the two phases are of two types, as follow (1) nonreactive compatibilization by involving a copolymer or graft homopolymer being miscible with the two phase and (2) reactive compatibilization by creating chemical linkages between the two copolymer at the interface (Stelescu, Manaila, and Niculescuaron, 2007). The formation of copolymers

at the interface will significantly reduce the dimensions of the phase domains and interfacial tension, stabilize the phase morphology, and strengthen the interface.

Zhang and Sun (2004) investigated the influence of a polymeric dioctyl maleate (DOM), a derivative of MA with a chemical structure similar to MA, on tensile strength and elongation of PLA/starch blends. PLA/starch blends at a fixed ratio of 55/45 at various DOM contents (1.0-15.0 wt%) were extruded using a twin screw extruder. The processing temperature profile was set at 125, 185, and 180°C from feed inlet to the die. By adding liquid DOM to a PLA/starch (55/45) blend, the tensile strength of the blend increased to a remarkable value of 40.0 MPa at 0.5% DOM and reached a maximum value of 43.6 MPa at 2% DOM. On further increasing DOM, the corresponding elongation was dramatically extended to 24.3% at 10% DOM, almost 7 times the elongation at 8% DOM, while tensile strength decreased to 19.9 MPa. The elongation then increased to 36.0% and the tensile strength reduced to 16.2 MPa at 15% DOM. There was probably a critical percentage of DOM between 8 and 10% that formed a continuous plasticizer phase. These results might be summarized that DOM acted as a compatibilizer for PLA/starch systems at concentrations below 8%. Further increasing DOM concentration, the tensile strength reduced while elongation markedly increased. This indicated that DOM acted as a polymeric plasticizer.

Harada, Iida, Okamoto, Hayashi, and Hirano (2008) studied mechanical and morphological properties of PLA/PCL (80/20) blends in the presence of isocyanate-lysine triisocyanate (LTI) as a reactive processing agent. LTI content was 1.5 phr. The blends were processed in a twin screw extruder at 190°C. The ultimate strain in the presence of LTI was 270% higher than that in the absence of LTI. The morphology

showed that PLA/PCL blends, in the presence of LTI, had sea-island structures, in which PLA formed a continuous phase and PCL formed a dispersed phase, thereby contributing to an increase in physical properties. This indicated that LTI might react with both PLA and PCL. Thus, the reaction might increase the interfacial adhesion between PLA and PCL.

Victor, Witold, Wunpen, and Betty (2009) prepared PLA-g-MA copolymer using dicumyl peroxide as an initiator. PLA-g-MA was used to improve interfacial adhesion between PLA and starch. The blends contained 15, 25, 35, 50, and 60 wt% starch. The blends were prepared in an internal mixer at 160°C with the blade speed of 80 rpm. SEM micrographs of all compatibilized blends showed better interaction between PLA and starch. Chemical interactions might result from a transesterification reaction among starch hydroxyl groups, grafted acid hydroxyl groups or anhydride groups on PLA. Physical interaction was possible through hydrogen bonds. PLA/starch blends without compatibilizer did not have sufficient interfacial adhesion.

Yuan, Liu, and Ren (2009) studied the influences of MAH and 2,5-dimethyl-2,5-di-(*tert*-butylperoxy)hexane (L101) on foaming behaviors of PLA/PBAT blends. The blends were extruded into foams using a twin screw extruder. Screw speed was fixed at 100 rpm for all formulations. The temperature profile during extrusion was 135/135/145/155/165/165/165/165/160/155/150°C from the barrel section just after the feeder throat to the die. Then PLA and PBAT were premixed at the weight ratios of 100/0 and 90/10 in a Hobart mixer. The mixtures were prepared as prefoaming masterbatches. L101 was used as a free-radicals initiator which attempted to capture the hydrogen atom both in PBAT and PLA chains. Then, MAH was grafted onto PBAT and PLA chains, which gave rise to better compatibility between PBAT and

PLA. The results showed that the addition of 10 wt% PBAT significantly increased elasticity and viscosity of PLA. Good compatibility of the PLA/PBAT composite foams was achieved when a small amount of both MA and L101 were added to PLA matrix.  $T_g$  of PLA decreased and its half-peak width of  $T_m$  values also decreased. In addition, the mechanical properties of the PLA/PBAT composite foams were improved by grafting reaction. The morphologies of no-foamed polymer before and after modification were observed by SEM. The fractures surface of PLA/PBAT blend showed several drawing belts along the direction of stress. This suggested that PBAT improved the elasticity of PLA. When 2 wt% of MAH and 0.5 wt% of L101 were added the dispersion of PBAT in PLA matrix was uniform. Although there were still some drawing belts, the fracture surface was smoother and those minimal filaments disappeared. This was due to the fact that when minute amounts of L101 were added, the intermolecular force of PLA and PBAT was enhanced.

Zhang, Wang, Ren, and Wang (2009) investigated mechanical properties of PLA/PBAT blend in the presence of a random terpolymer of ethylene, acrylic and glycidyl methacrylate (T-GMA) as a reactive processing agent. The blends were melt-blended using a co-rotating twin screw extruder. The blends contained 10, 20, 30, and 40 wt% PBAT. T-GMA was added at 1.0-10.0 wt% to the PLA/PBAT blends. With the addition of T-GMA to blend systems, tensile toughness of the blend increased without severe loss in tensile strength. SEM micrographs showed that PLA/PBAT blend was a kind of immiscible blend. With the presence of T-GMA (5 wt%), the blend of PLA and PBAT showed better miscibility and more shear yielding when it was fractured.

Lin, Guo, Chen, Ma, and Wang (2012) investigated effect of tetrabutyl titanate (TBT) on mechanical and morphological properties of PLA/PBAT blends at a fixed ratio of 70/30. TBT contents were 0.1, 0.2, 0.3, 0.4, and 0.5 wt%. The mechanical properties including tensile strength, elongation at break, toughness, and stiffness of PLA/PBAT blends were improved significantly with the incorporation of TBT. From DMA results, the addition of TBT not only improved the storage modulus of the blends but also promoted the cold crystallization process of PLA. Moreover, SEM micrographs demonstrated that the dispersed PBAT phase domain became smaller in the compatibilized blend indicating an increase in compatibility of PLA/PBAT blend.

#### **2.4 The effect of filler on properties of PLA blends**

Toughening PLA by incorporation of a flexible polymer is usually accompanied by reduction in strength and modulus. The addition of fillers into PLA increases modulus but reduces elongation and impact strength in most cases. Therefore, in an attempt to achieve balanced overall properties, PLA ternary composites containing both flexible polymer and fillers are recently studied.

Ludvik, Glenn, Klamczynski, and Wood (2007) prepared cellulose fiber/bentonite clay/biodegradable thermoplastic composites using a Hobart model N-50A mixer and their mechanical properties were investigated. PLA/PBAT 70/30 blends at various fiber contents (5.5 and 11 wt%) were studied. In order to obtain uniform dispersion of cellulose fiber in a biodegradable thermoplastic matrix, cellulose fiber and bentonite clay were soaked in water in the mixing bowl. With mixing, the fiber disintegrated into a uniform mass of hamburger-like consistency. The bentonite clay was added and mixed at medium speed for about ten minutes to

disperse the fiber uniformly. Then, the powder of PBAT and PLA were added and mixed to complete the mix. The incorporation of cellulose fiber and clay decreased tensile strength and elongation at break of PLA/PBAT blend but increased Young's modulus. Tensile strength and elongation at break decreased with increasing fiber and clay content. SEM micrographs of the failed ends of tensile bars of the composites showed that the fibers were pulled from the matrix, not broken. Holes in the matrix of pulled fibers were evident. This illustrated the relatively low adhesion between the fiber and the matrix.

Jiang, Liu, and Zhang (2009) investigated mechanical properties of PLA/PBAT/nanoparticle ternary composites. The nanoparticles were montmorillonite clay (MMT) or nanosized precipitated calcium carbonate (NPCC). The composites were prepared by a twin screw extruder. The extrusion temperature profile was set from 110 to 180°C along the barrel. The screw speed was maintained at 80 rpm for all runs. The concentration of PBAT was 10 wt% for all the composites. NPCC and MMT concentrations were 2.5 and 5 wt% on the basis of the total weight of PLA and PBAT. The composites containing MMT exhibited higher tensile strength and modulus but lower elongation compared to the composites containing NPCC. With the addition of PLA grafted with maleic anhydride (PLA-g-MA) as a compatibilizer into the ternary composites, the elongation of the ternary composites was substantially increased, possibly due to improved dispersion of the nanoparticles. SEM micrographs of PLA/PBAT/nanoparticle ternary composites showed that NPCC prime particles and agglomerates could be seen on the fracture surfaces of the PLA/PBAT/NPCC ternary composites. In contrast, MMT was not discernible from the fracture surfaces by SEM image because of its small size and good dispersion.

The nanoparticles also made the PBAT inclusions smaller (in case of NPCC) or hardly discernible (in case of MMT). As a result in case of MMT, the fracture surfaces appeared coarser due to the size reduction.

Ko, Hong, Park, Gupta, Choi, and Bhattacharya (2009) studied the morphological and rheological properties of biodegradable poly (lactic acid) (PLA)/poly (butyleneadipate-*co*-butyleneterephthalate) (PBAT)/multi-walled carbon nanotube (MWNT) nanocomposites. The PLA/PBAT/MWNT nanocomposites were prepared using a laboratory-scale twin screw extruder. The mixing temperature was varied from 160°C to 190°C and the screw speed was 250 rpm. The PLA/PBAT/MWNT nanocomposites were prepared for various compositions of PLA and PBAT (0, 10, 20, 30, 40, 50, and 100 wt% PBAT) with a fixed MWNT content (2 wt%). The experimental results showed that the PLA/PBAT blend was immiscible and MWNT had a good affinity to the PBAT phase due to an interfacial tension of polymer and MWNT. In addition, several factors such as viscosity of blend composition, flexibility of polymer chain, and polymer chemical structure were found to be related to the selectively localized MWNT in the PBAT phase. Storage modulus ( $G'$ ) of the PLA/PBAT/MWNT nanocomposites exhibited a cross-over point at an angular frequency of 6.5 (1/s). Three points of view were presented here to interpret their demonstrated rheological properties. First, to compare the degree of dispersion, the MWNT of PLA/PBAT (50/50) was more dispersed in a broad region. Thus, the storage modulus was higher than other compositions at a low angular frequency region. Second, regarding the filler structure of nanocomposites, MWNT bundles in PLA were highly aggregated but MWNT bundles in other compositions of the PLA/PBAT/MWNT nanocomposites were randomly presented. Highly aggregated

MWNT had more elastic properties based on  $G'$  below the crossover point. The last point of view was regarding the polymer–filler interactions. These results assumed that PBAT and MWNT had a better affinity, supporting the interaction between PBAT and MWNT. Thus,  $G'$  increased with increasing the content of PBAT.

Shahlari and Lee (2009) prepared PBAT/PLA/Cloisite® 30B composites. Rheological, morphological, and mechanical properties of the PBAT/PLA/Cloisite® 30B composites were investigated. The compounds of 80% PBAT, 20% PLA, and 3% Cloisite® 30B were premixed and then a counter-rotating twin screw extruder was used to compound the materials. In melt state, the composites showed higher storage modulus than loss modulus at low frequencies, unlike the neat blends melt, indicating formation of solid-like structure in the blend. Morphological studies showed that dispersed phase domain sizes were significantly reduced in the blends containing organoclay. TEM results indicated that the clay particles were mostly located at the interface of the two phases, which could explain the reduction of the dispersed phase size. Moreover, all of PLA/PBAT blends showed significantly higher moduli than pure PBAT sample. In addition, the blends containing clay showed improved mechanical performance compared to the similar blends without clay.

Kumar, Mohanty, Nayak, and Rahail Parvaiz (2010) investigated the effect of glycidyl methacrylate (GMA) and nanoclay (Cloisite® 20A) on mechanical and morphological behaviors of PLA/PBAT (75/25) blend. PLA/PBAT blend and its composite were prepared using melt blending technique. GMA contents were varied from 3 to 5 wt% and Cloisite® 20A content was 5 wt%. Incorporation of GMA increased the impact strength of PLA/PBAT blend while the tensile strength retained. When GMA content increased from 3 to 5 wt%, Young's modulus of PLA/PBAT

blend increased from 1314 to 1746 MPa which indicated reactivity control at the interface due to the formation of random terpolymer of ethylene acrylic ester and GMA. Adding Cloisite® 20A increased tensile modulus of virgin PLA. This behavior was mainly due to high stiffness and modulus of nanoclay platelets that reinforced the blend matrix. Furthermore, the addition of nanoclay also reduced the particle size of PBAT which led to efficient dispersion of PBAT particles within PLA matrix thereby enhancing the tensile modulus. Moreover, SEM micrographs revealed improved interfacial adhesion between the PLA/PBAT blend in the presence of GMA and nanoclay.

Pilla, Kim, Auer, Gong, and Park (2010) prepared foamed PLA/PBAT blends by the microcellular extrusion process using CO<sub>2</sub> as a blowing agent. Two types of blend systems were investigated: (1) Ecovio, which is a commercially available compatibilized PLA/PBAT blend and (2) a non-compatibilized PLA/PBAT blend at the same PLA/PBAT ratio (i.e., 45:55 by weight percent) as Ecovio. The effects of compatibilization and talc on crystallinity were evaluated. Talc had been added to promote heterogeneous nucleation. DSC was used to study the thermal characteristics (melting peaks and crystallization) of the foamed samples. The non-compatibilized blends exhibited two distinct melting peaks, at around 127°C and 168°C, representing PBAT and PLA, respectively. On the other hand, the compatibilized blends showed only one melting peak at 151°C. This showed that the distinctive melting peaks observed in non-compatibilized blends merged into a single melting peak in compatibilized blends and also the melting peak of non-compatibilized blends decreased. With the addition of talc, cold crystallization and recrystallization peak vanished for PLA. The disappearance of the cold crystallization peak indicated

enhanced crystallinity of PLA during the cooling cycle. Moreover, the addition of talc increased the degree of crystallinity for all the samples. This showed that talc had acted as a nucleating agent during the crystallization process and thereby increased the degree of crystallinity.



## **CHAPTER III**

### **EXPERIMENTAL**

#### **3.1 Materials**

Poly(lactic acid) (PLA, 4042D) was supplied from Nature Works LLC. Poly(butylene adipate-*co*-terephthalate) (PBAT, Ecoflex FBX 7011) was purchased from BASF Co., Ltd. Precipitated calcium carbonate (CaCO<sub>3</sub>, HICOAT 810) with an average particle size of 1.20-1.40 μm was supplied from Sand and Soil Co., Ltd. Maleic anhydride monomer (MA monomer, AR grade) and 2,5-bis(*tert*-butylperoxy)-2,5 dimethylhexane (Luperox101, AR grade) were supplied from Sigma-Aldrich.

#### **3.2 Experimental**

##### **3.2.1 Synthesis of poly (lactic acid) grafted with maleic anhydride**

Poly (lactic acid) grafted with maleic anhydride (PLA-*g*-MA) was prepared in an internal mixer (Haake Rheomix, 3000P). PLA pellet was dried at 70°C for 4 hrs before mixing. The mixing temperature was kept at 170°C. A rotor speed was 50 rpm and mixing time was 10 min. MA contents were 1.0, 2.5, 5.0, and 7.5 wt%. Luperox101 contents were 0, 0.1, 0.25, 0.5, and 1.0 wt%.

##### **3.2.2 Characterization of poly (lactic acid) grafted with maleic anhydride**

###### **3.2.2.1 Determination of maleic anhydride content**

The quantity of maleic anhydride content on PLA was determined by a titration of acid groups derived from anhydride functions using phenolphthalein as an indicator. Samples were dissolved in chloroform and precipitated with methanol to remove residual MA and initiator. Then, the grafted PLA was accurately weighed and completely dissolved in chloroform : methanol (80:20 %v/v) and it was titrated immediately with potassium hydroxide solution (KOH). The acid number and the graft content (%G) were calculated using Eq. (3.1) and Eq. (3.2), respectively. Pure PLA without MA was also titrated under the same condition to obtain blank values (Wu, 2003)

$$\text{Acid number (mg KOH/g)} = \frac{V_{\text{KOH}} (\text{ml}) \times N_{\text{KOH}} (\text{N})}{\text{sample(g)}} \times 56.1 \quad (3.1)$$

$$\%G = \frac{(\text{Acid number} - M_0)}{2 \times 561} \times 98.06 \quad (3.2)$$

Where N is the normality (mol/L), V is the volume (ml),  $M_0$  is the blank titration value of pure PLA, and 98.06 is the molecular weight of MA.

### 3.2.2.2 Fourier transform infrared spectroscopy

Infrared spectra of PLA-g-MA films were investigated and compared with the spectrum of PLA film using a Fourier transform infrared spectrometer (BRUKER, TENSOR 27). The spectra were recorded in the 400-4000  $\text{cm}^{-1}$  region with 4  $\text{cm}^{-1}$  resolution.

### 3.2.2.3 Gel permeation chromatography

Molecular weight and molecular weight distribution of PLA and PLA-g-MA were evaluated using a gel permeable chromatograph (GPC). The GPC instrument was equipped with a universal styrene-divinylbenzene copolymer

column (PLgel Mixed-C, 300×7.5 mm, 5µm), a differential refractometer detector (AGILENT/RI-G1362A), an online degasser (AGILENT/G1322A), a thermostatted column compartment (AGILENT/G1316A), and a quaternary pump (AGILENT/G1311A). Chloroform (HPLC grade) was used as an eluent. The eluent flow rate was kept constant at 0.5 ml/min. Temperatures of the column and the detector were maintained at 40°C and 35°C, respectively. The molecular weight of the sample was obtained from calibration curve using polystyrene standards (Shodek standard). The samples were dissolved, diluted using chloroform (2 mg/ml), and filtered with a 0.45 micron filter before injection to remove undissolved contaminants which may block the system.

### 3.2.3 Preparation of PLA/PBAT blends

Blends of PLA/PBAT at various compositions of 90/10, 80/20, and 70/30 wt% were investigated. Based on the mechanical properties of the blend, the blend giving the optimum mechanical properties with low material cost was selected to study the effect of PLA-g-MA content on the properties of the PLA/PBAT blend. The compatibilizer contents were varied as 2, 4, 6, 8, and 10 phr. Before blending, PLA and PBAT were dried in an oven at 70°C for 4 hrs. After that, they were premixed and fed in a co-rotating intermeshing twin screw extruder (Brabender, DSE 35/17D) at the barrel temperature of 160/165/170/165/160°C. The screw speed was 25 rpm. After exiting die, the extrudates were cooled in air before being granulated by a pelletizer. After that, granulated blends were dried at 70°C for 2 hrs. The test specimens were prepared by a compression molding machine (LabTech, LP20-B). The compression condition was processed at the temperature of 170°C and the pressure of 100 MPa. In addition, PLA/PBAT blend and compatibilized PLA/PBAT

blend giving the optimum mechanical properties with low material cost were chosen to prepare the blown films and investigate their tensile properties.

### **3.2.4 Preparation of PLA/PBAT/CaCO<sub>3</sub> composites**

In case of PLA/PBAT/CaCO<sub>3</sub> composite, CaCO<sub>3</sub> was added in the compatibilized PLA/PBAT blend giving the optimum mechanical properties. CaCO<sub>3</sub> contents were 5, 10, 15, and 30 wt%. Before blending, PLA, PBAT and CaCO<sub>3</sub> were dried in an oven at 70°C for 4 hrs. Then, they were mixed in a co-rotating intermeshing twin screw extruder (Brabender, DSE 35/17D). PLA and PBAT were premixed and fed in a polymer feeder while CaCO<sub>3</sub> was fed in an additive feeder with the same feed throat location. The extrusion temperature was independently controlled on four heating zones and the die along the extruder barrel to achieve a temperature profile was 160/165/170/165/160°C. The screw speed was 25 rpm. After exiting die, the extrudates were cooled in air before being granulated by a pelletizer. After that, granulated blends were dried at 70°C for 2 hrs. The test specimens were prepared using a compression molding machine (LabTech, LP20-B). The compression condition was processed at the temperature and the pressure of 170°C and 100 MPa, respectively. In addition, the blown film of compatibilized PLA/PBAT/CaCO<sub>3</sub> composite giving the optimum mechanical properties with low material cost was prepared and its tensile properties were examined.

### **3.2.5 Preparation of blown films from PLA/PBAT blends and PLA/PBAT/CaCO<sub>3</sub> composite**

Blown films of PLA/PBAT blends and their composite were performed on a blown film extrusion machine (ILIE Plastic, EP-HA 45 mm) at the temperature range of 160-170°C. The film die had a diameter of 70 mm and die gap of 1.4 mm.

Blow up ratio was 3.85 and draw ratio was 24.24. The thickness of resulting films was about 10  $\mu\text{m}$ .

### **3.2.6 Characterization of PLA, PBAT, PLA/PBAT blends, and PLA/PBAT/CaCO<sub>3</sub> composites**

#### **3.2.6.1 Mechanical properties**

Tensile properties of PLA, PLA/PBAT blends, and PLA/PBAT/CaCO<sub>3</sub> composite were obtained according to ASTM D638 using a universal testing machine (Instron, 5565) with a load cell of 5 kN and a crosshead speed of 5 mm/min.

Impact properties of PLA, PLA/PBAT blends, and PLA/PBAT/CaCO<sub>3</sub> composite were studied using an impact testing machine (Atlas, BPI). Impact tests were performed according to notched Izod impact strength (ASTM D256). A pendulum of 2.7 J was selected.

#### **3.2.6.2 Morphological properties**

Morphological properties of PLA, PBAT, PLA/PBAT blends, and PLA/PBAT/CaCO<sub>3</sub> composite were examined by a scanning electron microscope (JEOL, JSM-6400). Acceleration voltage of 10-15 kV was used to collect SEM images of sample. The samples were freeze-fractured in liquid nitrogen and coated with gold before analysis.

#### **3.2.6.3 Thermal properties**

Thermal properties of PLA, PBAT, PLA/PBAT blends, and PLA/PBAT/CaCO<sub>3</sub> composites were investigated using a differential scanning calorimeter (Perkin Elmer, DSC7). All samples were heated from 25°C to 200°C with a heating rate of 5°C/min (heating scan) and kept isothermal for 2 min under a

nitrogen atmosphere to erase previous thermal history. Then, the sample was cooled to 25°C with a cooling rate of 10°C/min and heated again to 200°C with a heating rate of 5°C/min (2<sup>nd</sup> heating scan). The crystallinity of PLA ( $\chi_c$ ) was estimated using the following equation:

$$\chi_c = \frac{\Delta H_m}{w_f \times \Delta H_m^0} \times 100\% \quad (3.3)$$

Where  $\Delta H_m$  is the enthalpy of melting during the heating;  $\Delta H_m^0$  is the enthalpy for 100% crystalline PLA homopolymers (93.7 J/g) (Garlotta, 2001) and  $w_f$  is the weight fraction of PLA component in blends and composites.

Thermogravimetric analysis of PLA, PBAT, PLA/PBAT blends, and PLA/PBAT/CaCO<sub>3</sub> composites were examined using a thermogravimetric analyzer (Perkin Elmer, SDT 2960). Thermal decomposition temperature of each sample was examined under nitrogen atmosphere. The sample with a weight between 10 to 20 mg was used for each run. Each sample was heated from room temperature to 600°C at a heating rate of 10°C/min. The weight change was recorded as a function of temperature.

#### 3.2.6.4 Rheological properties

Melt flow index (MFI) of PLA, PBAT, PLA/PBAT blends, and PLA/PBAT/CaCO<sub>3</sub> composites was characterized using a melt flow indexer (Kayeness, 4004). All samples were measured at 170°C with a load of 2.16 kgs. Shear viscosity at various shear rates (shear rate ranges of 10-10000 s<sup>-1</sup>) of PLA, PBAT, PLA/PBAT blends, and PLA/PBAT/CaCO<sub>3</sub> composites were measured using a capillary rheometer (Kayeness, D5052m) at 170°C.

### **3.2.7 Properties of blown films prepared from PLA/PBAT blends and PLA/PBAT/CaCO<sub>3</sub> composite**

The transparency of blown films prepared from PLA/PBAT blend, compatibilized PLA/PBAT blend, and PLA/PBAT/CaCO<sub>3</sub> composite were examined by visual observation.

Tensile test of blown films prepared from PLA/PBAT blend, compatibilized PLA/PBAT blend, and PLA/PBAT/CaCO<sub>3</sub> composite was carried out using a universal testing machine (Instron, 5565) in accordance with ASTM-D882. A load cell and a crosshead speed were 5 kN and 50 mm/min, respectively. For each run of the film, 10 of rectangular pieces were cut from the blown film with the long dimension parallel to extrusion in the machine direction (MD) and perpendicular to extrusion in the transverse direction (TD).



## CHAPTER IV

### RESULTS AND DISCUSSION

#### 4.1 The effects of initiator and monomer content on graft content of PLA-g-MA

##### 4.1.1 Identification of PLA-g-MA

Melt grafting of maleic anhydride (MA) onto PLA was prepared by an internal mixer. Infrared spectrometry was used to identify the grafting reaction of PLA-g-MA. This analysis was performed with a Fourier transform infrared spectrophotometer (FTIR). The FTIR spectra of PLA, MA, and PLA-g-MA with different compositions of MA (1.0, 2.5, 5.0, and 7.5 wt%) and Luperox101 (0, 0.1, 0.25, 0.5, and 1.0 wt%) were scanned. The second derivative of FTIR spectra were used for improving resolution of strongly overlapping peaks. The graft content was determined by a non-aqueous titration method. Moreover, molecular weight and molecular weight distribution were also determined by a gel permeable chromatography (GPC).

The second derivative IR spectra of PLA and PLA-g-MA with different monomer contents (1.0, 2.5, 5.0, and 7.5 wt% MA) at a constant Luperox101 content of 0.5 wt% and different initiator contents (0, 0.1, 0.25, 0.5, and 1.0 wt% Luperox101) at a constant MA content of 5.0 wt% are shown in Figures 4.1 and 4.2, respectively. The unreacted MA may exhibit the peak of MA in the same region as the PLA-g-MA therefore the removal of the unreacted MA was necessary (Wu, 2003). The second derivative IR spectra of PLA-g-MA showed the absorption at  $1785\text{ cm}^{-1}$

corresponding to the characteristic absorption band of the succinic anhydride groups. It could be clearly seen that the peak at  $1785\text{ cm}^{-1}$  was due to the cyclic anhydride group absorption. This cyclic anhydride exhibited an intensive absorption band near  $1780\text{ cm}^{-1}$  and weak band near  $1850\text{ cm}^{-1}$  due to the symmetric and the asymmetric stretching of  $\text{C}=\text{O}$ , respectively (Mani, Bhattacharya, and Tang, 1999). This result confirmed that the grafting of MA onto PLA occurred. Moreover, the peak at  $1785\text{ cm}^{-1}$  tended to increase with amount of MA and Luperox101. The similar result was observed by Wootthikanokkhan et al. (2011).

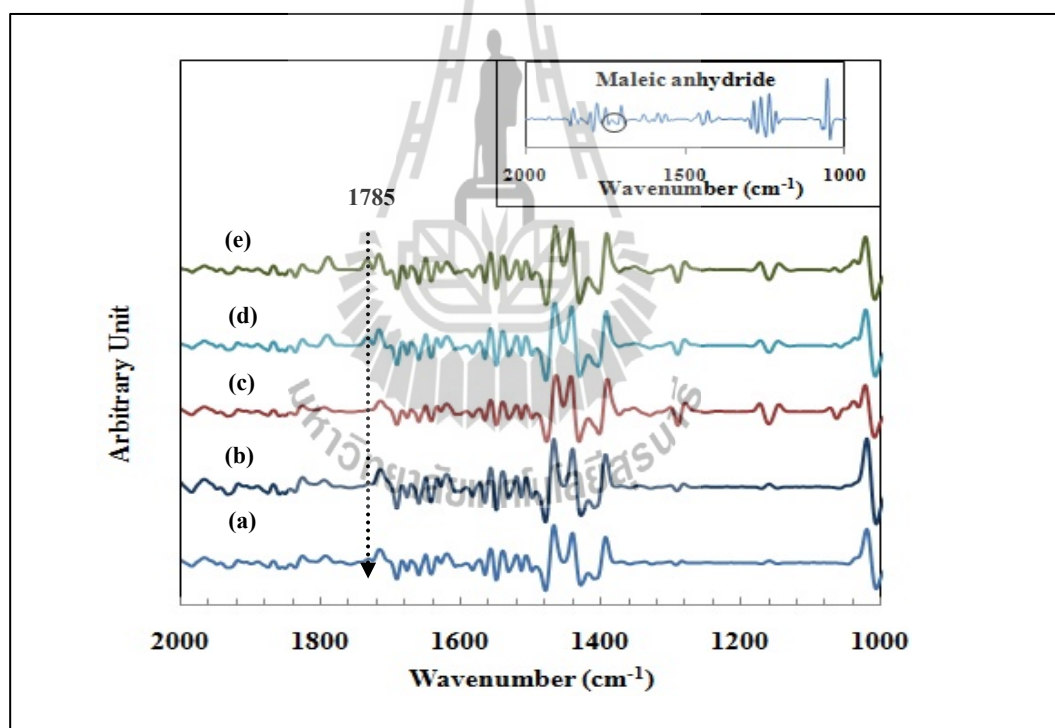


**Figure 4.1** FTIR second derivative spectra of MA, PLA, and PLA-g-MA at a constant Luperox101 content of 0.5 wt% and various contents of MA (a) PLA, (b) PLA-g-MA (1.0 wt%), (c) PLA-g-MA (2.5 wt%), (d) PLA-g-MA (5.0 wt%), and (e) PLA-g-MA (7.5 wt%).

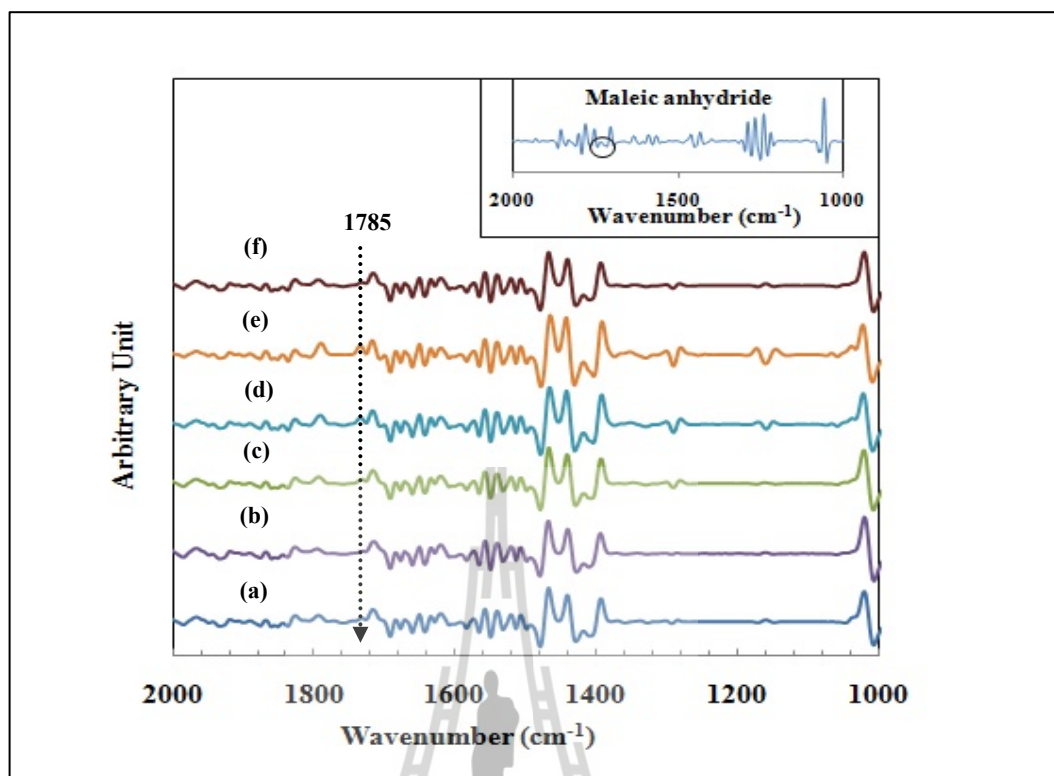


**Figure 4.2** FTIR second derivative spectra of MA, PLA, and PLA-g-MA at a constant MA content of 5.0 wt% and various contents of Luperox101 (a) PLA, (b) PLA-g-MA (0.1 wt%), (c) PLA-g-MA (0.25 wt%), (d) PLA-g-MA (0.5 wt%), (e) PLA-g-MA (1.0 wt%), and (f) PLA-g-MA (none).

Mani, Bhattacharya, and Tang (1999) reported that the probability of hydrogen abstraction depended mainly upon the structure of the polymer molecules. When organic peroxide was used as an initiator the proton at the  $\alpha$ -carbon atom of the carboxylic acid was abstracted due to the radical stabilization. On the basis of the evidence from FTIR, the probable mechanism for grafting reaction was suggested in Figure 4.3.

The reaction started with the homolytical scission of organic peroxide. This was followed by the hydrogen abstraction of the  $\alpha$ -carbon atom relative to the ester carbonyl group and resulted in the formation of a polyester macroradical. A single molecule of MA or another radical (peroxide, polymer radicals, or hydrogen) may be grafted onto the macroradical.

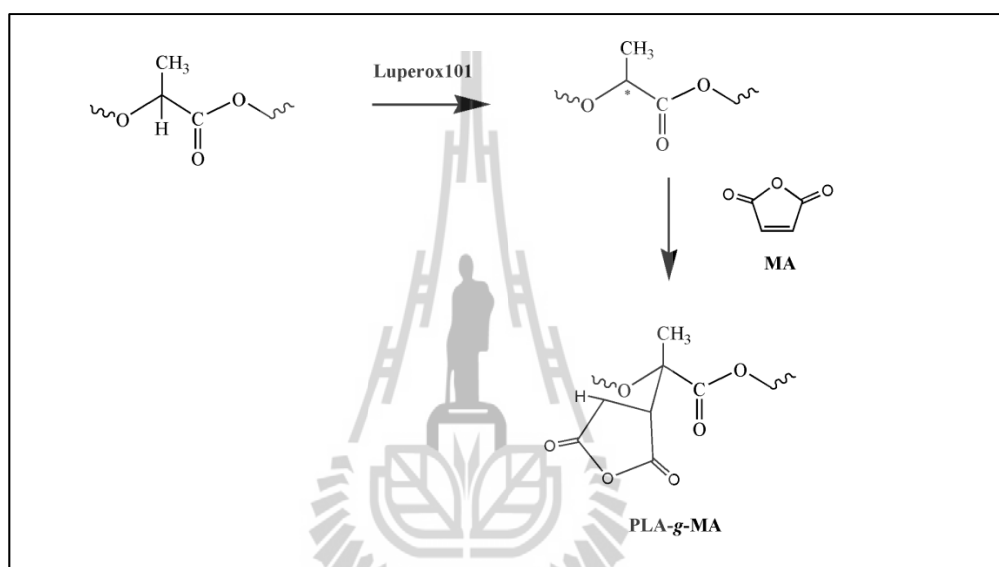


**Figure 4.3** Proposed grafting reaction pathway for the reaction of MA on PLA (Mani, Bhattacharya, and Tang, 1999).

#### 4.1.2 Determination of graft content

##### 4.1.2.1 Effect of monomer content

The influence of monomer (MA) content on the graft content (%G) of PLA-g-MA is shown in Figure 4.4. The data results are summarized in Table 4.1. Introduction of MA on the non-polar polymers backbone had overcome the disadvantage of low surface energy of these polymers leading to improved hydrophilicity (Rzayew, 2011). Moreover, it was well-recognized that MA was a

good monomer candidate for grafting reaction because its homopolymerization was very difficult to take place due to its symmetrical chemical structure (Merijan and Rahway, 1968). Therefore, MA tended to attach to the PLA backbone and the graft content mainly depended on the possibility that macromolecules collided with MA. As MA content increased at constant Luperox101 content of 1.0 wt%, the graft content was increased. Increasing MA content would enhance the chances of macroradicals reacting with MA, hence the graft content increased. Similar observations were reported by Yang et al. (2003); Chuai, Iqbal, Aijaz, Iqbal, and Hiu (2010). However, the graft content did not change significantly with adding MA content at 7.5 wt%.

From Table 4.1, the number average molecular weight ( $\overline{M}_n$ ) and the weight average molecular weight ( $\overline{M}_w$ ) of PLA passed an internal mixer were lower than that of neat PLA. This indicated that PLA was degraded after processing due to its thermal instability. The addition of MA monomer at 1.0 wt% resulted in a decrease in  $\overline{M}_n$  and  $\overline{M}_w$  of PLA-g-MA. This could be due to more chain scission which resulted from more radical formation generated through the decomposition of initiator at high peroxide/monomer ratio. However,  $\overline{M}_n$  and  $\overline{M}_w$  of PLA-g-MA increased with increasing MA content up to 5.0 wt% due to an increase in the probability of reaction between MA monomer and radical from initiator. This may decrease the reaction of PLA and radical from initiator resulting in a decrease in PLA chain scission and an increase in the molecular weight of PLA-g-MA.

**Table 4.1** Graft content, the number average molecular weight ( $\overline{M}_n$ ), the weight average molecular weight ( $\overline{M}_w$ ), and the molecular weight distribution (MWD) of PLA-g-MA at various MA contents and a constant Luperox101 content of 0.5 wt% in chloroform: methanol (80:20 %v/v) solvent.

MA content (wt%)	Graft content (%)	$\overline{M}_n$ (g/mol)	$\overline{M}_w$ (g/mol)	MWD
PLA <sup>a</sup>	-	44581	80847	1.813
PLA <sup>b</sup>	-	24463	53916	1.984
1.0	0.13	10217	18175	1.779
2.5	0.15	17564	43695	2.488
5.0	0.24	25662	52646	2.052
7.5	0.23	21600	53194	2.463

<sup>a</sup> Not internal mixer passed

<sup>b</sup> Internal mixer passed

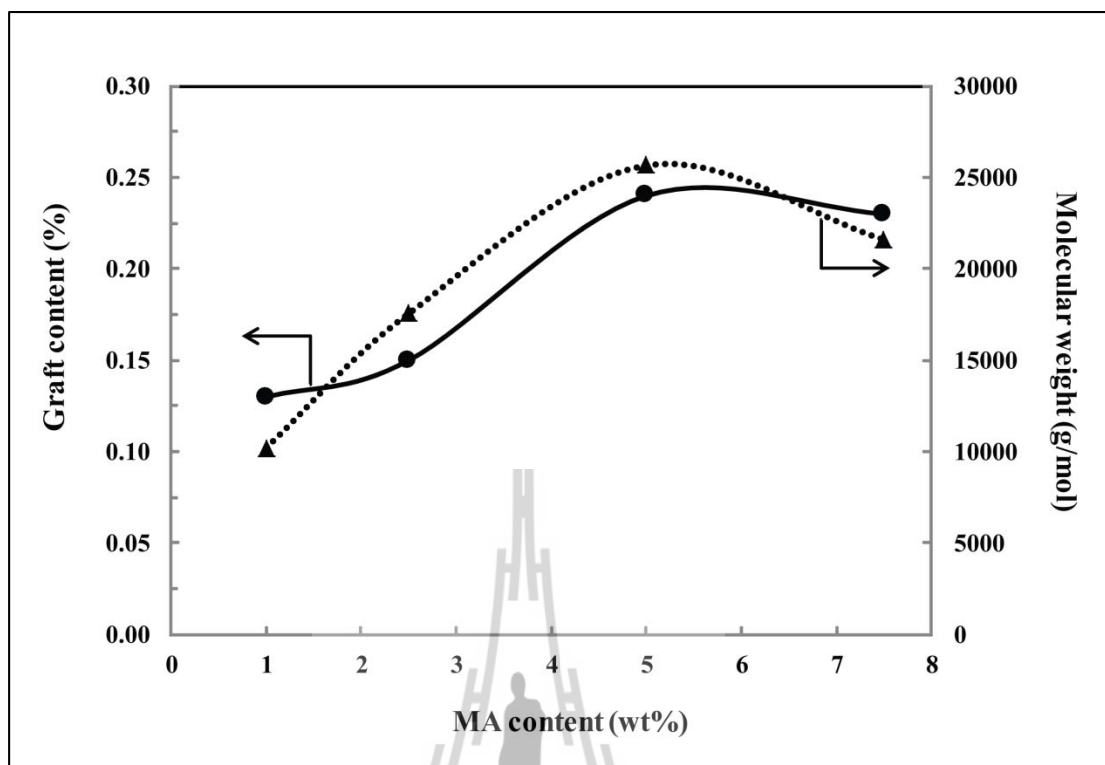


**Figure 4.4** Graft content and the number average molecular weight of PLA-g-MA at various MA contents and a constant Luperox101 content of 0.5 wt%.

#### 4.1.2.2 Effect of initiator content

Initiator is a necessary component for melt free radical grafting process. Amount of the initiator is among the most important parameter in grafting reaction (Li, Zhang, and Zhang, 2003).

The influence of initiator content on the graft content (%G) of PLA-g-MA is shown in Figure 4.5. The data results are summarized in Table 4.2. In the absence of Luperox101, no grafting occurred. From Figure 4.5, the graft content increased when initiator content was increased at a constant MA content of 5.0 wt% due to an enhancement of radical formation in the radical decomposition. As initiator content was increased the probability along with the reaction of MA and PLA

backbone improved leading to an increase in the graft content. The similar result had been reported by Mani, Bhattacharya, and Tang (1999). They investigated the effect of peroxide initiator on the graft content of PBS-g-MA, PBSA-g-MA, and PLA-g-MA. They found that the enhancement of total free radical content and the graft content were manipulated by the initiator content.

From Table 4.2,  $\overline{M}_n$  and  $\overline{M}_w$  of PLA-g-MA insignificantly changed with increasing Luperox101 content due to small difference of peroxide/monomer ratio.

**Table 4.2** Graft content, the number average molecular weight ( $\overline{M}_n$ ), the weight average molecular weight ( $\overline{M}_w$ ), and the molecular weight distribution (MWD) of PLA-g-MA at various Luperox101 contents and a constant MA content of 5.0 wt% in chloroform: methanol (80:20 %v/v) solvent.

Luperox 101 content (wt%)	Graft content (%)	$\overline{M}_n$ (g/mol)	$\overline{M}_w$ (g/mol)	MWD
PLA <sup>a</sup>	-	44581	80847	1.813
PLA <sup>b</sup>	-	24463	53916	1.984
0.10	0.14	23262	49390	2.123
0.25	0.19	24576	50305	2.372
0.50	0.26	25431	55868	2.197
1.00	0.41	27777	57410	2.067

<sup>a</sup> Not internal mixer passed

<sup>b</sup> Internal mixer passed

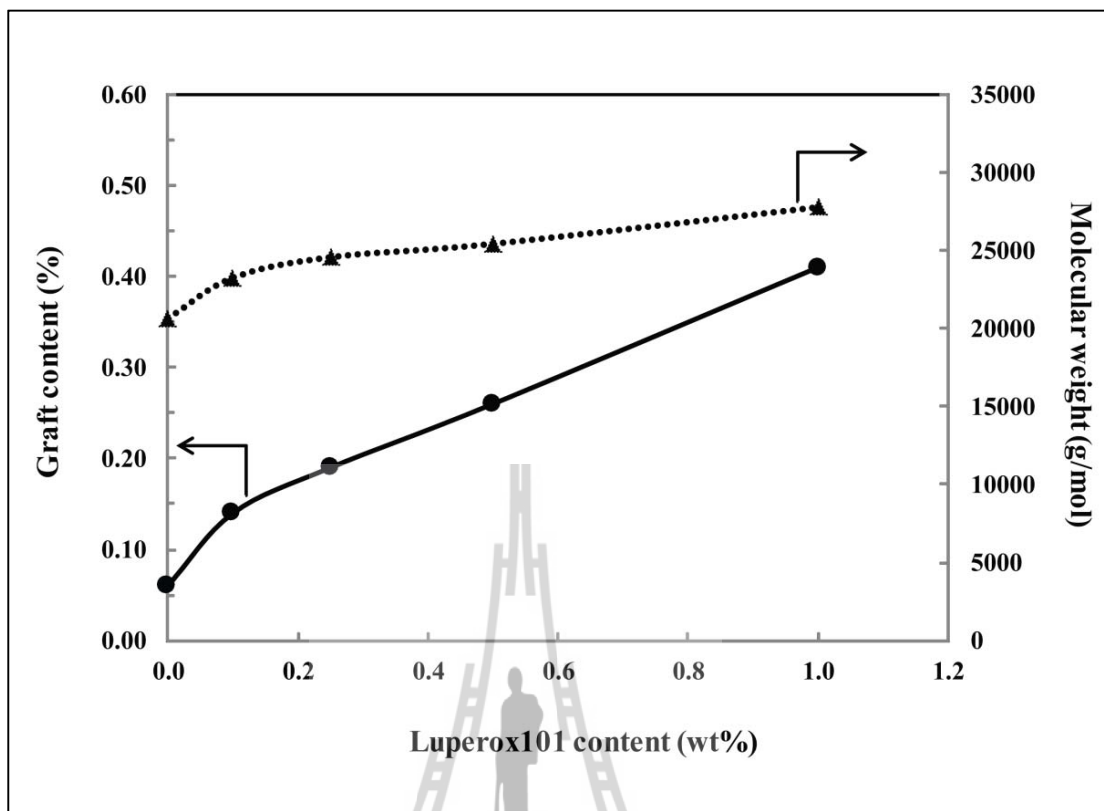


**Figure 4.5** Graft content and the number average molecular weight of PLA-g-MA at various Luperox101 contents and a constant MA content of 5.0 wt%.

The investigation of effects of monomer and initiator content on the graft content can be concluded that the initiator content exhibited more significant effect on the graft content than monomer content. As initiator content was increased the probability along with the reaction between radical from initiator and MA or PLA backbone increased leading to an increase in the graft content. However, the monomer content affected the improvement of graft content and the molecular weight measurement at high peroxide/monomer ratio (low MA content). This was due to the existing high total radical molecules leading to improved MA and radical from

initiator decomposition reaction. The high peroxide/monomer ratio led to an increase in chain scission of PLA.

The highest graft content of PLA-g-MA obtained from 1.0 wt% Luperox101 and 5.0 wt% MA was 0.41%. Therefore, this PLA-g-MA was used as a compatibilizer throughout this study.

## **4.2 The effect of blend composition on properties of PLA/PBAT blends**

### **4.2.1 Mechanical properties**

Mechanical properties of PLA and PLA/PBAT blends at various PBAT contents are listed in Table 4.3.

During tensile testing, it was observed that fracture behavior of the specimen changed from brittle fracture of neat PLA to ductile fracture of PLA/PBAT blends. This was demonstrated in the tensile stress-strain curves as shown in Figure 4.6. Pure PLA fractured in a brittle manner without any necking. On the contrary, PLA/PBAT blends demonstrated necking and cold drawing. As PBAT content increased, stable neck growth through cold drawing was also found. The optical photographs of tensile fracture of PLA and PLA/PBAT blends are shown in Figure 4.7. Tensile strength and Young's modulus of PLA/PBAT blends decreased with increasing PBAT content as shown in Figure 4.8 and Figure 4.9, respectively. However, PLA/PBAT blends showed higher elongation at break than pure PLA as shown in Figure 4.10. Elongation at break of the blends increased with increasing PBAT content. The similar result was observed by Jiang, Wolcott, and Zhang (2006). This was expected since PBAT had lower Young's modulus and tensile strength than PLA resulting in a noticeable improvement of PLA ductility. This was consistent with the tensile strength results.

The correlation between notched impact strength and composition of PLA/PBAT blends are shown in Figure 4.11. The notched impact strength of PLA/PBAT blends increased with increasing PBAT content. This suggested that PBAT may act as sites of local stress concentration and these sites were capable of initiation of craze and shear band. Therefore, the interfacial debonding, the pullout of PBAT, and the yielding information (including cavitation, crazing, and shear band, etc.) were important mechanisms to dissipate the impact energy (Lin, Guo, Chen, Ma, and Wang, 2012). This resulted in improved toughness of the blends. It could be concluded that the addition of PBAT into PLA can remarkably improve the toughness of PLA.

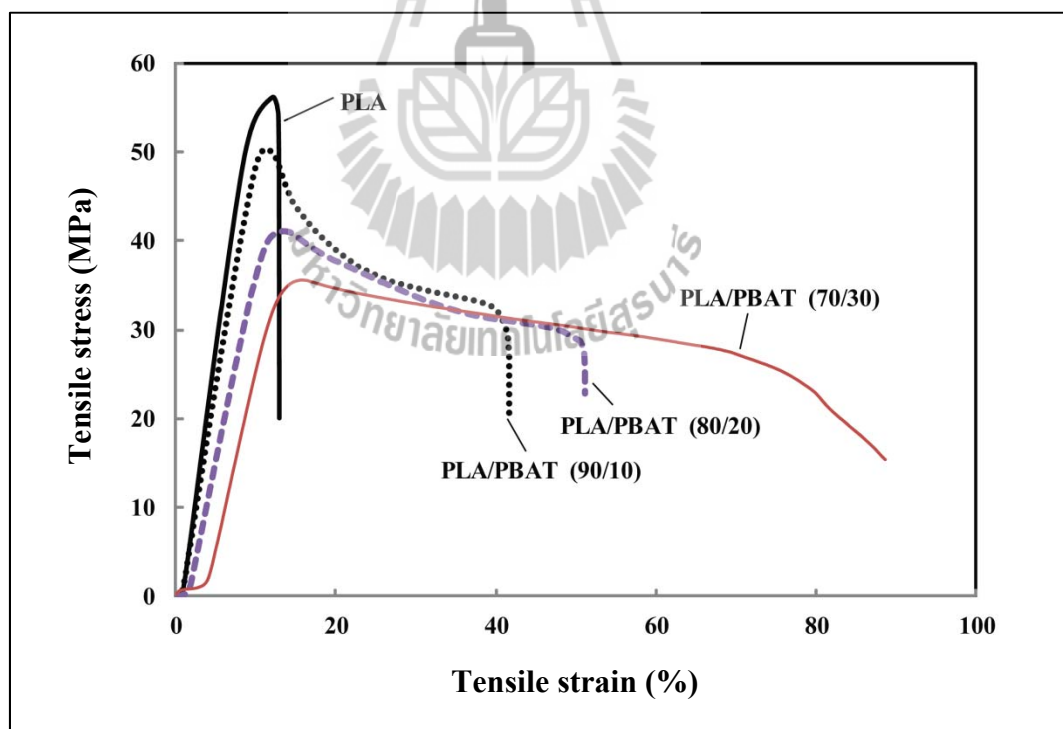


**Figure 4.6** Stress-strain curves of PLA and PLA/PBAT blends at various PBAT contents.



**Figure 4.7** Optical photographs of tensile-fractured samples of (a) PLA, (b) PLA/PBAT 90/10 blend, (c) PLA/PBAT 80/20 blend, and (d) PLA/PBAT 70/30 blend.

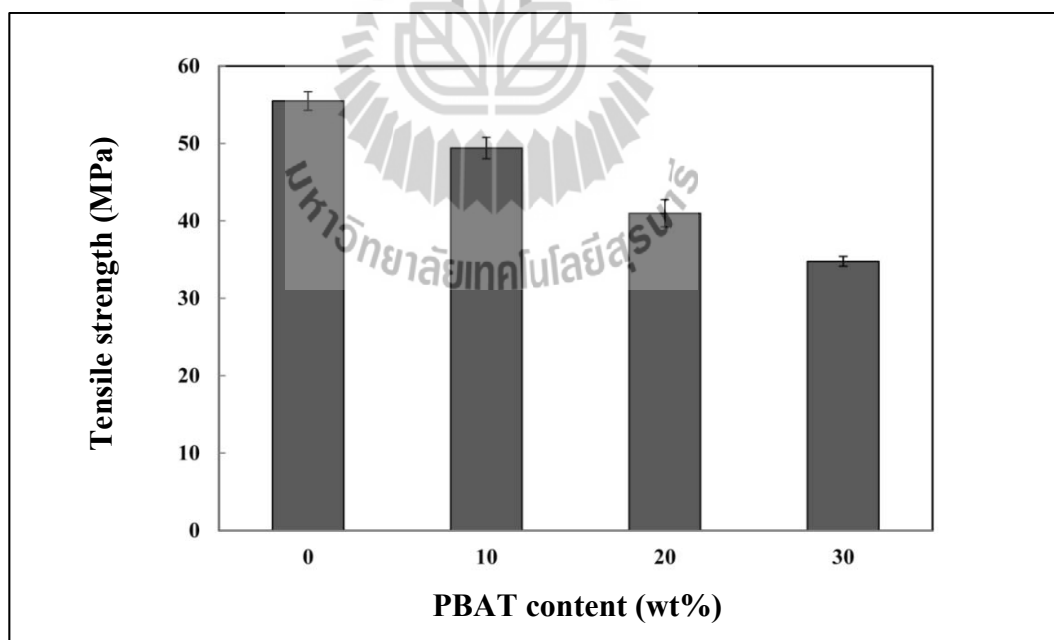


**Figure 4.8** Tensile strength of PLA and PLA/PBAT blends at various PBAT contents.

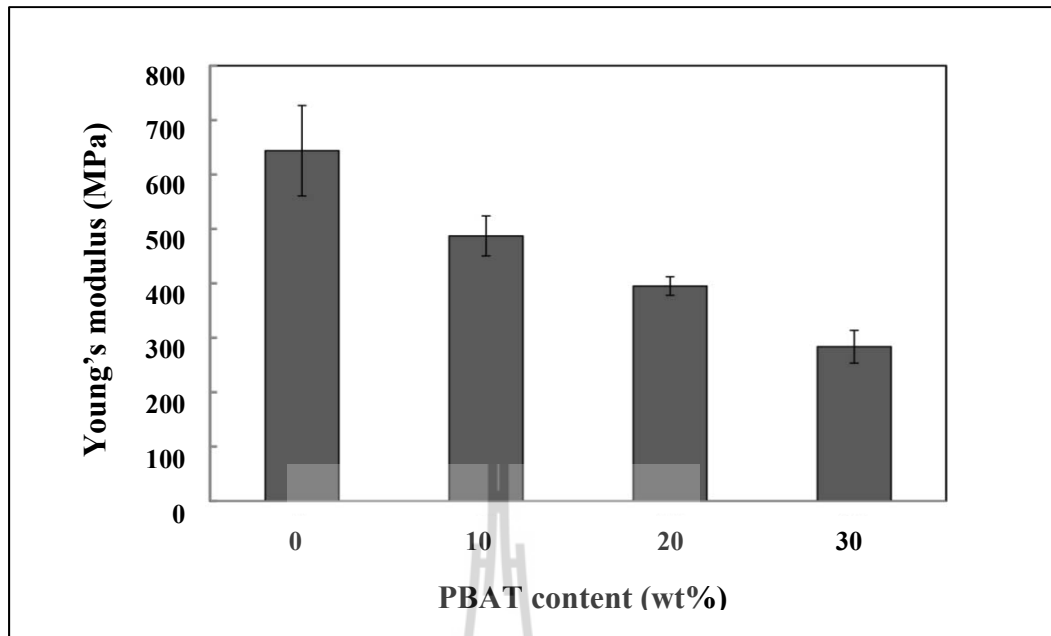


**Figure 4.9** Young's modulus of PLA and PLA/PBAT blends at various PBAT contents.

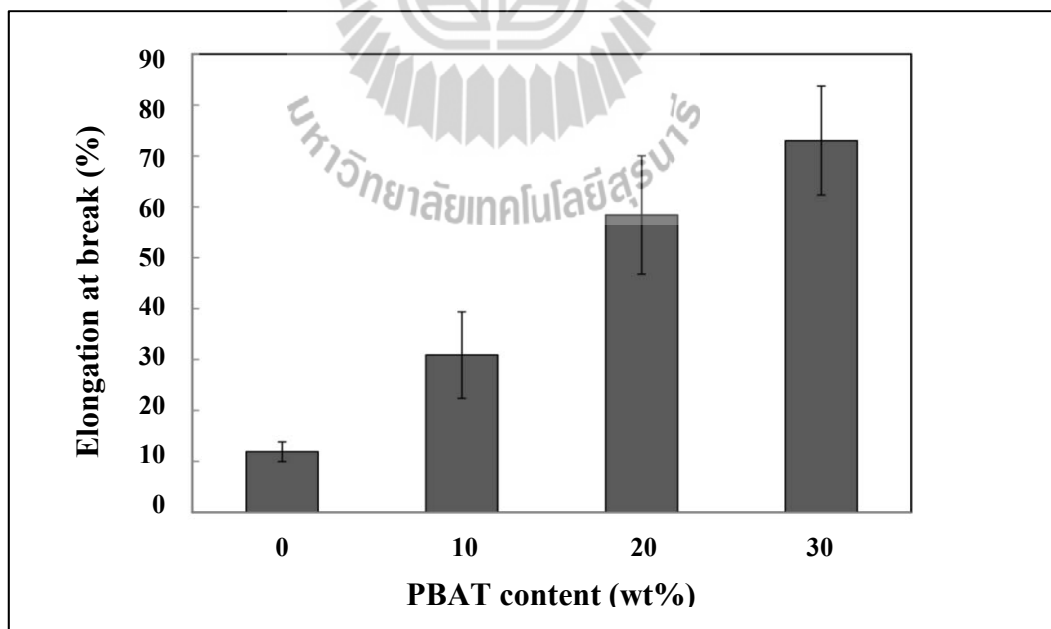


**Figure 4.10** Elongation at break of PLA and PLA/PBAT blends at various PBAT contents.

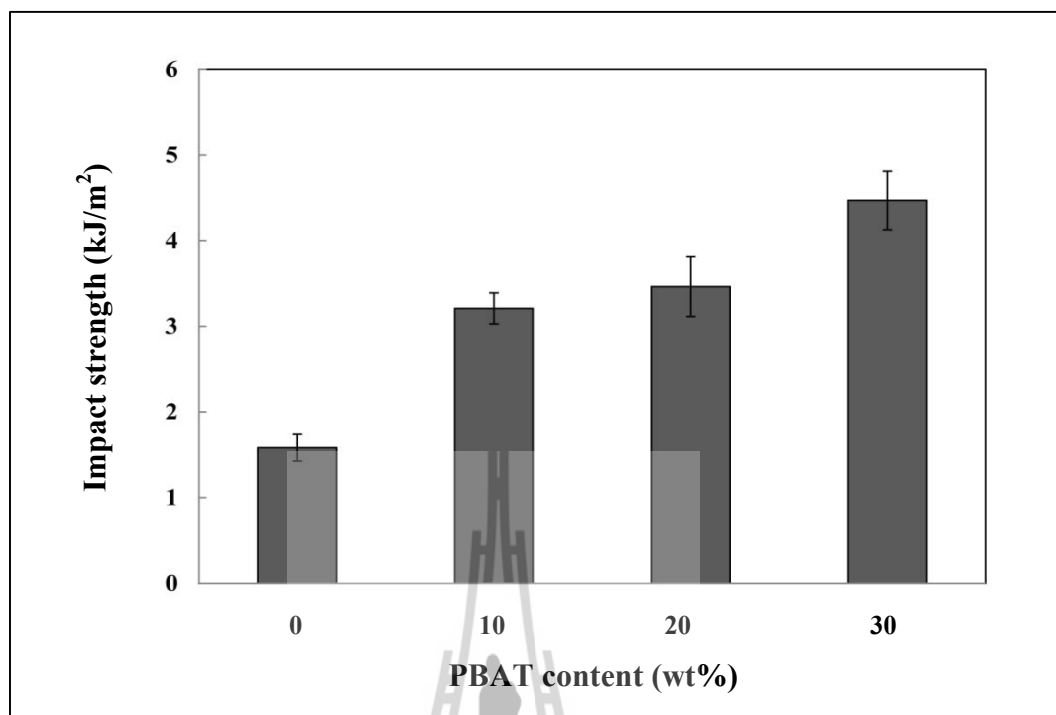


**Figure 4.11** Impact strength of PLA and PLA/PBAT blends at various PBAT contents.

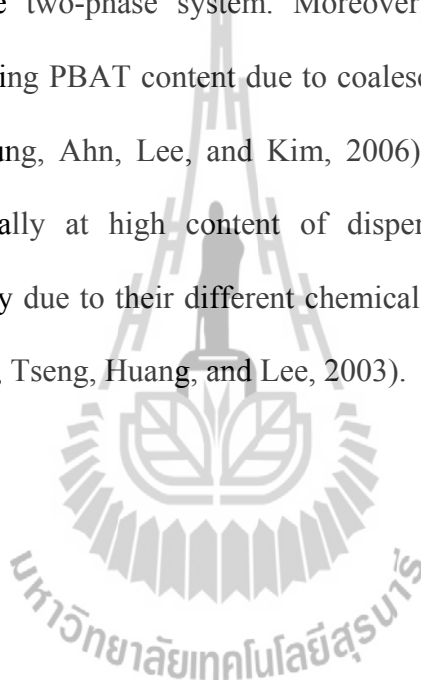
**Table 4.3** Mechanical properties of PLA and PLA/PBAT blends at various PBAT contents.

<b>Composition (wt%)</b>	<b>Tensile strength (MPa)</b>	<b>Young's modulus (MPa)</b>	<b>Elongation at break (%)</b>	<b>Impact strength (kJ/m<sup>2</sup>)</b>
PLA	55.49±1.22	643.95±83.13	11.89±1.92	1.58±0.16
PLA/PBAT 90/10	49.40±1.37	487.10±36.77	44.72±8.51	3.21±0.18
PLA/PBAT 80/20	40.98±1.76	395.13±17.15	58.42±11.62	3.46±0.35
PLA/PBAT 70/30	34.77±0.63	283.66±30.15	73.02±10.72	4.47±0.34



#### 4.2.2 Morphological properties

SEM micrographs of the fractured surface of PLA and PLA/PBAT blends with various PBAT contents are shown in Figure 4.12. From Figure 4.12(a), relatively brittle and smooth fracture surface morphology was found on the fracture surface of PLA. After blending PBAT in PLA, many PBAT droplets were found in the PLA matrix as shown in Figure 4.12(b-d). This result indicated that the blend was a kind of immiscible two-phase system. Moreover, the size of PBAT domain increased with increasing PBAT content due to coalescence of PBAT droplets in the blends (Hong, Namkung, Ahn, Lee, and Kim, 2006). Generally, in an immiscible blend system, especially at high content of dispersed phase, polymers always coagulated individually due to their different chemical structures and high molecular weights (Chen, Chueh, Tseng, Huang, and Lee, 2003).



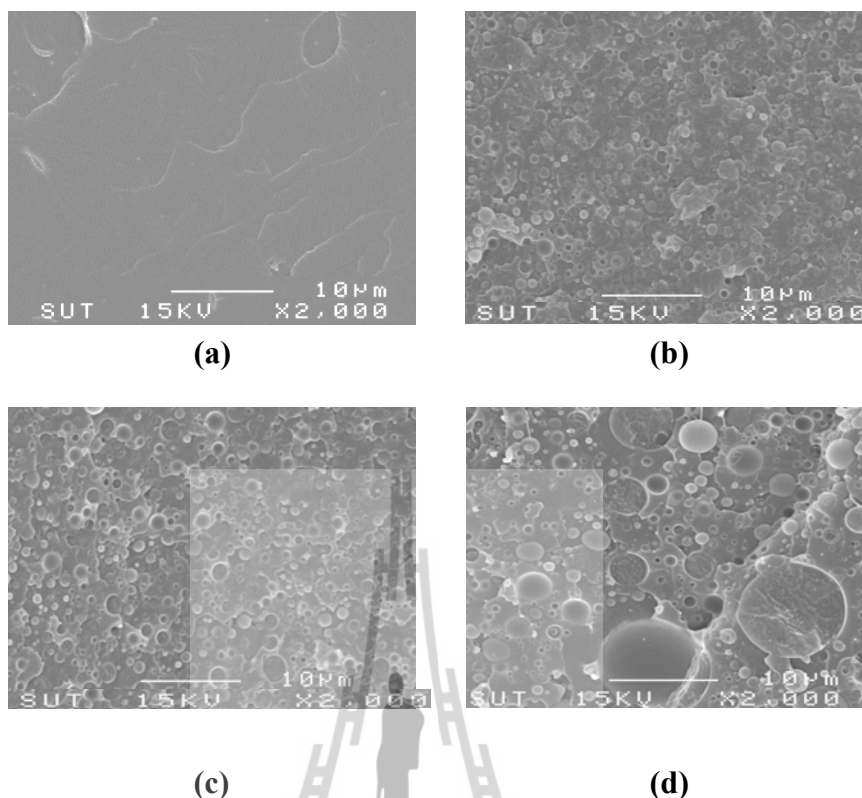


**Figure 4.12** SEM micrographs at 2000x magnification of (a) PLA, (b) PLA/PBAT 90/10 blend, (c) PLA/PBAT 80/20 blend, and (d) PLA/PBAT 70/30 blend.

### 4.2.3 Thermal properties

DSC thermograms of PLA, PBAT, and PLA/PBAT blends are shown in Figure 4.13. The second heating curves of melt-quenched samples were chosen in order to remove previous thermal history and make glass transition ( $T_g$ ) more clear and obvious. The determined data are listed in Table 4.4.  $T_g$ , cold crystallization temperature ( $T_{cc}$ ), and melting temperature ( $T_m$ ) of the blends were observed. Neat PLA showed  $T_g$ ,  $T_{cc}$ ,  $T_{m1}$ , and  $T_{m2}$  at 58.1, 112.2, 148.7, and 155.2°C, respectively. Moreover,  $T_m$  of PLA at 148.67°C ( $T_{m1}$ ) accompanied with a shoulder-melting peak ( $T_{m2}$ ) at 155.17°C was observed. The double melting endotherms of neat PLA

suggested that different size and/or perfection of ordering of PLA were taken place. The peak at low temperature was attributed to re-melting of newly formed crystallite during heating (Sarasua, Prud'homme, Wisniewski, Le Borgne, and Spassky, 1998). PBAT showed  $T_m$  at 119°C. Additionally,  $T_g$  of PLA in PLA/PBAT blends did not change with varying PBAT content. Jiang, Wolcott, and Zhang, (2006) also observed similar result in PLA/PBAT blend indicating the lack of significant molecular interactions between PLA and PBAT. Incorporating PBAT decreased  $T_{cc}$  approximately 5°C indicating an enhancement of crystalline ability of PLA. Yokohara and Yamaguchi (2008) also found similar result in PLA/PBS blends. The addition of PBAT into PLA had no effect on  $T_m$  of PLA. However, heat of crystallization ( $\Delta H_c$ ), heat of fusion ( $\Delta H_m$ ), and degree of crystallinity ( $\chi_c$ ) decreased with incorporating PBAT. It was well known that for polymer containing a semi-crystalline component, the variation in the value of  $\chi_c$  was usually due to the interaction between components (Zhang, Goh, and Lee, 1998). Therefore, the decrease in  $\chi_c$  of PLA/PBAT blend implied that PLA/PBAT blend was partially miscible. The miscibility of PLA/PBAT (90/10) blend was higher than other blend ratios due to the higher decrease in  $\chi_c$ . Liu, Lin, Yang, and Chen, (2005) also found similar result in poly (l-lactide) and poly (tetramethylene adipate-*co*-terephthalate) (PLA/PTAT) blend.

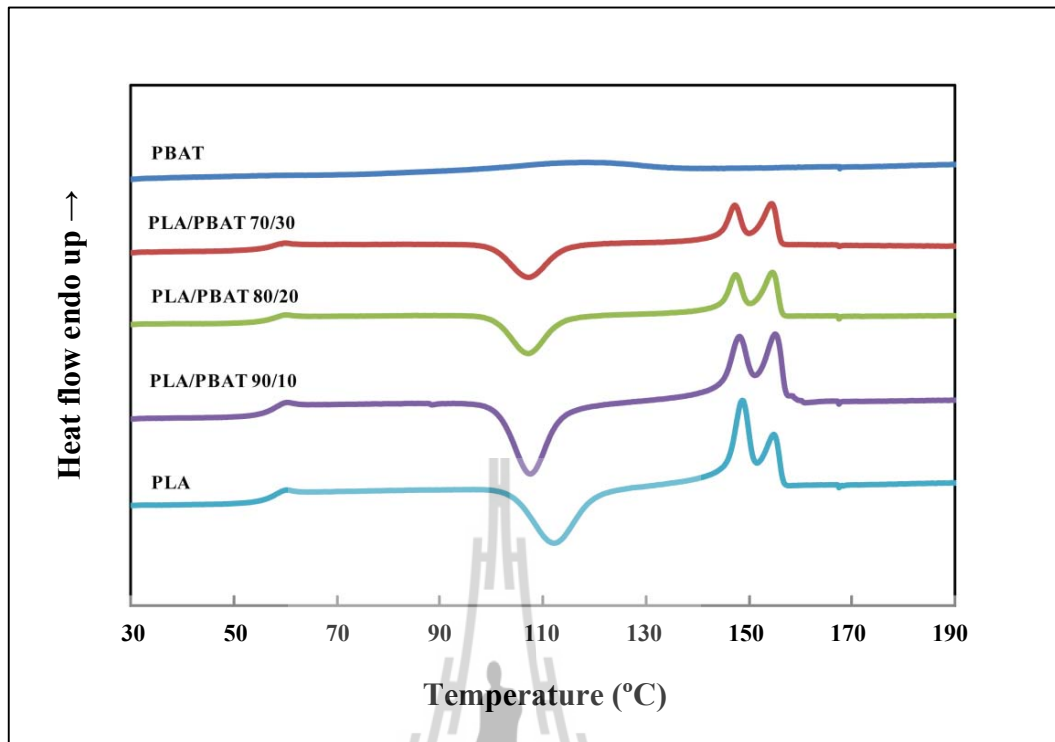


**Figure 4.13** DSC thermograms of PLA, PBAT, and PLA/PBAT blends at various PBAT contents (the second heating, heating rate 5°C/min).

**Table 4.4** Thermal characteristics of PLA and PLA/PBAT blends at various PBAT contents (the second heating, heating rate 5°C/min).

<b>Composition (wt%)</b>	<b>T<sub>g</sub> (°C)</b>	<b>T<sub>cc</sub> (°C)</b>	<b>T<sub>m1</sub> (°C)</b>	<b>T<sub>m2</sub> (°C)</b>	<b>ΔH<sub>c</sub> (J/g)</b>	<b>ΔH<sub>m</sub> (J/g)</b>	<b>χ<sub>c</sub> (%)</b>
PLA	57.63	112.20	148.67	155.17	27.02	24.65	26.33
PLA/PBAT 90/10	57.70	107.61	148.08	154.91	23.32	19.31	22.90
PLA/PBAT 80/20	57.38	107.17	147.34	154.59	17.89	17.91	23.89
PLA/PBAT 70/30	58.12	107.20	147.17	154.41	15.23	16.12	24.58



#### 4.2.4 Rheological properties

Shear viscosity of PLA, PBAT, and their blends at 170°C is shown in Figure 4.14. The shear viscosity of PLA/PBAT blend decreased with an increase in shear rate. The blend showed shear thinning behavior. Similar behavior was observed in biodegradable aliphatic polyester (BDP)/poly (vinyl acetate) (PVAc) blend (Shin, Kim, Choi, and Jhon, 2000) and PLA/PCL blend (Umamaheswara Rao, Suman, Kesava Rao, and Bhanukiran, 2011). At low shear rate, PBAT exhibited higher shear viscosity than PLA. The viscosity of the blends increased with increasing PBAT content. However, at high shear rate, no significant difference in the viscosity of PLA, PBAT, and PLA/PBAT blends was found. Thus, the addition of PBAT insignificantly affected processability of PLA in extrusion.

MFI of PLA, PBAT, and PLA/PBAT blends is shown in Figure 4.15. MFI of PLA and PBAT were 17.70 and 3.44 g/10 min, respectively. PLA/PBAT blends showed lower MFI than PLA. MFI of the blends insignificantly changed with PBAT content.

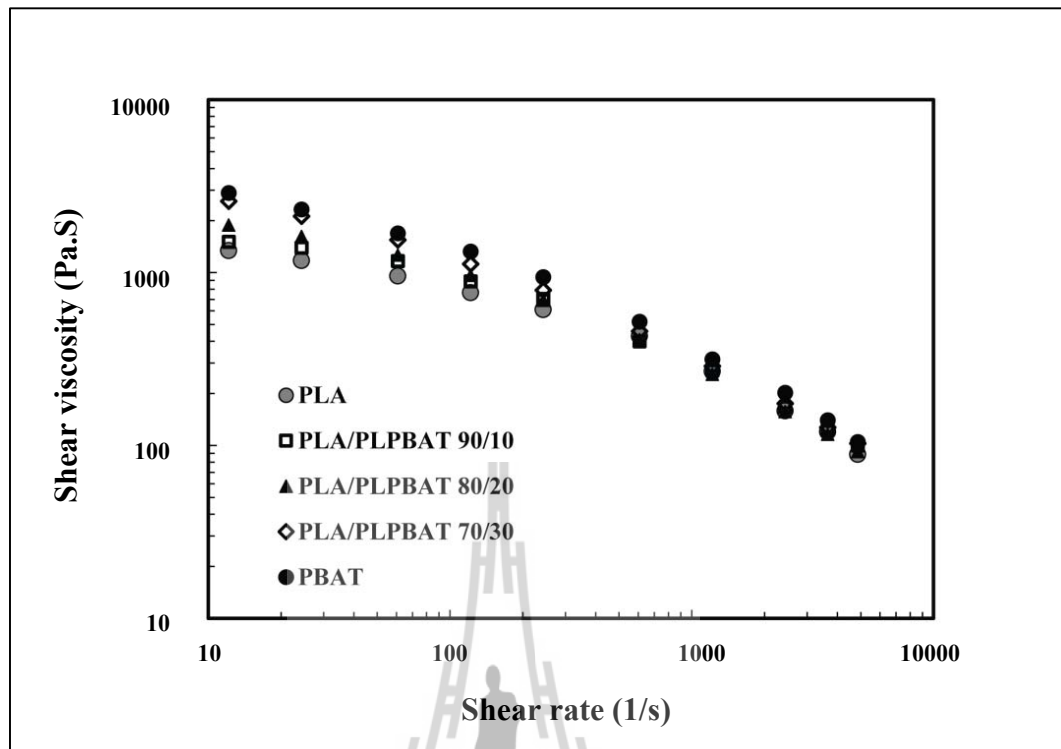


**Figure 4.14** Shear viscosity of PLA, PBAT, and PLA/PBAT blends at various PBAT contents.

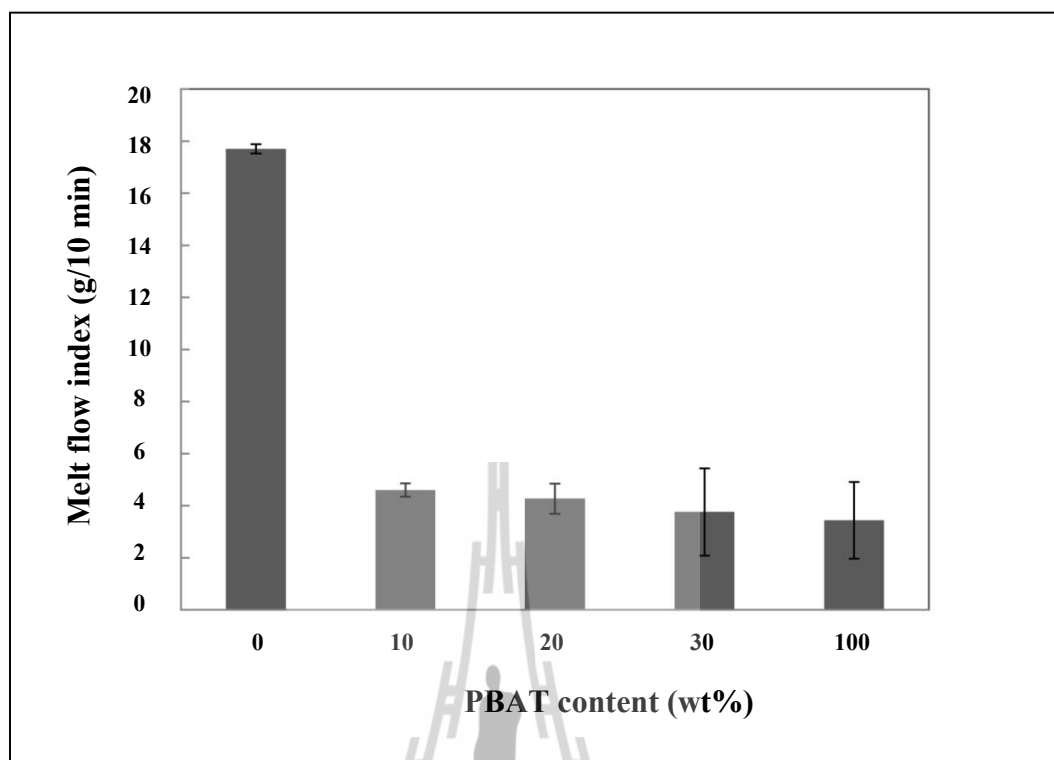


**Figure 4.15** MFI of PLA, PBAT, and PLA/PBAT blends at various PBAT contents.

From mechanical properties of the PLA/PBAT blends, the blend having optimum mechanical properties with low material cost was selected to study effect of compatibilizer content on the properties of PLA/PBAT blends. The costs of PLA and PBAT were 120 and 270 bath/kg, respectively. Moreover, this PLA/PBAT blend was chosen to prepare blown films and its tensile properties were investigated. Therefore, PLA/PBAT 90/10 blend was chosen to further study.

#### **4.3 The effect of compatibilizer content on properties of PLA/PBAT blends**

To study the effect of PLA-g-MA content on mechanical, morphological, thermal, and rheological properties of PLA/PBAT blends, PLA/PBAT 90/10 blend was chosen according to its optimum mechanical properties and low material cost.

### 4.3.1 Mechanical properties

Mechanical properties of uncompatibilized PLA/PBAT blend and compatibilized PLA/PBAT blends at various compatibilizer contents are illustrated in Table 4.5.

Mechanical properties of the blends were related to morphology, domain size, and size homogeneity (Díaz, Barbosa, and Capiati, 2005). The uncompatibilized PLA/PBAT blend exhibited a decrease in tensile strength, Young's modulus, and elongation at break due to weak adhesion at the interface. Adding 2 phr of PLA-g-MA significantly improved the tensile strength of the blend because the intermolecular force between PLA-g-MA and polymer backbone might be formed (Yuan, Liu, and Ren, 2009). The increase in tensile strength (at 2 phr PLA-g-MA) was in agreement with the adhesion improvement shown in the phase morphology of the compatibilized PLA/PBAT blend (Figure 4.20). This indicated that the compatibility between PLA and PBAT was improved when PLA-g-MA was used as a compatibilizer. Nevertheless, tensile strength of the blend slightly decreased with increasing compatibilizer content as showed in Figure 4.16. This may be due to the saturation of the interface (Lomellini, Matos, and Favis, 1996). An excess compatibilizer was difficult to reach the interface and it may trapped in one of the phases (Sailaja, Reddy, and Chanda, 2001). PLA-g-MA exhibited insignificant effect on Young's modulus of the PLA/PBAT blends as shown in Figure 4.17. Elongation at break of the blend slightly increased with the addition of 2 phr of PLA-g-MA. However, when PLA-g-MA content was increased from 4 to 10 phr, elongation at break of the blends was decreased as shown in Figure 4.18.

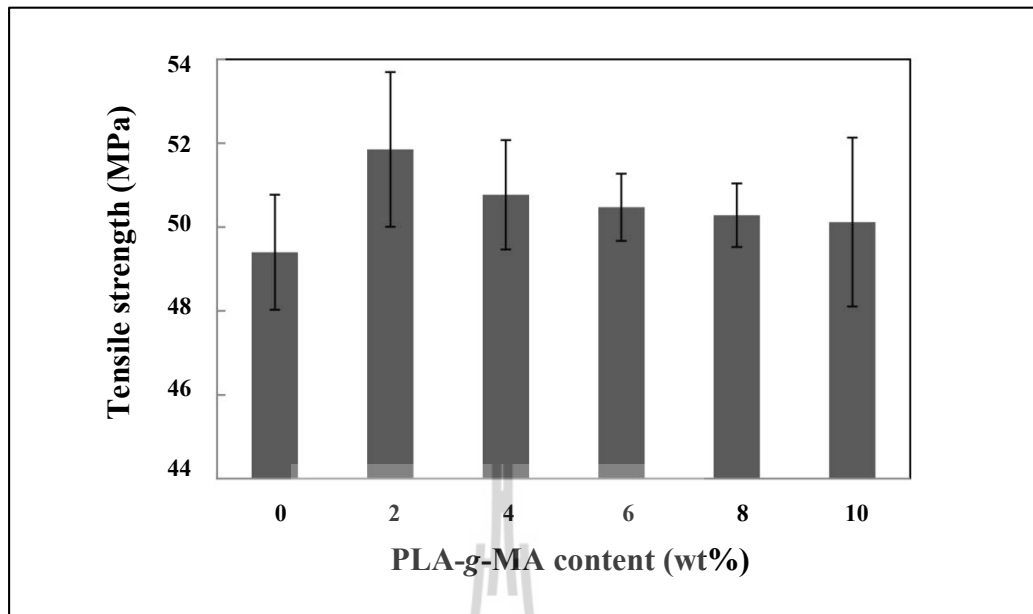


**Figure 4.16** Tensile strength of PLA/PBAT blend and PLA/PBAT/PLA-g-MA blends at various PLA-g-MA contents.

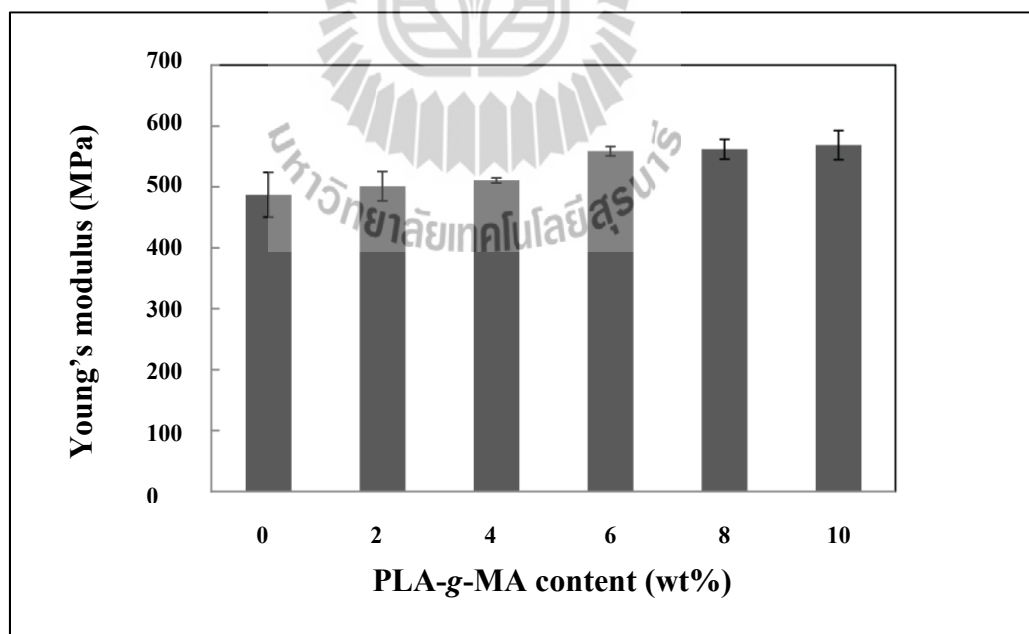


**Figure 4.17** Young's modulus of PLA/PBAT blend and PLA/PBAT/PLA-g-MA blends at various PLA-g-MA contents.

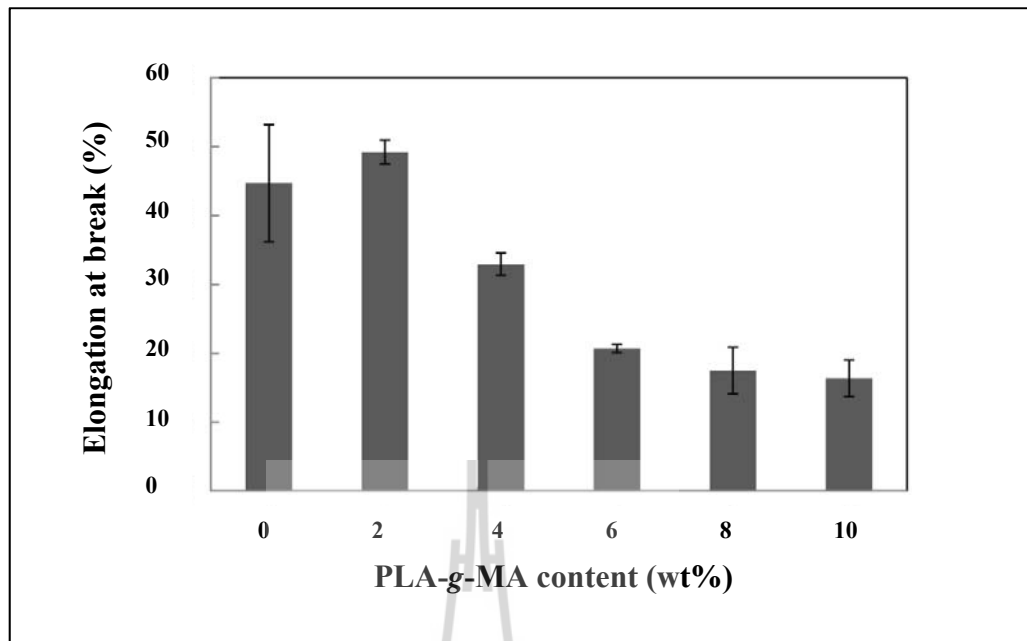


**Figure 4.18** Elongation at break of PLA/PBAT blend and PLA/PBAT/PLA-g-MA blends at various PLA-g-MA contents.

The correlation between notched impact strength of PLA/PBAT blends and PLA-g-MA content is shown in Figure 4.19. With incorporation of PLA-g-MA at 2 phr, the notched impact strength of PLA/PBAT blend increased. It could be implied that the addition of PLA-g-MA into the PLA/PBAT blend can improve the toughness of PLA/PBAT blend. However, when PLA-g-MA content was increased from 4 to 10 phr, the impact strength of the blends was slightly decreased. Similar result was also found by Lin, Guo, Chen, Ma, and Wang (2012) and Zhang, Wang, Ren, and Wang (2009). Zhang et al. (2009) observed that impact strength of PLA/PBAT blends increased with adding 1 wt% T-GMA and then trended to saturate. Lin et al. (2012) reported that impact strength of the PLA/PBAT blend containing 0.2 wt% TBT was

increased by 76% as compared to pure PLA. However, the impact strength of the blends did not change with further increasing TBT loading.

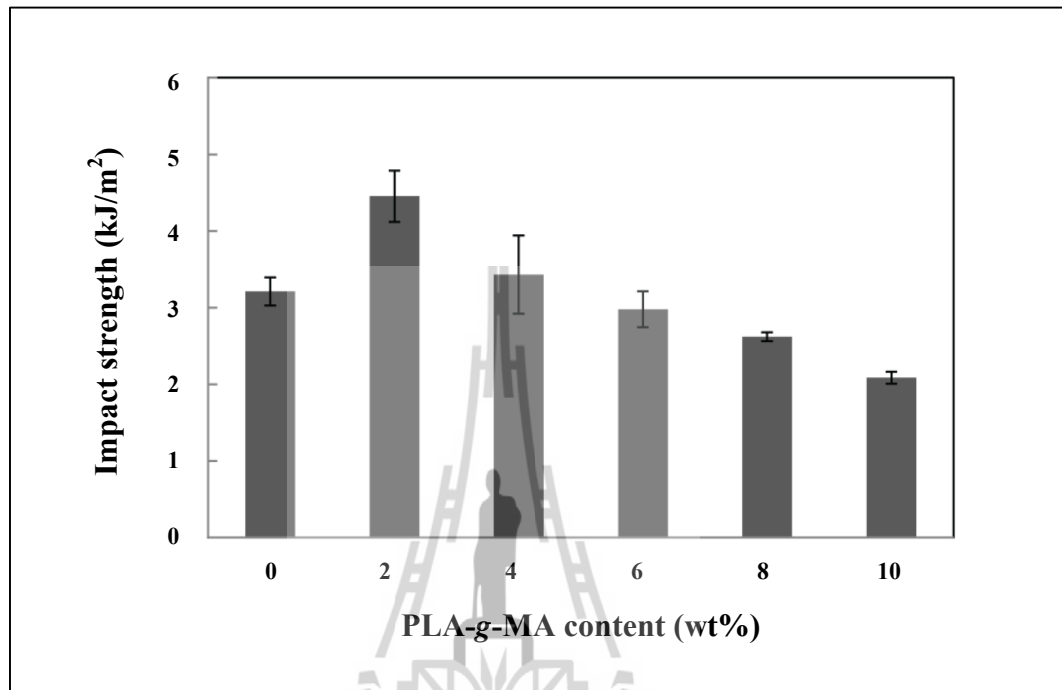


**Figure 4.19** Impact strength of PLA/PBAT blend and PLA/PBAT/PLA-g-MA blends at various PLA-g-MA contents.

**Table 4.5** Mechanical properties of PLA/PBAT blend and compatibilized PLA/PBAT blends at various PLA-g-MA contents.

<b>Composition (wt%)</b>	<b>Tensile strength (MPa)</b>	<b>Young's modulus (MPa)</b>	<b>Elongation at break (%)</b>	<b>Impact strength (kJ/m<sup>2</sup>)</b>
PLA/PBAT 90/10	49.40±1.37	487.10±36.7	44.72±8.51	3.21±0.18
PLA/PBAT/PLA-g-MA 90/10/2phr	51.67±1.85	543.65±24.19	49.25±1.69	4.45±0.33
PLA/PBAT/PLA-g-MA 90/10/4phr	50.77±1.30	550.73±4.37	32.92±1.63	3.43±0.51
PLA/PBAT/PLA-g-MA 90/10/6phr	50.47±0.80	558.72±7.79	20.66±0.58	2.98±0.23
PLA/PBAT/PLA-g-MA 90/10/8phr	50.28±0.76	561.89±16.27	17.48±3.37	2.62±0.06
PLA/PBAT/PLA-g-MA 90/10/10phr	50.12±2.01	568.70±24.09	16.35±2.67	2.09±0.08

### 4.3.2 Morphological properties

Morphologies of the fracture surface of PLA, PLA/PBAT blend, and compatibilized PLA/PBAT blends are shown in Figure 4.20. The uncompatibilized blend showed a coarse morphology with larger domain size in comparison to the compatibilized PLA/PBAT blends. The compatibilizer controlled the morphology of the blends by preventing coalescence and reducing interfacial tension. When 2 phr of PLA-g-MA was added, PBAT particle size decreased. This indicated that the compatibility between PLA and PBAT was improved. However, when PLA-g-MA content was higher than 2 phr, some large domain sizes of the third phase could be found in the PLA/PBAT blend. This phenomenon may be due to segregation and formation of unreacted PLA-g-MA as the third phase in the PLA/PBAT blend as shown in Figure 4.20(d-g). This morphology led to poor mechanical properties. A similar behavior was reported by Juntuek, Ruksakulpiwat, Chumsamrong, and Ruksakulpiwat (2011).

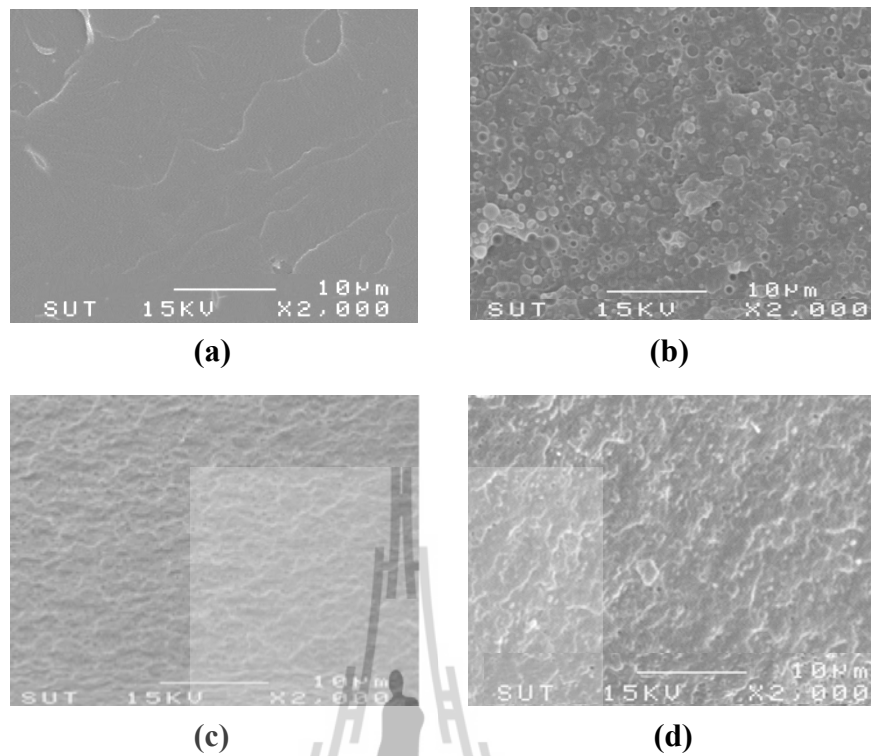


**Figure 4.20** SEM micrographs at 2000x magnification of (a) PLA, (b) PLA/PBAT 90/10 blend, (c) PLA/PBAT/PLA-g-MA 90/10/2 phr blend, (d) PLA/PBAT/PLA-g-MA 90/10/4 phr blend, (e) PLA/PBAT/PLA-g-MA 90/10/6 phr blend, (f) PLA/PBAT/PLA-g-MA 90/10/8 phr blend, and (g) PLA/PBAT/PLA-g-MA 90/10/10 phr blend.

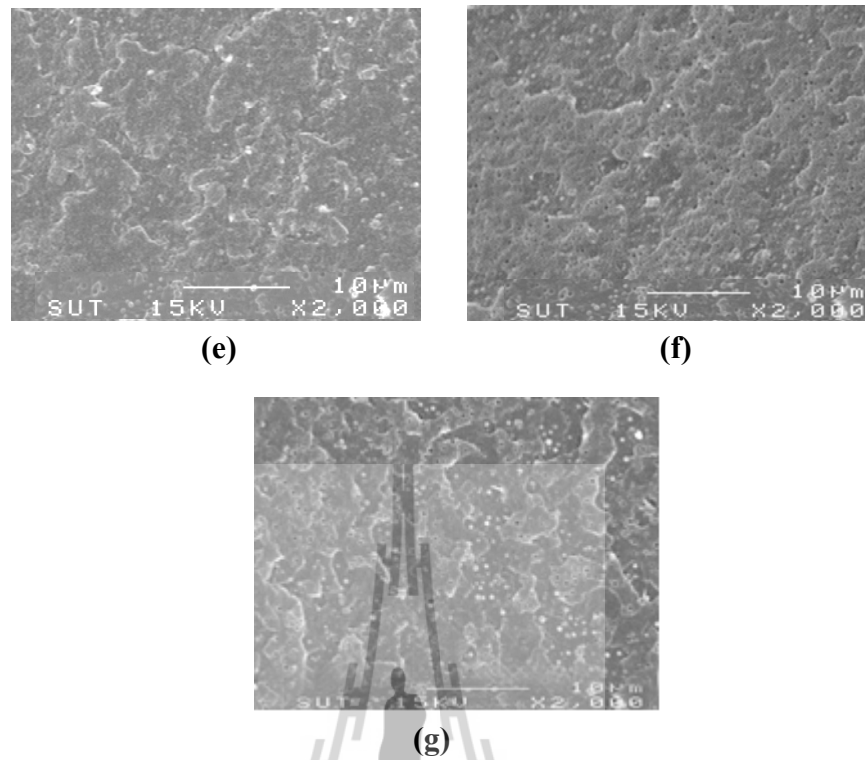


**Figure 4.20** SEM micrographs at 2000x magnification of (a) PLA, (b) PLA/PBAT 90/10 blend, (c) PLA/PBAT/PLA-g-MA 90/10/2 phr blend, (d) PLA/PBAT/PLA-g-MA 90/10/4 phr blend, (e) PLA/PBAT/PLA-g-MA 90/10/6 phr blend, (f) PLA/PBAT/PLA-g-MA 90/10/8 phr blend, and (g) PLA/PBAT/PLA-g-MA 90/10/10 phr blend. (continued)

### 4.3.3 Thermal properties

DSC curves of PLA, PLA/PBAT blend, and compatibilized PLA/PBAT blends with different PLA-g-MA contents are shown in Figure 4.21. The determined data of thermal characteristics of PLA/PBAT blend and compatibilized PLA/PBAT blends are illustrated in Table 4.6. PLA/PBAT blend showed  $T_g$ ,  $T_{cc}$ , and  $T_m$  at 57.7, 107.6, and 154.91°C, respectively. Additionally, PLA-g-MA exhibited insignificant effect on  $T_g$  of PLA in PLA/PBAT blends. Zhang and He (2002) also found the similar result in compatibilized polysulfone (PSF)/thermotropic liquid crystalline polymer (TLCP) blend. They suggested that the addition of PSF-g-MA improved compatibility of PSF/TLCP blend by enhanced interfacial adhesion. This often insignificantly affected on  $T_g$  of the blend component, thus did not affect properties of bulk polymer components. Although the size of dispersed phase was significantly reduced  $T_{cc}$  of the compatibilized blends at 2 and 4 phr of PLA-g-MA insignificantly changed when compared with the uncompatibilized PLA/PBAT blend. Further increasing PLA-g-MA content,  $T_{cc}$  was shifted to lower value. This suggested that adding PLA-g-MA had an influence on crystallizability of PLA/PBAT blend. When PLA-g-MA content increased,  $T_{cc}$  of the blend was reduced. However, the addition of PLA-g-MA to the blends did not significantly affect  $T_m$  of PLA component. With increasing PLA-g-MA content,  $\Delta H_c$ ,  $\Delta H_m$ , and  $\chi_c$  of the compatibilized blend insignificantly changed.

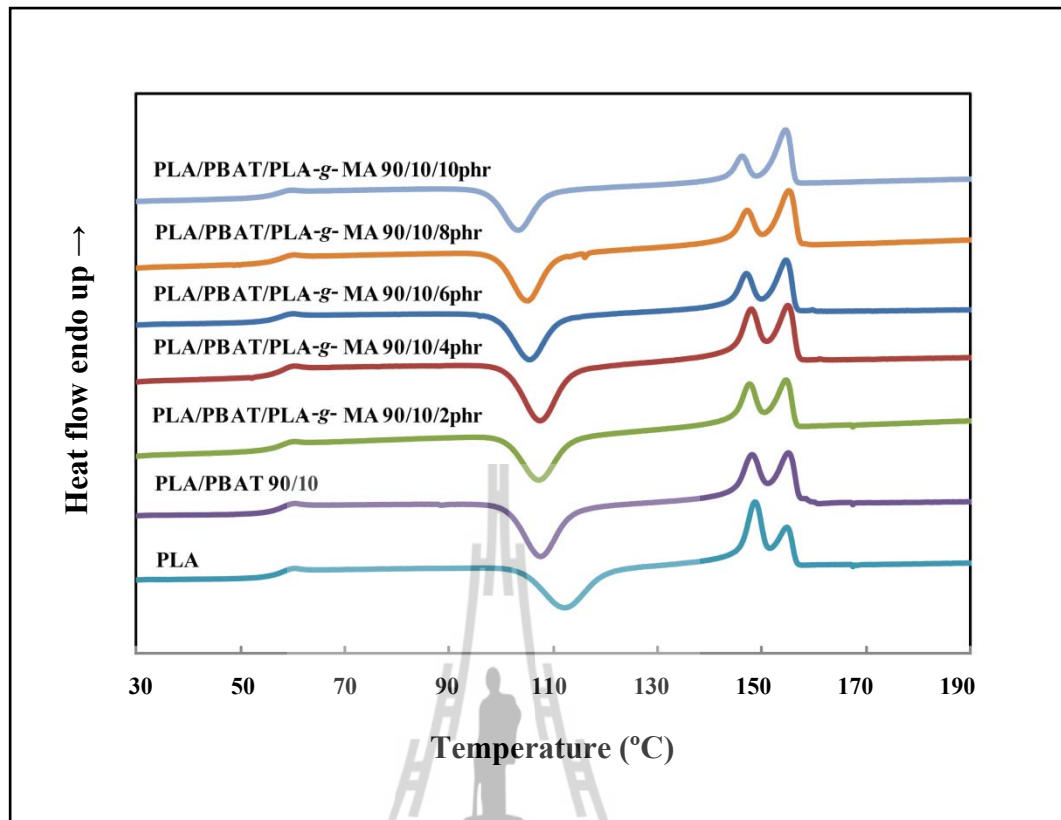
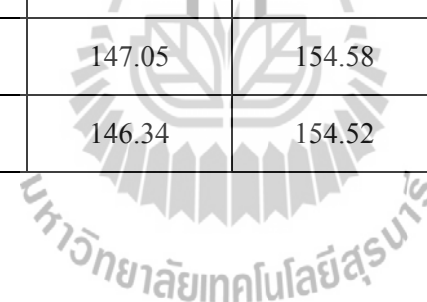


**Figure 4.21** DSC thermograms of PLA, PLA/PBAT blend, and PLA/PBAT/PLA-g-MA blends at various PLA-g-MA contents (the second heating, heating rate 5°C/min).

**Table 4.6** Thermal characteristics of PLA/PBAT blend and compatibilized PLA/PBAT blends at various PLA-g-MA contents.

<b>Composition (wt%)</b>	<b>T<sub>g</sub> (°C)</b>	<b>T<sub>cc</sub> (°C)</b>	<b>T<sub>m1</sub> (°C)</b>	<b>T<sub>m2</sub> (°C)</b>	<b>ΔH<sub>c</sub> (J/g)</b>	<b>ΔH<sub>m</sub> (J/g)</b>	<b>χ<sub>c</sub> (%)</b>
PLA/PBAT 90/10	57.70	107.61	148.08	154.91	23.32	19.31	22.90
PLA/PBAT/PLA-g-MA 90/10/2phr	57.44	107.19	147.58	154.75	23.22	19.05	23.07
PLA/PBAT/PLA-g-MA 90/10/4phr	57.42	107.39	147.58	154.94	22.60	20.88	25.78
PLA/PBAT/PLA-g-MA 90/10/6phr	56.73	105.36	147.24	154.60	22.10	20.76	26.12
PLA/PBAT/PLA-g-MA 90/10/8phr	57.26	105.60	147.05	154.58	21.83	20.55	26.35
PLA/PBAT/PLA-g-MA 90/10/10phr	56.75	103.20	146.34	154.52	21.53	20.21	26.39



TGA and DTG curves of PLA, PBAT, PLA/PBAT blend, and compatibilized PLA/PBAT blend at 2 phr of PLA-g-MA are shown in Figure 4.22 and 4.23, respectively. It was evident that the thermal degradation of PLA and PBAT showed only single step of weight loss. Thermal degradation at 5 % weight loss ( $T_5$ ), thermal degradation at 50% weight loss ( $T_{50}$ ), and final degradation ( $T_f$ ) of PLA, PBAT, PLA/PBAT blend and compatibilized PLA/PBAT blend are listed in Table 4.7.  $T_5$ ,  $T_{50}$ , and  $T_f$  of neat PLA were at 333.70°C, 362.01°C, and 387.96°C, respectively.  $T_5$ ,  $T_{50}$ , and  $T_f$  of neat PBAT were at 362.79°C, 403.22°C, and 444.14°C, respectively. PBAT displayed higher  $T_5$ ,  $T_{50}$ , and  $T_f$  than PLA. This indicated PBAT had better thermal stability than PLA. The addition of PBAT into PLA increased  $T_f$  of PLA indicating the improvement of thermal stability of PLA. DTG curve of the blend showed two peaks with incorporating PLA-g-MA. Furthermore, the compatibilized PLA/PBAT blend showed higher  $T_5$ ,  $T_{50}$ , and  $T_f$  than PLA/PBAT blend due to enhanced interaction between PLA and PBAT. This suggested that thermal stability of the blend was enhanced with addition of PLA-g-MA. PLA, PLA/PBAT blend, and compatibilized PLA/PBAT blend left no char residue at 600°C.

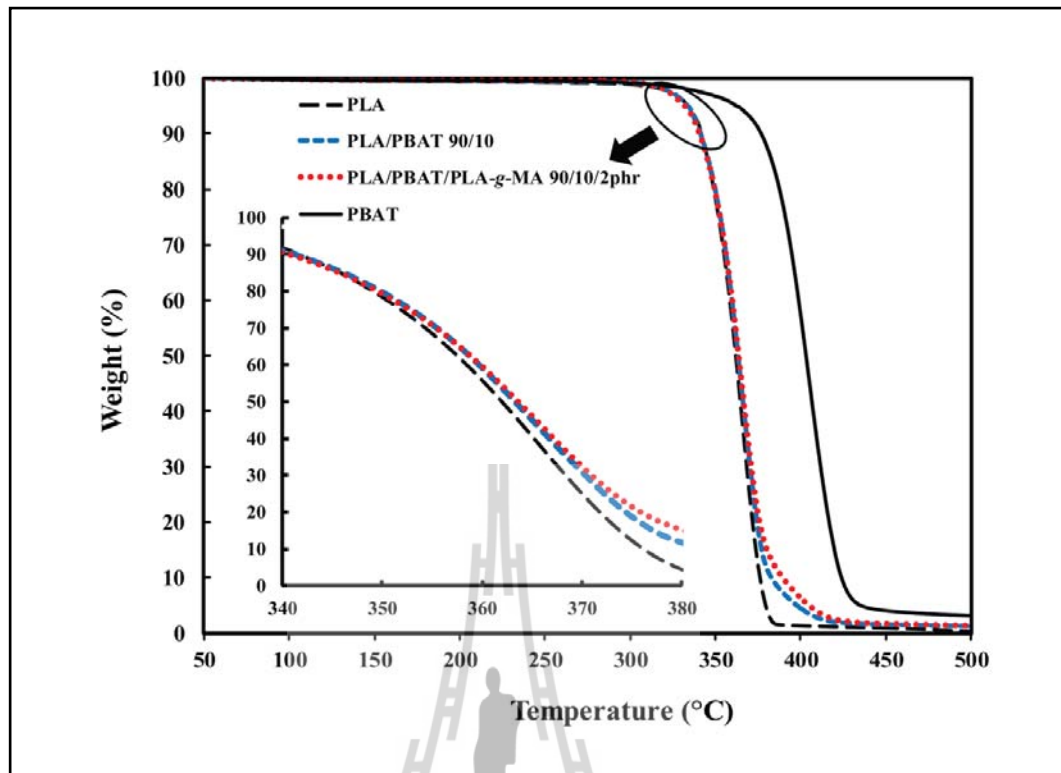


**Figure 4.22** TGA thermograms of PLA, PBAT, PLA/PBAT 90/10 blend, and PLA/PBAT/PLA-g-MA 90/10/2 phr blend.

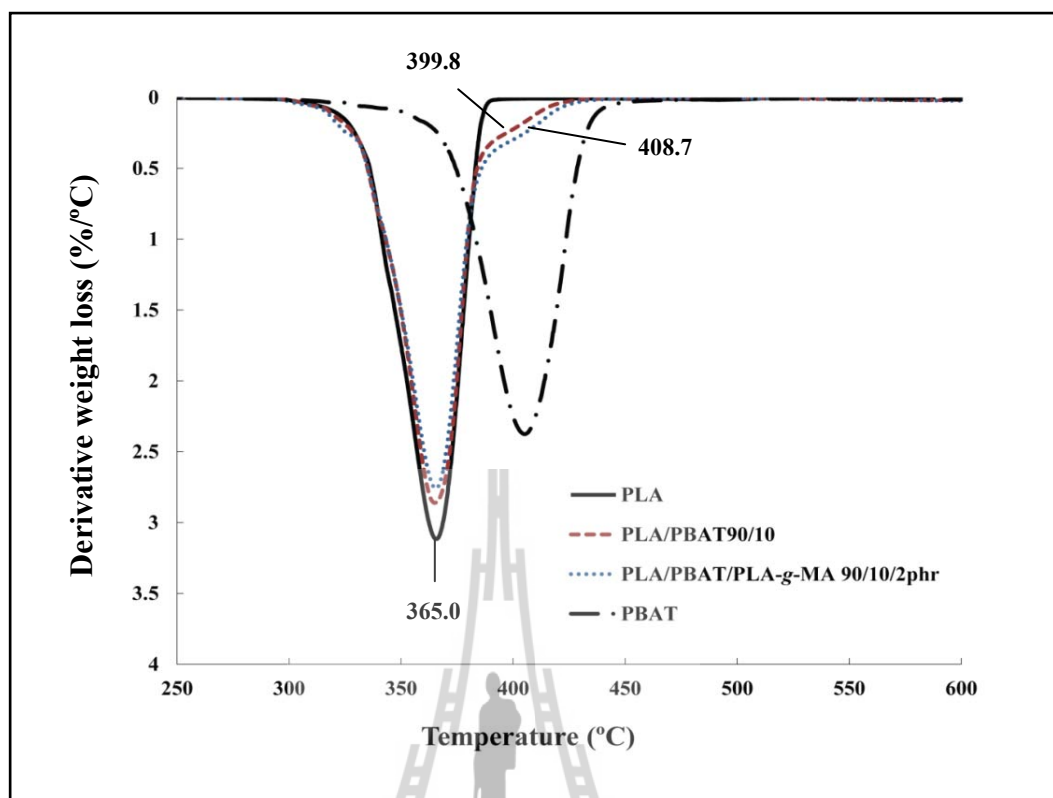


**Figure 4.23** DTG thermograms of PLA, PBAT, PLA/PBAT 90/10 blend and PLA/PBAT/PLA-g-MA 90/10/2 phr blend.

**Table 4.7** Thermal degradation temperature and % char of PLA, PBAT, and PLA/PBAT blends.

Composition (wt%)	T <sub>5</sub> (°C)	T <sub>50</sub> (°C)	T <sub>f</sub> (°C)	Char residual (%)
PLA	333.70	362.01	387.96	-
PBAT	362.39	403.22	444.14	2.2
PLA/PBAT 90/10	333.71	363.30	428.80	-
PLA/PBAT/PLA-g-MA 90/10/2phr	340.76	363.72	434.96	-

#### 4.3.4 Rheological properties

Shear viscosity of PLA, PLA/PBAT blend, and compatibilized PLA/PBAT blends are shown in Figure 4.24. The shear viscosity of the PLA/PBAT blends decreased with increasing shear rate. At low shear rate, the viscosity of the blends with PLA-g-MA content of 2 and 4 phr appeared to be relatively greater than that of the uncompatibilized blend while at high shear rate the viscosity seemed to be unaffected by compatibilization. The increase in viscosity at low shear rate was probably due to a compatibilizing effect of PLA-g-MA. However, further increasing the amount of PLA-g-MA (6 to 10 phr) resulted in a decrease in the viscosity of the blends. This phenomenon was more pronounced at low shear rate. When PLA-g-MA content was above 4 phr, the interface of polymer matrices was already saturated with PLA-g-MA and no further increase in viscosity was observed. At high content of PLA-g-MA, PLA-g-MA formed the third phase in PLA/PBAT blend resulting in a decrease in the blend viscosity due to its low molecular weight. The similar result was reported by Macaúbas and Demarquette (2001). They found that adding SBS and SEBS as compatibilizers at high content (above 10 wt%) led to a decrease in the viscosity of PP/PS blend due to the segregation of SBS or SEBS in the third phase. This behavior could explain the decrease in the viscosity of the blend.

Melt flow index (MFI) of PLA, PLA/PBAT blend, and compatibilized PLA/PBAT blends are shown in Figure 4.25. MFI of PLA/PBAT blends increased with increasing compatibilizer content. This result indicated that the viscosity of the blends decreased with increasing quantity of the compatibilizer.

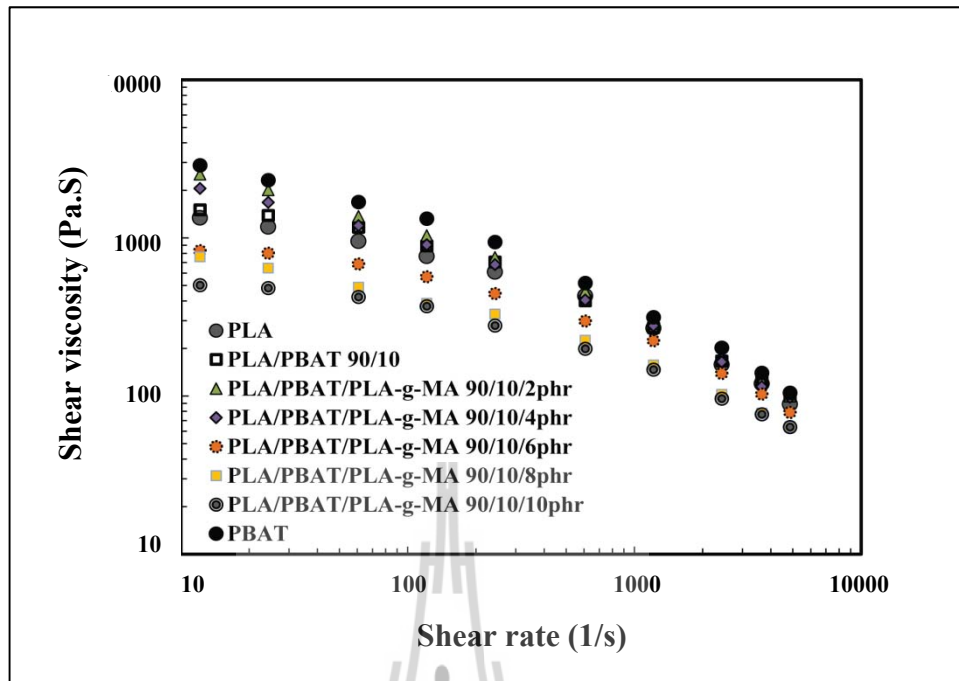


**Figure 4.24** Shear viscosity of PLA, PBAT, PLA/PBAT blend, and PLA/PBAT/PLA-g-MA blends at various PLA-g-MA contents.

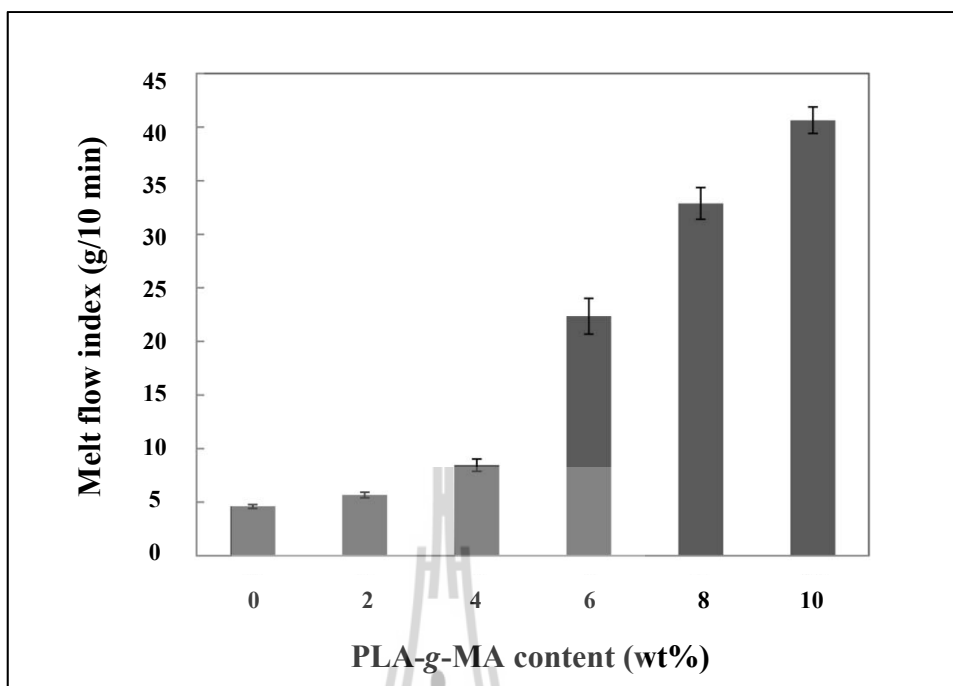


**Figure 4.25** MFI of PLA/PBAT blend and PLA/PBAT/PLA-g-MA blends at various PLA-g-MA contents.

From mechanical properties results, the compatibilized PLA/PBAT blend containing 2 phr of PLA-g-MA was selected to study effect of  $\text{CaCO}_3$  content on the properties of PLA/PBAT/ $\text{CaCO}_3$  composites. Furthermore, the compatibilized PLA/PBAT blend with 2 phr of PLA-g-MA was chosen to prepare blown films and its tensile properties were evaluated.

#### **4.4 The effect of $\text{CaCO}_3$ content on properties of compatibilized PLA/PBAT blend**

##### **4.4.1 Mechanical properties**

Mechanical properties of compatibilized PLA/PBAT blend and PLA/PBAT/ $\text{CaCO}_3$  composites at various  $\text{CaCO}_3$  contents are listed in Table 4.8. The

PLA/PBAT/CaCO<sub>3</sub> composites showed lower tensile strength, elongation at break, and impact strength than the compatibilized PLA/PBAT blend. Tensile strength of the composite decreased with increasing CaCO<sub>3</sub> content as shown in Figure 4.26. The reduction of tensile strength might be attributed to the agglomeration of CaCO<sub>3</sub>, especially at high CaCO<sub>3</sub> content. These results were corresponding to SEM observation. The agglomeration of CaCO<sub>3</sub> caused high stress concentration and led to large voids during tension process. Moreover, this large void could develop into cracks resulting in significant reduction in the tensile strength of the composite (Jiang, Liu, and Zhang, 2009). Young's modulus of the composites insignificantly changed with increasing CaCO<sub>3</sub> content (Figure 4.27). However, elongation at break decreased with increasing CaCO<sub>3</sub> content as expected (Figure 4.28) due to adding rigid phase in PLA/PBAT blend resulting in a reduction of the blend ductility. When 5 %wt CaCO<sub>3</sub> was added, impact strength of the composite decreased. However, further increasing CaCO<sub>3</sub> content, the impact strength slightly increased as shown in Figure 4.29.

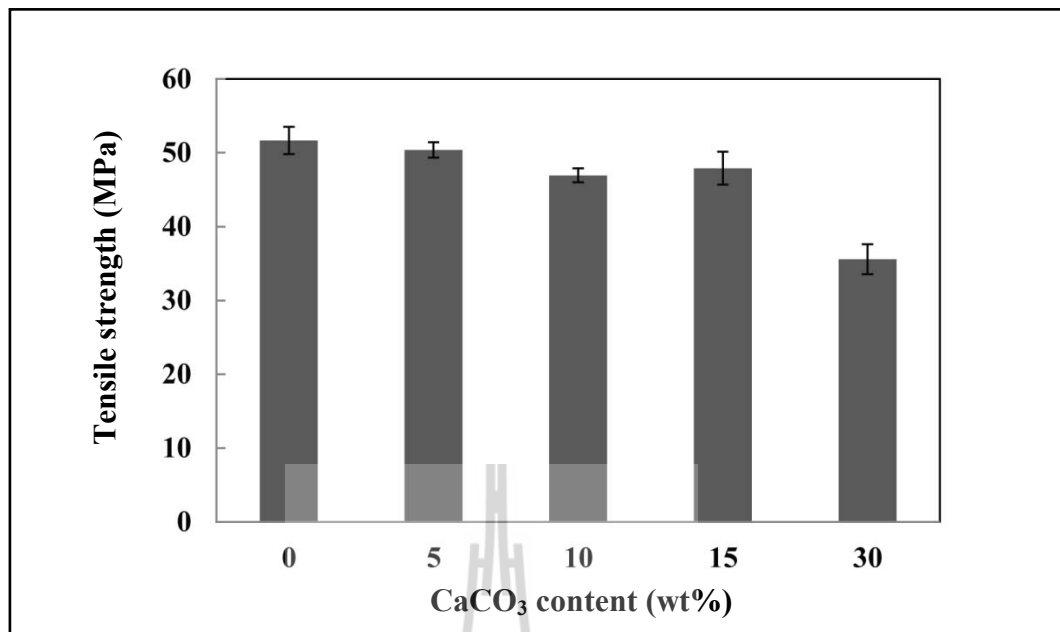


**Figure 4.26** Tensile strength of compatibilized PLA/PBAT blend and PLA/PBAT/CaCO<sub>3</sub> composites at various CaCO<sub>3</sub> contents.

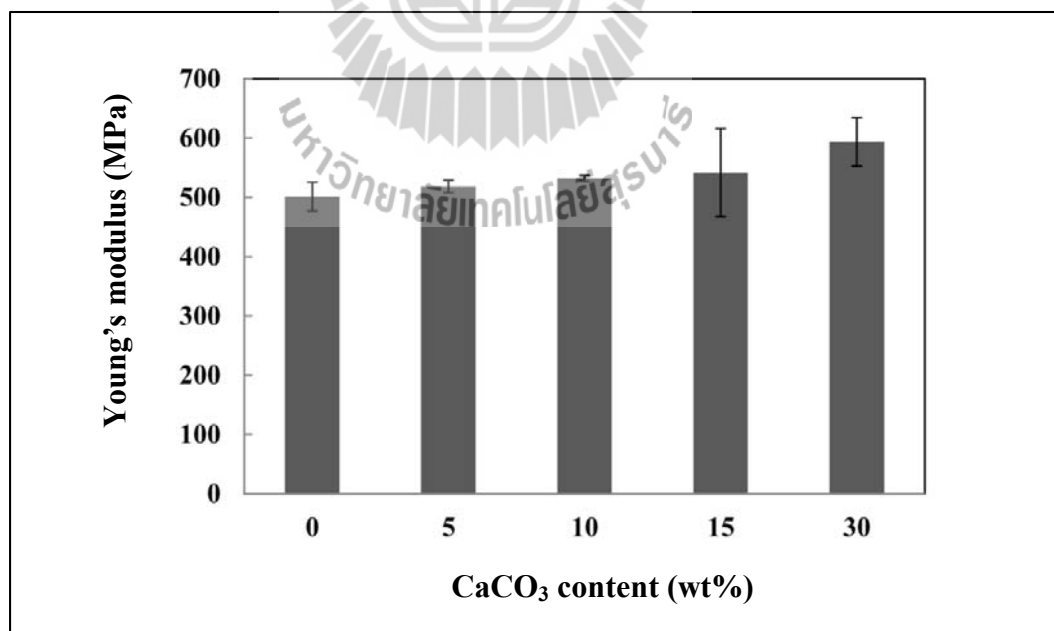


**Figure 4.27** Young's modulus of compatibilized PLA/PBAT blend and PLA/PBAT/CaCO<sub>3</sub> composites at various CaCO<sub>3</sub> contents.

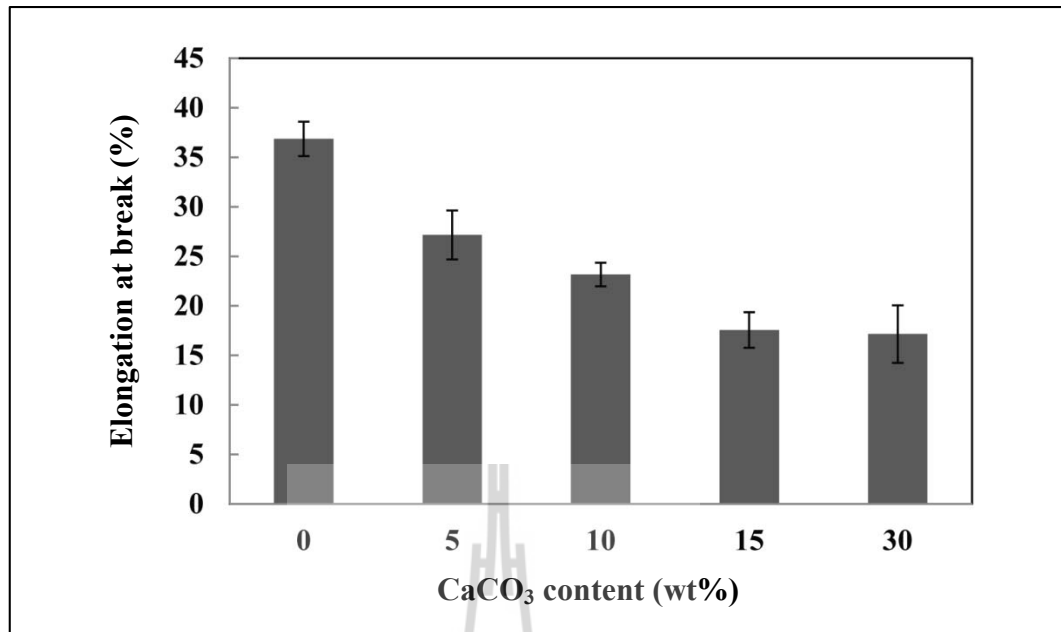


**Figure 4.28** Elongation at break of compatibilized PLA/PBAT blend and PLA/PBAT/CaCO<sub>3</sub> composites at various CaCO<sub>3</sub> contents.

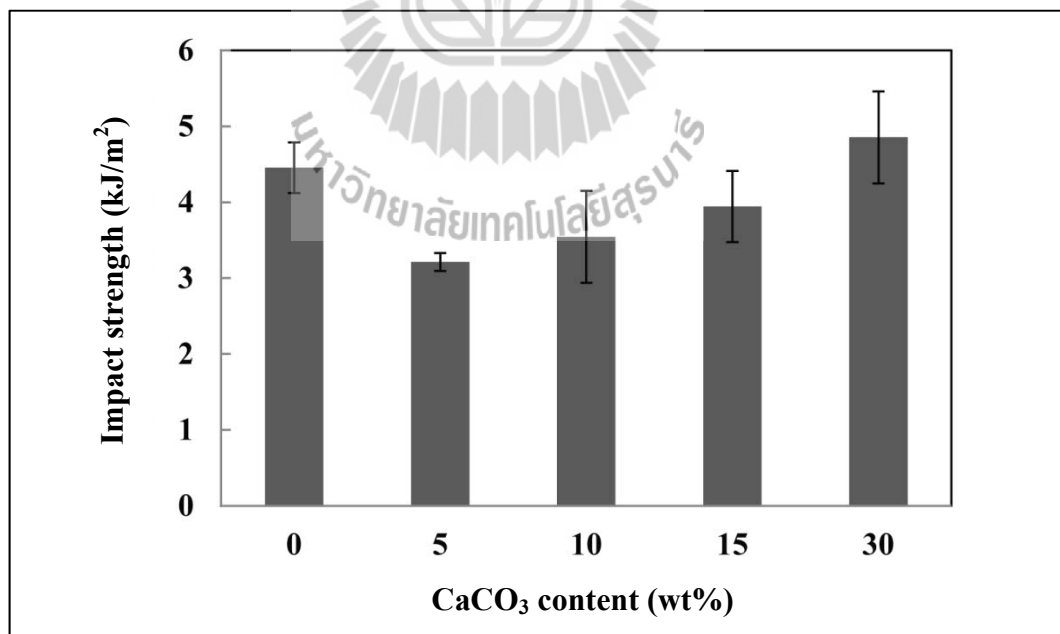


**Figure 4.29** Impact strength of compatibilized PLA/PBAT blend and PLA/PBAT/CaCO<sub>3</sub> composites at various CaCO<sub>3</sub> contents.

**Table 4.8** Mechanical properties of compatibilized PLA/PBAT blend and PLA/PBAT/CaCO<sub>3</sub> composites at various CaCO<sub>3</sub> contents.

<b>Composition (wt%)</b>	<b>Tensile strength (MPa)</b>	<b>Young's modulus (MPa)</b>	<b>Elongation at break (%)</b>	<b>Impact strength (kJ/m<sup>2</sup>)</b>
PLA/PBAT/PLA-g-MA 90/10/2 phr	51.85±1.85	543.65±24.19	49.25±1.69	4.45±0.33
PLA/PBAT/PLA-g-MA/CaCO <sub>3</sub> 90/10/2 phr/5	50.38±1.04	518.36±10.26	27.16±2.46	3.21±0.12
PLA/PBAT/PLA-g-MA/CaCO <sub>3</sub> 90/10/2 phr/10	46.94±0.93	532.10±4.89	23.17±1.18	3.54±0.61
PLA/PBAT/PLA-g-MA/CaCO <sub>3</sub> 90/10/2 phr/15	47.91±2.25	541.28±74.55	17.56±0.47	3.94±0.47
PLA/PBAT/PLA-g-MA/CaCO <sub>3</sub> 90/10/2 phr/30	35.58±2.02	593.34±40.77	17.15±2.91	4.85±0.61



#### 4.4.2 Morphological properties

SEM micrographs of the fracture surface of compatibilized PLA/PBAT blend and PLA/PBAT/CaCO<sub>3</sub> composites are shown in Figure 4.30. From the point of view of the performance of a composite, the mean size, the size distribution, as well as the shape of the particles, are of importance. As seen in Figure 4.30(b), at low CaCO<sub>3</sub> content, CaCO<sub>3</sub> well dispersed in the polymer matrices. When CaCO<sub>3</sub> content was increased from 10 to 30 wt%, agglomerates of CaCO<sub>3</sub> were observed as shown in Figure 4.30(c-e) leading to PLA/PBAT/CaCO<sub>3</sub> composites with poor mechanical properties.



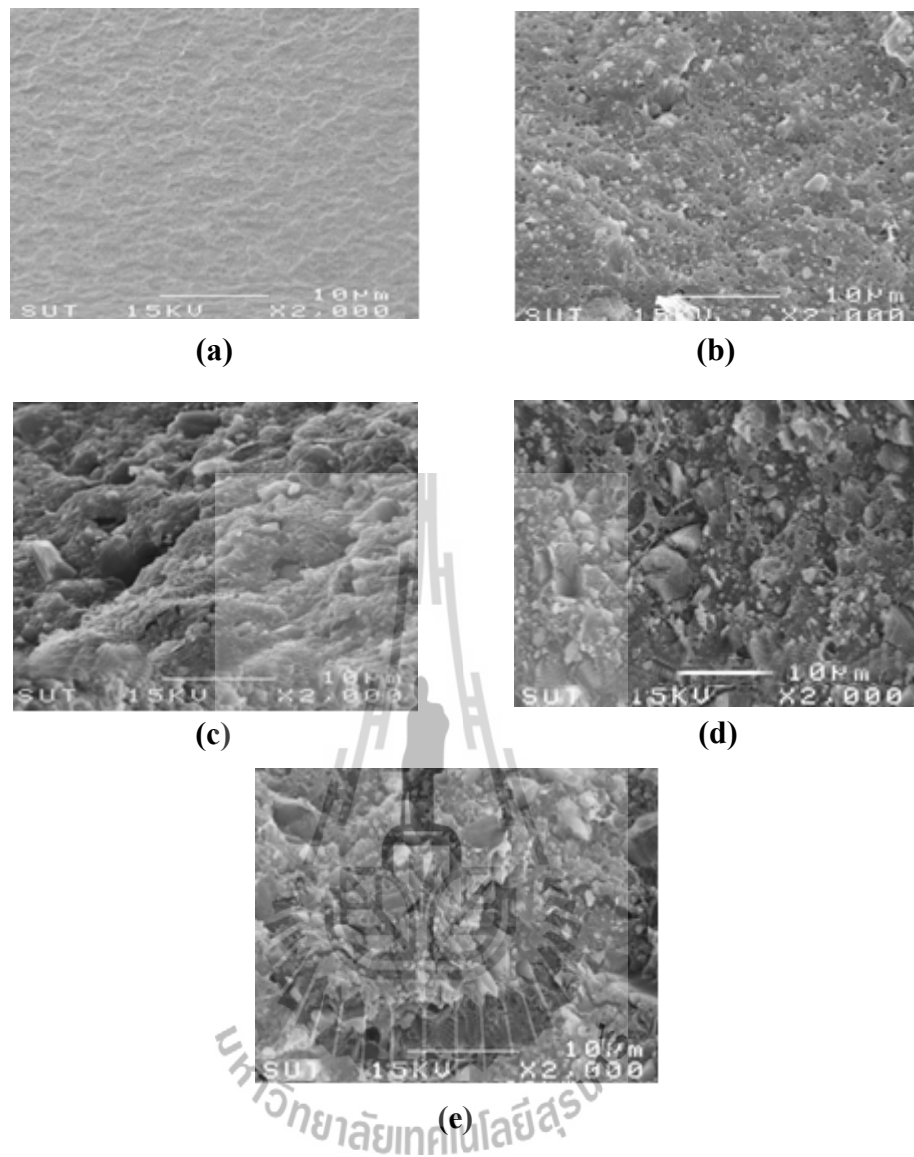


**Figure 4.30** SEM micrographs at 2000x magnification of (a) PLA/PBAT/PLA-g-MA 90/10/2 phr blend, (b) PLA/PBAT/PLA-g-MA/CaCO<sub>3</sub> 90/10/2 phr/5 composite, (c) PLA/PBAT/PLA-g-MA/CaCO<sub>3</sub> 90/10/2 phr/10 composite, (d) PLA/PBAT/PLA-g-MA/CaCO<sub>3</sub> 90/10/2 phr/15 composite, and (e) PLA/PBAT/PLA-g-MA/CaCO<sub>3</sub> 90/10/2 phr/30 composite.

#### 4.4.3 Thermal properties

Thermal properties of compatibilized PLA/PBAT blend and PLA/PBAT/CaCO<sub>3</sub> composites were investigated by DSC. The determined data are listed in Table 4.9. DSC curves of compatibilized PLA/PBAT blend and PLA/PBAT/CaCO<sub>3</sub> composites with different CaCO<sub>3</sub> contents are shown in Figure 4.31. Adding CaCO<sub>3</sub> showed insignificant effect on  $T_g$ ,  $T_{cc}$ , and  $T_m$  of PLA/PBAT blend but led to reduced  $\Delta H_c$  and  $\Delta H_m$ . However,  $\chi_c$  increased with increasing CaCO<sub>3</sub>. This indicated that crystallization ability of PLA was enhanced (Zhang, Meng, Chen, Tao, and Wu, 2012). The rigid CaCO<sub>3</sub> particles acted as a nucleating agent for crystallization and contributed to higher crystallinity. This concluded that adding CaCO<sub>3</sub> into PLA/PBAT/CaCO<sub>3</sub> composite had an influence on crystallizability of PLA/PBAT blend.



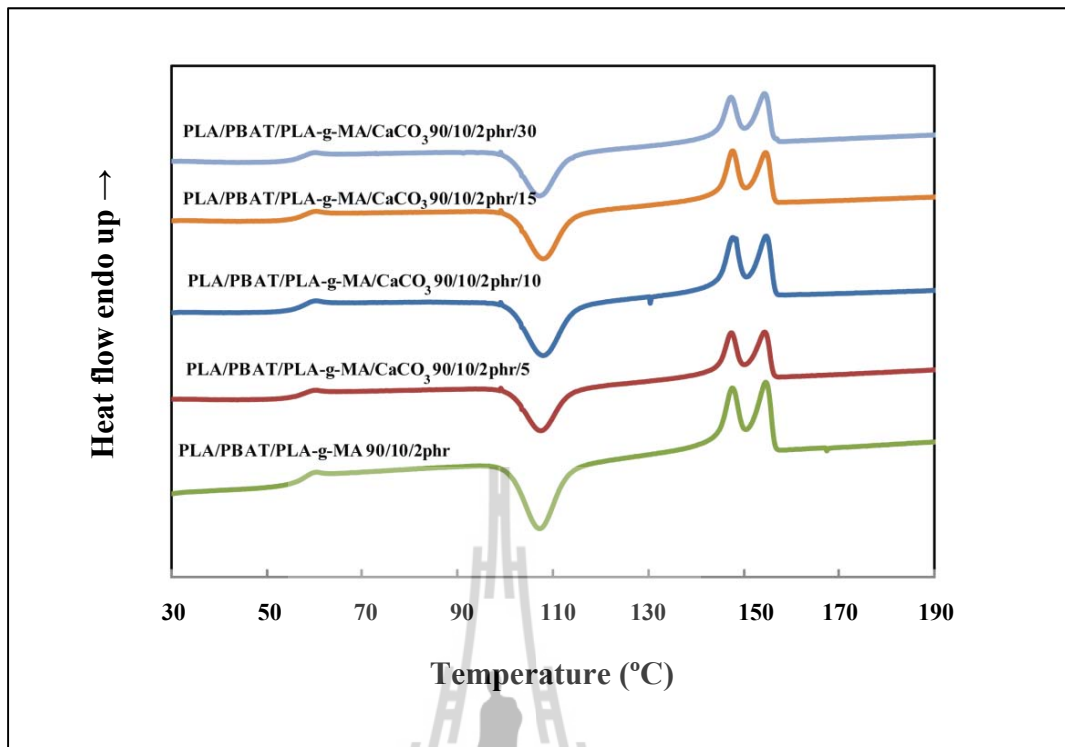


**Figure 4.31** DSC thermograms of compatibilized PLA/PBAT blend and PLA/PBAT/CaCO<sub>3</sub> composites at various CaCO<sub>3</sub> contents.

**Table 4.9** Thermal characteristics of compatibilized PLA/PBAT blend and PLA/PBAT/CaCO<sub>3</sub> composites at various CaCO<sub>3</sub> contents.

Composition (wt%)	T <sub>g</sub> (°C)	T <sub>cc</sub> (°C)	T <sub>m1</sub> (°C)	T <sub>m2</sub> (°C)	ΔH <sub>c</sub> (J/g)	ΔH <sub>m</sub> (J/g)	χ <sub>c</sub> (%)
PLA/PBAT/PLA-g-MA 90/10/2phr	57.44	107.19	147.58	154.75	23.22	19.05	23.07
PLA/PBAT/PLA-g-MA/CaCO <sub>3</sub> 90/10/2phr/5	57.49	107.49	147.40	154.37	22.04	20.92	26.14
PLA/PBAT/PLA-g-MA/CaCO <sub>3</sub> 90/10/2phr/10	57.48	107.95	147.66	154.74	21.45	20.91	27.58
PLA/PBAT/PLA-g-MA/CaCO <sub>3</sub> 90/10/2phr/15	57.82	107.99	147.70	154.52	20.34	20.92	28.90
PLA/PBAT/PLA-g-MA/CaCO <sub>3</sub> 90/10/2phr/30	57.05	107.19	147.33	154.33	15.66	17.91	30.37



TGA and DTG curves of PLA, PBAT, and PLA/PBAT/CaCO<sub>3</sub> composites are presented in Figure 4.32 and 4.33, respectively. Thermal degradation of PLA and PBAT showed only single step of weight loss. However, all PLA/PBAT/CaCO<sub>3</sub> composites showed two step degradation behaviors of PLA (at lower 350°C) and PBAT (at lower 400°C). Thermal degradation at 5% weight loss (T<sub>5</sub>), thermal degradation at 50% weight loss (T<sub>50</sub>), final degradation temperature (T<sub>f</sub>), and char residual of PLA, PBAT, PLA/PBAT blends, and PLA/PBAT/CaCO<sub>3</sub> composites are listed in Table 4.10. T<sub>5</sub>, T<sub>50</sub>, and T<sub>f</sub> of PLA/PBAT/CaCO<sub>3</sub> composites were lower than that of the blends. This suggested that thermal stability of PLA/PBAT blend significantly decreased with compounding with CaCO<sub>3</sub>. The basic nature of CaCO<sub>3</sub> had catalyzed the depolymerization of the ester bonds of PLA, thus it was responsible for reduced thermal stability (Kim, Park, Choi, and Yoon, 2008). Moreover, when 5, 10, 15, and 30 wt% CaCO<sub>3</sub> were added into PLA/PBAT blend, the composites left the char residual of CaCO<sub>3</sub> at 4.92, 10.54, 15.59, and 32.02%, respectively. This result confirmed that CaCO<sub>3</sub> was added into the blend.

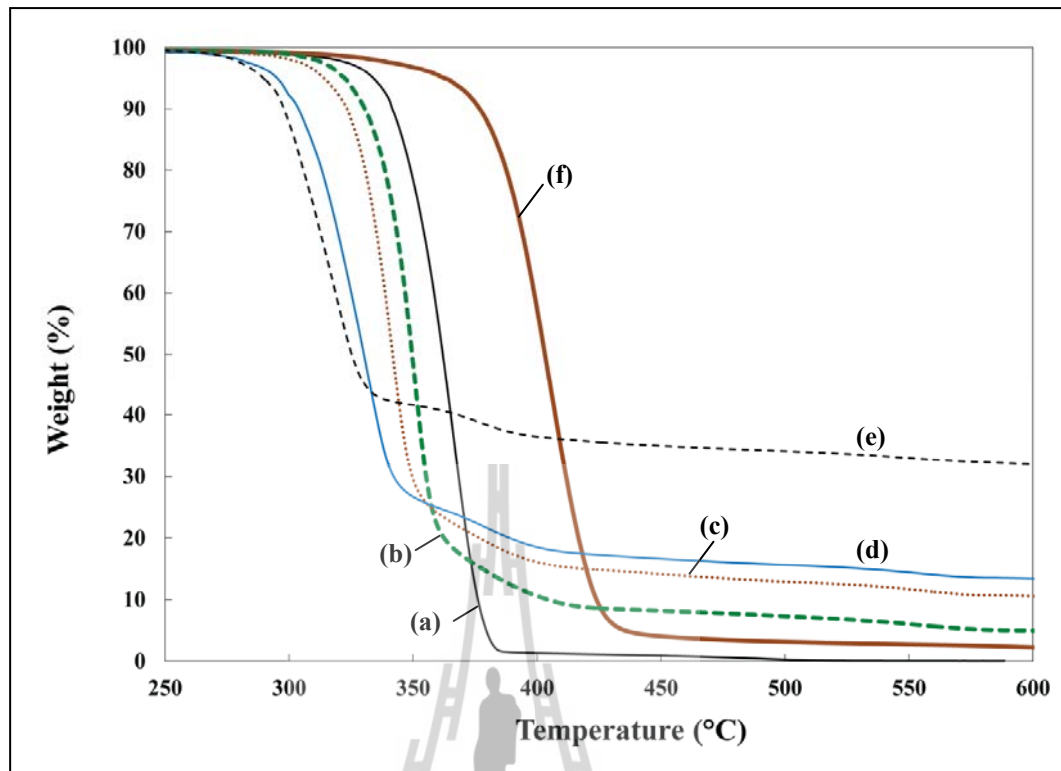


**Figure 4.32** TGA thermograms of (a) PLA, (b) PLA/PBAT/PLA-g-MA/CaCO<sub>3</sub> 90/10/2 phr/5 composite, (c) PLA/PBAT/PLA-g-MA/CaCO<sub>3</sub> 90/10/2 phr/10 composite, (d) PLA/PBAT/PLA-g-MA/CaCO<sub>3</sub> 90/10/2 phr/15 composite, (e) PLA/PBAT/PLA-g-MA/CaCO<sub>3</sub> 90/10/2 phr/30 composite, and (f) PBAT.

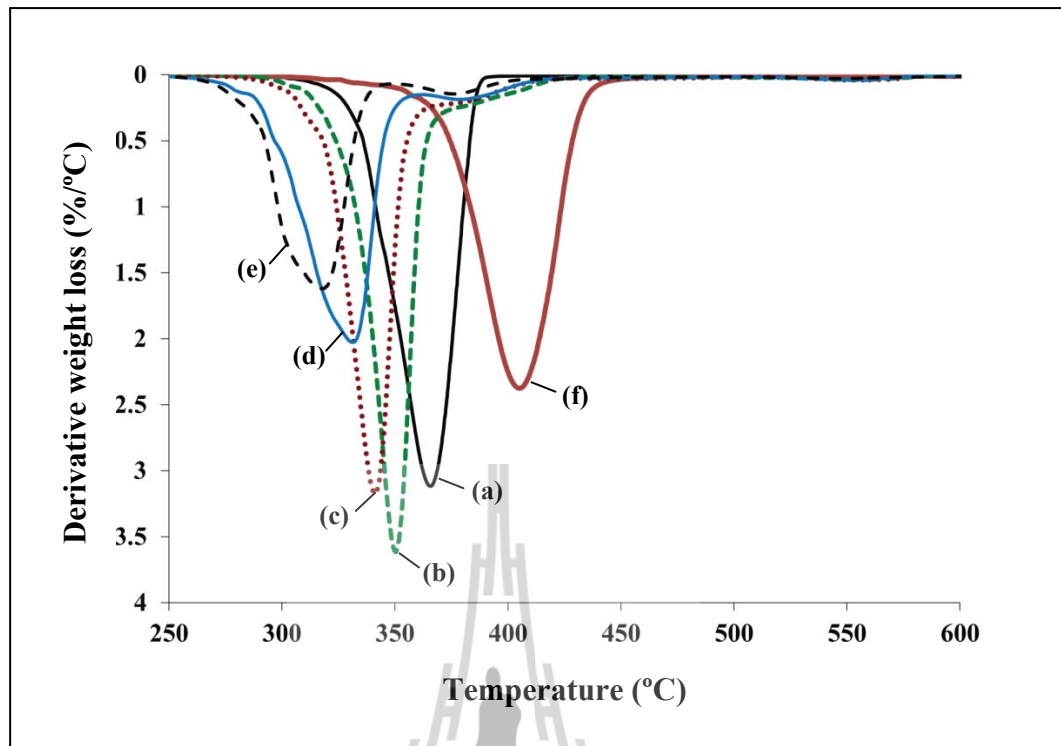


**Figure 4.33** DTG thermograms of (a) PLA, (b) PLA/PBAT/PLA-g-MA/CaCO<sub>3</sub> 90/10/2 phr/5 composite, (c) PLA/PBAT/PLA-g-MA/CaCO<sub>3</sub> 90/10/2 phr/10 composite, (d) PLA/PBAT/PLA-g-MA/CaCO<sub>3</sub> 90/10/2 phr/15 composite, (e) PLA/PBAT/PLA-g-MA/CaCO<sub>3</sub> 90/10/2 phr/30 composite, and (f) PBAT.

**Table 4.10** Thermal degradation temperature and % char of PLA, PBAT, PLA/PBAT blends, and PLA/PBAT/CaCO<sub>3</sub> composites.

Composition (wt%)	T <sub>5%</sub> (°C)	T <sub>50%</sub> (°C)	T <sub>f</sub> (°C)	Char residual (%)
PLA	333.70	362.01	387.96	-
PBAT	362.39	403.22	444.14	2.2
PLA/PBAT	333.71	363.30	428.80	-
PLA/PBAT/PLA-g-MA 90/10/2phr	340.76	363.72	434.96	-
PLA/PBAT/PLA-g-MA/CaCO <sub>3</sub> 90/10/2phr/5	322.28	349.65	424.96	4.92
PLA/PBAT/PLA-g-MA/CaCO <sub>3</sub> 90/10/2phr/10	313.28	341.85	426.28	10.54
PLA/PBAT/PLA-g-MA/CaCO <sub>3</sub> 90/10/2phr/15	289.42	325.24	426.02	15.59
PLA/PBAT/PLA-g-MA/CaCO <sub>3</sub> 90/10/2phr/30	287.97	324.77	434.81	32.02

#### 4.4.4 Rheological properties

Shear viscosity of PLA/PBAT blend and its composites with various CaCO<sub>3</sub> contents at 170°C are shown in Figure 4.34. At low shear rate, the viscosity of PLA/PBAT/CaCO<sub>3</sub> composites gradually decreased with increasing CaCO<sub>3</sub> content. Nekhamanurak, Patanathabutr, and Hongsriphan (2009) found that the viscosity of PLA/CaCO<sub>3</sub> composite decreased with increasing CaCO<sub>3</sub> content. They suggested that CaCO<sub>3</sub> particles (or agglomerated particles) could lubricate the movement of polymer chain during flow. In addition, high CaCO<sub>3</sub> content would create self-lubrication during flow. However, at high shear rate, no significant difference in the viscosity of PLA/PBAT/CaCO<sub>3</sub> composites was found.

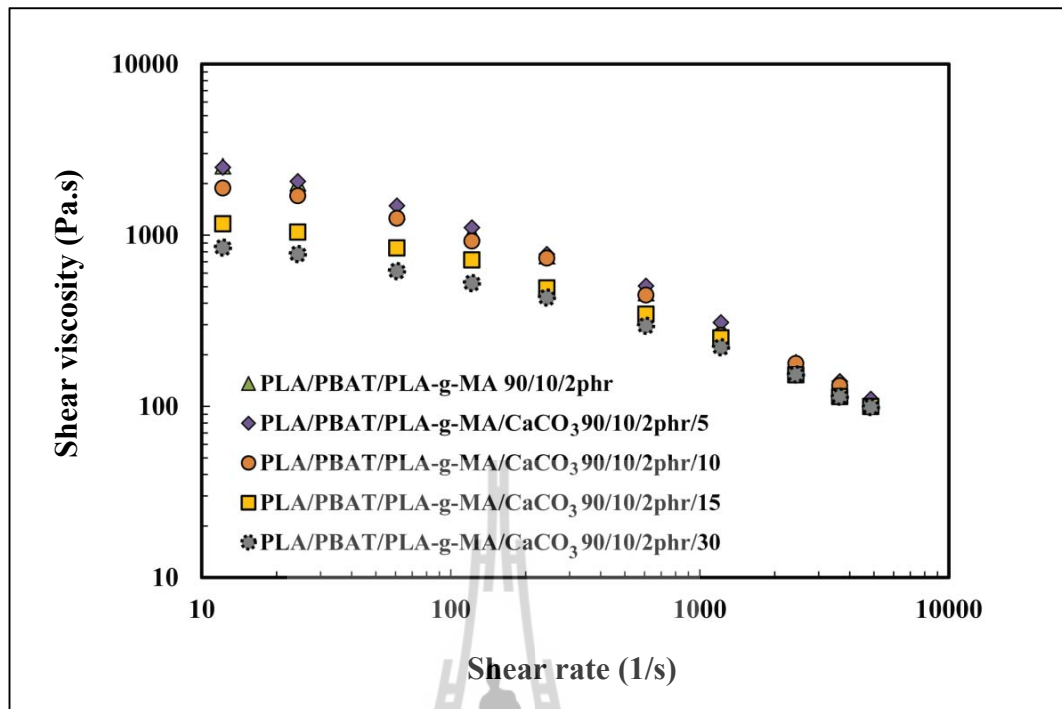


**Figure 4.34** Shear viscosities of compatibilized PLA/PBAT blend and PLA/PBAT/CaCO<sub>3</sub> composites at various CaCO<sub>3</sub> contents.

Melt flow index (MFI) of compatibilized PLA/PBAT blend and PLA/PBAT/CaCO<sub>3</sub> composites are shown in Figure 4.35. It clearly demonstrated that increasing CaCO<sub>3</sub> content resulted in the composites with higher MFI. This indicated that the viscosity of the composites decreased with increasing CaCO<sub>3</sub> content.

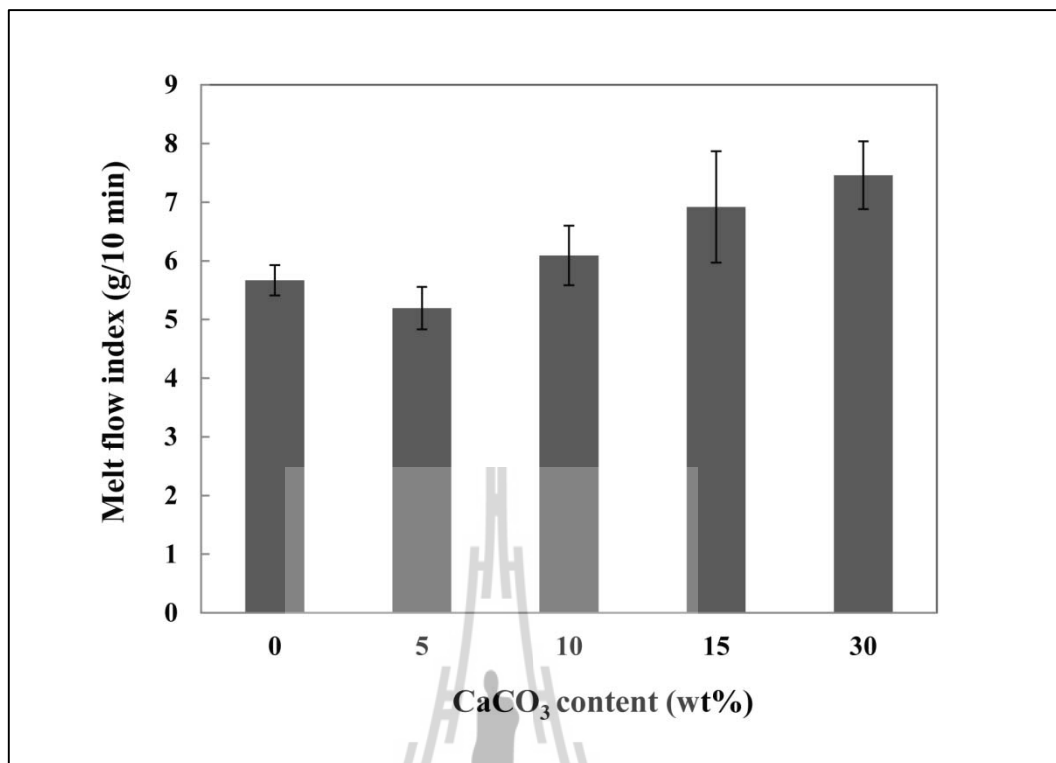


**Figure 4.35** MFI of compatibilized PLA/PBAT blend and PLA/PBAT/CaCO<sub>3</sub> composites at various CaCO<sub>3</sub> contents.

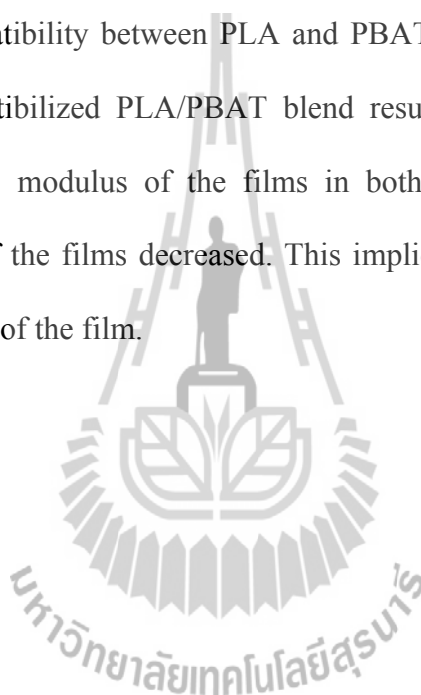
From mechanical properties results, PLA/PBAT/CaCO<sub>3</sub> composite with 5 wt% CaCO<sub>3</sub> was chosen to prepare blown films and its tensile properties were investigated.

#### **4.5 The properties of blown films prepared from PLA/PBAT blends and PLA/PBAT/CaCO<sub>3</sub> composite**

Blown films of PLA/PBAT blend, compatibilized PLA/PBAT blend, and PLA/PBAT/CaCO<sub>3</sub> composite can be prepared using a commercial blown film extruder. The thickness of the film was 10 micrometers. From visual observation, the films of PLA/PBAT blend and compatibilized PLA/PBAT blend showed higher

transparency than the film of PLA/PBAT/CaCO<sub>3</sub> composite as shown in Figure 4.36 (a–c).

Tensile properties in machine direction (MD) and transverse direction (TD) of blown films prepared from PLA/PBAT blends and their composite are illustrated in Figure 4.37 and Table 4.11. The addition of PLA-g-MA improved tensile strength, Young's modulus, and elongation at break of the films in both MD and TD due to the relatively good compatibility between PLA and PBAT. Furthermore, incorporating CaCO<sub>3</sub> in the compatibilized PLA/PBAT blend resulted in an increase in tensile strength and Young's modulus of the films in both the MD and TD. However, elongation at break of the films decreased. This implied that the addition of CaCO<sub>3</sub> increased the stiffness of the film.



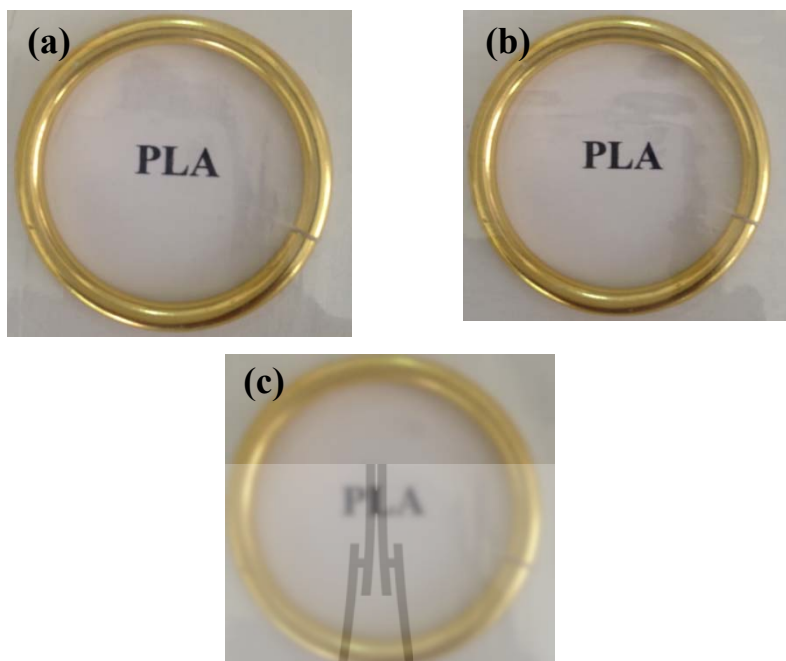


**Figure 4.36** Photographs of films prepared from PLA/PBAT blends and PLA/PBAT/CaCO<sub>3</sub> composite (10  $\mu\text{m}$  thickness) on a graphic pattern a) PLA/PBAT 90/10 blend, (b) PLA/PBAT/PLA-g-MA 90/10/2phr blend, and (c) PLA/PBAT/PLA-g-MA/CaCO<sub>3</sub> 90/10/2phr/5 composite.

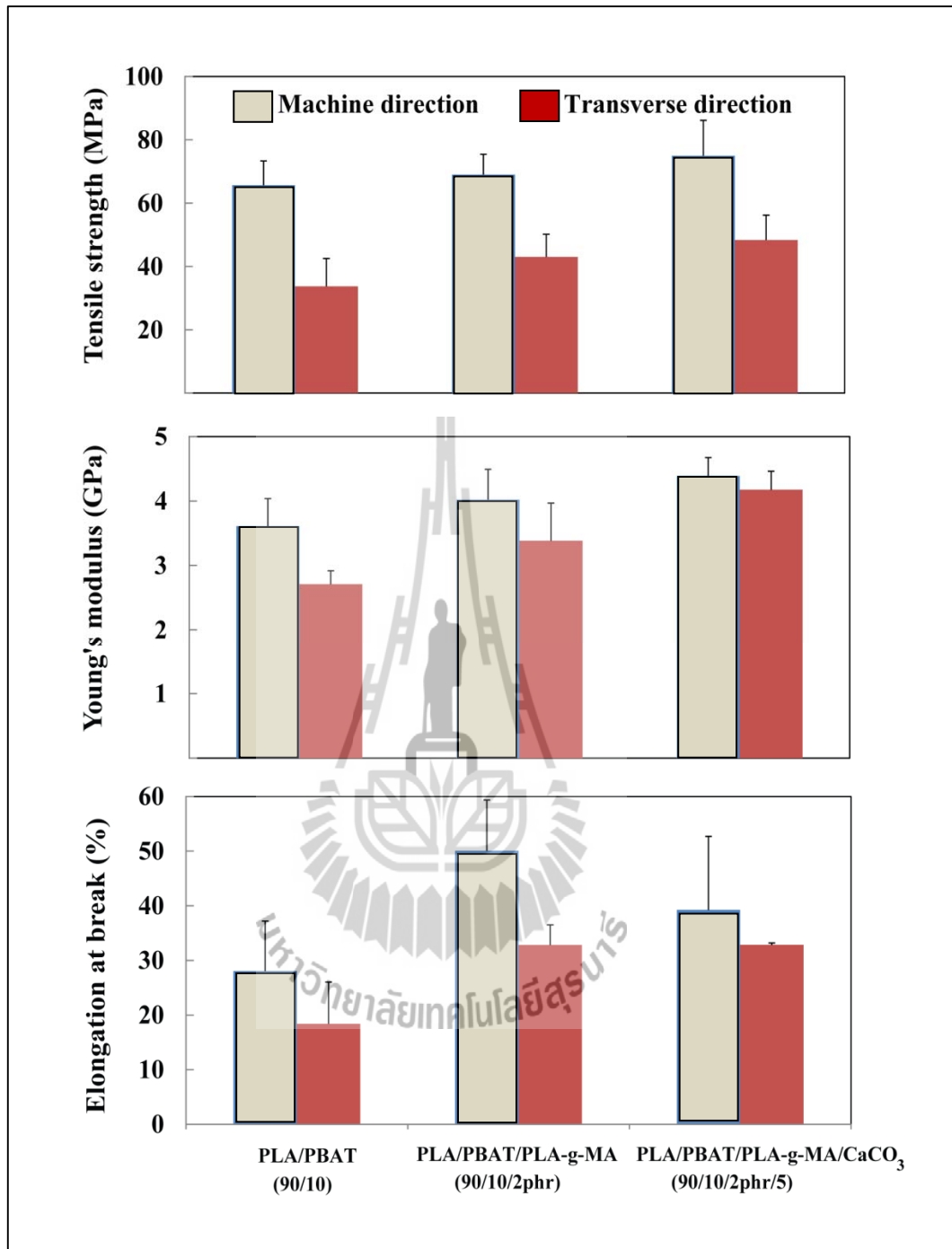
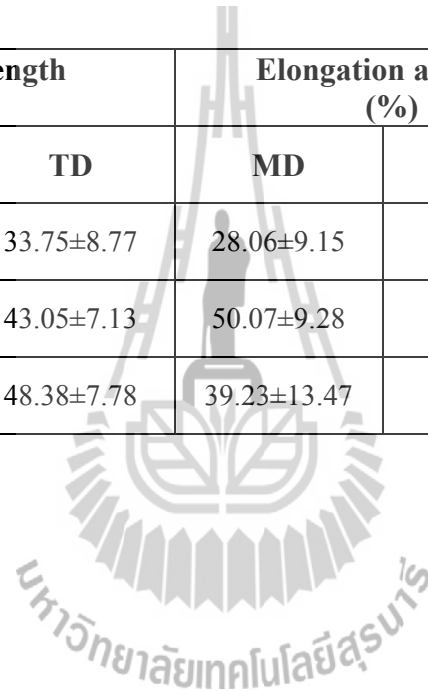


**Figure 4.37** Tensile properties of blown films prepared from PLA/PBAT blend, compatibilized PLA/PBAT blend, and PLA/PBAT/CaCO<sub>3</sub> composite.

**Table 4.11** Tensile properties of blown films prepared from PLA/PBAT blend, compatibilized PLA/PBAT blend, and PLA/PBAT/CaCO<sub>3</sub> composite.

Sample	Tensile strength (MPa)		Elongation at break (%)		Young's modulus (GPa)	
	MD	TD	MD	TD	MD	TD
PLA/PBAT 90/10	65.65±7.69	33.75±8.77	28.06±9.15	18.42±7.63	3.61±0.43	2.71±0.21
PLA/PBAT/PLA-g-MA 90/10/2phr	69.03±6.41	43.05±7.13	50.07±9.28	32.84±3.68	4.02±0.47	3.38±0.58
PLA/PBAT/PLA-g-MA/CaCO <sub>3</sub> 90/10/2phr/5	74.94±11.18	48.38±7.78	39.23±13.47	32.87±0.32	4.39±0.28	4.17±0.28



## CHAPTER V

### CONCLUSIONS

The effects of monomer and initiator content on graft content of MA grafted onto PLA molecule were studied. Fourier transform infrared spectroscopy (FTIR) was used to identify the MA grafted onto PLA molecule. The second derivative IR spectra of PLA-g-MA showed the absorption at  $1785\text{ cm}^{-1}$  corresponding to the characteristic absorption band of the succinic acid anhydride groups that assigned to the MA grafted onto PLA molecule. The highest graft content of MA grafted onto PLA molecule determined from the titration method was 0.41% with the addition of 1.0 wt% of 2,5-bis(*tert*-butylperoxy)-2,5 dimethylhexane and 5.0 wt% of MA.

With the addition of PBAT, elongation at break and impact strength of PLA significantly improved while tensile strength and Young's modulus decreased due to addition of ductile phase. PLA/PBAT blend was a kind of immiscible two-phase system. Moreover, the size of PBAT domain increased with increasing PBAT content due to coalescence of PBAT droplet in the blend. PBAT exhibited insignificant effect on  $T_g$  and  $T_m$  of PLA. Incorporating PBAT decreased  $T_{cc}$  indicating an enhancement of crystallizability of PLA. Furthermore, rheological results revealed that PBAT had higher viscosity than PLA and viscosity of PLA/PBAT blends gradually increased with increasing PBAT content.

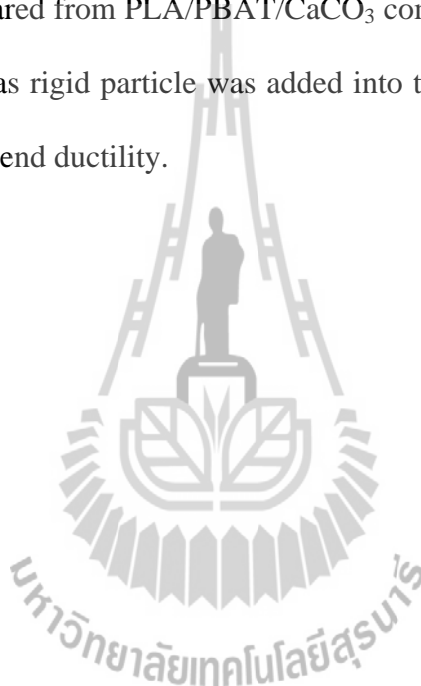
Incorporating PLA-g-MA improved the mechanical properties of PLA/PBAT blend due to enhanced interfacial adhesion between PLA and PBAT. The

compatibilized blend had a smaller size of disperse phase than that of the uncompatibilized blend. However, with increasing PLA-g-MA content (4 to 10 phr), the formation of a third phase in the compatibilized blend was observed resulting in decreased mechanical properties. PLA-g-MA exhibited insignificant effect on  $T_g$  and  $T_m$  of PLA/PBAT blend but led to a decrease in  $T_{cc}$ . This suggested that adding PLA-g-MA had an influence on crystallizability of PLA/PBAT blend. Moreover, thermal stability of the blend was enhanced with addition of PLA-g-MA. The compatibilized PLA/PBAT blend containing 2 and 4 phr of PLA-g-MA had higher viscosity than that of PLA/PBAT blend due to a compatibilizing effect of PLA-g-MA.

PLA/PBAT/ $\text{CaCO}_3$  composites showed lower tensile strength, elongation at break, and impact strength than the compatibilized blend. With increasing  $\text{CaCO}_3$  content, Young's modulus of the composites did not change while tensile strength decreased due to the agglomeration of  $\text{CaCO}_3$ , especially at high  $\text{CaCO}_3$  content.  $\text{CaCO}_3$  revealed insignificant effect on  $T_g$  and  $T_{cc}$  of the blend but reduced  $\Delta H_m$  and  $\Delta H_c$ . However,  $\chi_c$  increased with increasing  $\text{CaCO}_3$ . This indicated that crystallization ability of PLA was enhanced.  $\text{CaCO}_3$  might behave as nucleating agents. Furthermore, all of the composites exhibited two step degradation behaviors.  $T_5$ ,  $T_{50}$ , and  $T_f$  of PLA/PBAT/ $\text{CaCO}_3$  composites were lower than that of the blend. This suggested that thermal stability of PLA/PBAT blend significantly decreased with adding  $\text{CaCO}_3$ . In addition, the composites showed lower viscosity than the compatibilized blend.

Moreover, blown films of PLA/PBAT blend, compatibilized PLA/PBAT blend, and PLA/PBAT/ $\text{CaCO}_3$  composites can be processed using a commercial blown film extruder. The thickness of film was 10 micrometers. The films of

uncompatibilized and compatibilized PLA/PBAT blends showed higher transparency than that of PLA/PBAT/CaCO<sub>3</sub> composite. The addition of PLA-g-MA improved tensile strength, Young's modulus, and elongation at break of the films in both machine direction (MD) and transverse direction (TD) due to the relatively good compatibility between PLA and PBAT. Incorporating CaCO<sub>3</sub> resulted in increased tensile strength and Young's modulus of the films in both MD and TD. Elongation at break of the film prepared from PLA/PBAT/CaCO<sub>3</sub> composite decreased in MD. This might be that CaCO<sub>3</sub> as rigid particle was added into the PLA/PBAT blend resulting in a reduction of the blend ductility.



## REFERENCES

- Ajji, A. (2003). **Interphase and compatibilization by addition of a compatibilizer.**  
**In L. A. Utracki (Ed.), Polymer Blends Handbook** (pp. 295-338).  
Netherlands: Kluwer Academic Publishers.
- Bajer, K., Malinowski, R., Bajer, D., and Richert, S. (2010). Properties of poly (lactic acid)/Ecoflex rigid foil sheets applied in thermoforming process. **Polimery.** 55 (7/8): 591-593.
- Bartczak, Z., Argon, A. S., Cohen, R. E., and Weinberg, M. (1999). Toughness mechanism in semi-crystalline polymer blends: II. High-density polyethylene toughened with calcium carbonate filler particles. **Polymer.** 40 (9): 2347-2365.
- Bhatia, A., Gupta, R. K., Bhattacharya, S. N., and Choi, H. J. (2007). Compatibility of biodegradable poly (lactic acid) (PLA) and poly (butylene succinate) (PBS) blends for packaging application. **Korea-Australia Rheol. J.** 19 (3): 125-131.
- Broz, M. E., VanderHart, D. L., and Washburn, N. R. (2003). Structure and mechanical properties of poly (d,l-lactic acid)/poly ( $\epsilon$ -caprolactone) blends. **Biomaterials.** 24 (23): 4181-4190.
- Carlson, D., Nie, L., Narayan, R., and Dubois, P. (1999). Maleation of polylactide (PLA) by reactive extrusion. **J. Appl. Polym. Sci.** 72 (4): 477-485.
- Chen, C.-C., Chueh, J.-Y., Tseng, H., Huang, H.-M., and Lee, S.-Y. (2003). Preparation and characterization of biodegradable PLA polymeric blends. **Biomaterials.** 24 (7): 1167-1173.

- Chen, C., Peng, S., Fei, B., Zhuang, Y., Dong, L., Feng, Z., Chen, S., and Xia, H. (2003). Synthesis and characterization of maleated poly (3-hydroxybutyrate). **J. Appl. Polym. Sci.** 88 (3): 659-668.
- Chen, G.-X., Kim, H.-S., Kim, E.-S., and Yoon, J.-S. (2005). Compatibilization-like effect of reactive organoclay on the poly (l-lactide)/poly (butylene succinate) blends. **Polymer.** 46 (25): 11829-11836.
- Chuai, C., Iqbal, M., Aijaz, M., Iqbal, M., and Hiu, L. (2010). Effect of grafting ratio on rheological and mechanical properties of high density polyethylene-graft-maleic anhydride/polyamide 6 blends. **J. Chem. Soc. Pak.** 32 (1): 20-26.
- Coltelli, M.-B., Maggiore, I. D., Bertoldo, M., Signori, F., Bronco, S., and Ciardelli, F. (2008). Poly (lactic acid) properties as a consequence of poly (butylene adipate-*co*-terephthalate) blending and acetyl tributyl citrate plasticization. **J. Appl. Polym. Sci.** 110 (2): 1250-1262.
- Díaz, M. F., Barbosa, S. E., and Capiati, N. J. (2005). Improvement of mechanical properties for PP/PS blends by in situ compatibilization. **Polymer.** 46 (16): 6096-6101.
- Gan, Z., Kuwabara, K., Yamamoto, M., Abe, H., and Doi, Y. (2004). Solid-state structures and thermal properties of aliphatic-aromatic poly (butylene adipate-*co*-butylene terephthalate) copolyesters. **Polym. Degrad. Stab.** 83 (2): 289-300.
- Garlotta, D. (2001). A literature review of poly (lactic Acid). **J. Polym. Environ.** 9 (2): 63-84.
- Gu, S.-Y., Zhang, K., Ren, J., and Zhan, H. (2008). Melt rheology of polylactide/poly (butylene adipate-*co*-terephthalate) blends. **Carbohydr. Polym.** 74 (1): 79-85.

- Harada, M., Iida, K., Okamoto, K., Hayashi, H., and Hirano, K. (2008). Reactive compatibilization of biodegradable poly (lactic acid)/poly ( $\epsilon$ -caprolactone) blends with reactive processing agents. **Polym. Eng. Sci.** 48 (7): 1359-1368.
- Hiljanen-Vainio, M., Karjalainen, T., and Seppälä, J. (1996). Biodegradable lactone copolymers. I. Characterization and mechanical behavior of  $\epsilon$ -caprolactone and lactide copolymers. **J. Appl. Polym. Sci.** 59 (8): 1281-1288.
- Hong, J. S., Namkung, H., Ahn, K. H., Lee, S. J., and Kim, C. (2006). The role of organically modified layered silicate in the breakup and coalescence of droplets in PBT/PE blends. **Polymer.** 47 (11): 3967-3975.
- Hwang, S. W., Lee, S. B., Lee, C. K., Lee, J. Y., Shim, J. K., Selke, S. E. M., Soto-Valdez, H., Matuana, L., Rubino, M., and Auras, R. (2012). Grafting of maleic anhydride on poly (l-lactic acid). Effects on physical and mechanical properties. **Polym. Test.** 31 (2): 333-344.
- Jiang, L., Liu, B., and Zhang, J. (2009). Properties of poly (lactic acid)/poly (butylene adipate-*co*-terephthalate)/nanoparticle ternary composites. **Ind. Eng. Chem. Res.** 48 (16): 7594-7602.
- Jiang, L., Wolcott, M. P., and Zhang, J. (2006). Study of biodegradable poly (lactide)/poly (butylene adipate-*co*-terephthalate) blends. **Biomacromolecules.** 7 (1): 199-207.
- Jiang, L., Zhang, J., and Wolcott, M. P. (2007). Comparison of polylactide/nano-sized calcium carbonate and polylactide/montmorillonite composites: Reinforcing effects and toughening mechanisms. **Polymer.** 48 (26): 7632-7644.

- Juntuek, P., Ruksakulpiwat, C., Chumsamrong, P., and Ruksakulpiwat, Y. (2011). Effect of glycidyl methacrylate-grafted natural rubber on physical properties of polylactic acid and natural rubber blends. **J. Appl. Polym. Sci.** 125 (1): 745-754.
- Kim, H.-S., Park, B. H., Choi, J. H., and Yoon, J.-S. (2008). Mechanical properties and thermal stability of poly (l-lactide)/calcium carbonate composites. **J. Appl. Polym. Sci.** 109 (5): 3087-3092.
- Kim, Y. F., Choi, C. N., Kim, Y. D., Lee, K. Y., and Lee, M. S. (2004). Compatibilization of immiscible poly (l-lactide) and low density polyethylene blends. **Fiber Polym.** 5 (4): 270-274.
- Ko, S., Hong, M., Park, B., Gupta, R., Choi, H., and Bhattacharya, S. (2009). Morphological and rheological characterization of multi-walled carbon nanotube/PLA/PBAT blend nanocomposites. **Polym. Bull.** 63 (1): 125-134.
- Ko, S. W., Gupta, R. K., Bhattacharya, S. N., and Choi, H. J. (2010). Rheology and physical characteristics of synthetic biodegradable aliphatic polymer blends dispersed with MWNTs. **Macromol. Mater. Eng.** 295 (4): 320-328.
- Kumar, M., Mohanty, S., Nayak, S. K., and Rahail Parvaiz, M. (2010). Effect of glycidyl methacrylate (GMA) on the thermal, mechanical and morphological property of biodegradable PLA/PBAT blend and its nanocomposites. **Bioresour. Technol.** 101 (21): 8406-8415.
- Kuo, S.-W., Huang, C.-F., Tung, Y.-C., and Chang, F.-C. (2006). Effect of bisphenol A on the miscibility, phase morphology, and specific interaction in immiscible biodegradable poly ( $\epsilon$ -caprolactone)/poly (l-lactide) blends. **J. Appl. Polym. Sci.** 100 (2): 1146-1161.

- Lee, J.-W. and Lee, S.-M. (2005). Characterization and processing of biodegradable polymer blends of poly (lactic acid) with poly (butylene succinate adipate). **Korea-Australia Rheol. J.** 17 (2): 71-77.
- Li, C., Zhang, Y., and Zhang, Y. (2003). Melt grafting of maleic anhydride onto low-density polyethylene/polypropylene blends. **Polym. Test.** 22 (2): 191-195.
- Li, H. and Huneault, M. A. (2007). Effect of nucleation and plasticization on the crystallization of poly (lactic acid). **Polymer.** 48 (23): 6855-6866.
- Lin, S., Guo, W., Chen, C., Ma, J., and Wang, B. (2012). Mechanical properties and morphology of biodegradable poly (lactic acid)/poly (butylene adipate-*co*-terephthalate) blends compatibilized by transesterification. **Mater. Design.** 36: 604-608.
- Liu, T.-Y., Lin, W.-C., Yang, M.-C., and Chen, S.-Y. (2005). Miscibility, thermal characterization and crystallization of poly (l-lactide) and poly (tetramethylene adipate-*co*-terephthalate) blend membranes. **Polymer.** 46 (26): 12586-12594.
- Lomellini, P., Matos, M., and Favis, B. D. (1996). Interfacial modification of polymer blends-the emulsification curve: 2. Predicting the critical concentration of interfacial modifier from geometrical considerations. **Polymer.** 37 (25): 5689-5694.
- Ludvik, C., Glenn, G., Klamczynski, A., and Wood, D. (2007). Cellulose fiber/bentonite clay/biodegradable thermoplastic composites. **J. Polym. Environ.** 15 (4): 251-257.
- Macaúbas, P. H. P. and Demarquette, N. R. (2001). Morphologies and interfacial tensions of immiscible polypropylene/polystyrene blends modified with triblock copolymers. **Polymer.** 42 (6): 2543-2554.

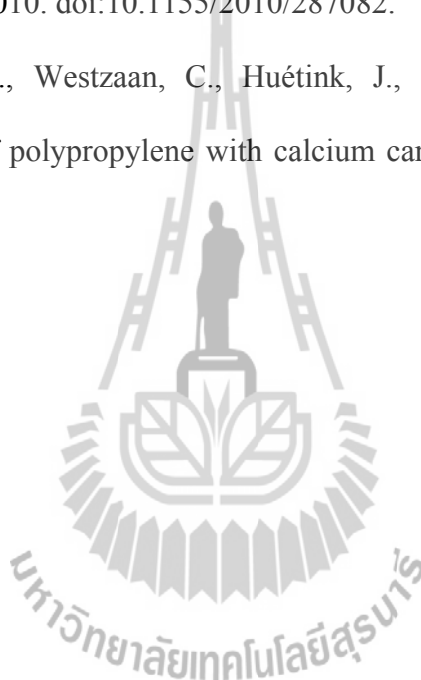
- Mani, R., Bhattacharya, M., and Tang, J. (1999). Functionalization of polyesters with maleic anhydride by reactive extrusion. **J. Polym. Sci. Pol. Chem.** 37 (11): 1693-1702.
- Martin, O. and Averous, L. (2001). Poly (lactic acid): plasticization and properties of biodegradable multiphase systems. **Polymer.** 42 (14): 6209-6219.
- Meng, B., Deng, J., Liu, Q., Wu, Z., and Yang, W. (2012). Transparent and ductile poly (lactic acid)/poly (butyl acrylate) (PBA) blends: Structure and properties. **Eur. Polym. J.** 48 (1): 127-135.
- Merijan, A. and Rahway, N. J. (1968). US Patent Office Patent No. 3,385,834.
- Murariu, M., Da Silva Ferreira, A., Degée, P., Alexandre, M., and Dubois, P. (2007). Polylactide compositions. Part 1: Effect of filler content and size on mechanical properties of PLA/calcium sulfate composites. **Polymer.** 48 (9): 2613-2618.
- Nekhamanurak, B., Patanathabutr, P., and Hongsrirphan, N. (2009). The influence of size and loading of calcium carbonate on melt flow index and thermal properties of polylactic acid and extrusion sheet. In **35<sup>th</sup> Congress on Science and Technology of Thailand (STT35)** Chonburi, Thailand.
- Pilla, S., Kim, S. G., Auer, G. K., Gong, S., and Park, C. B. (2010). Microcellular extrusion foaming of poly (lactide)/poly (butylene adipate-*co*-terephthalate) blends. **Mater. Sci. Eng.** 30 (2): 255-262.
- Pillin, I., Montrelay, N., and Grohens, Y. (2006). Thermo-mechanical characterization of plasticized PLA: Is the miscibility the only significant factor? **Polymer.** 47 (13): 4676-4682.

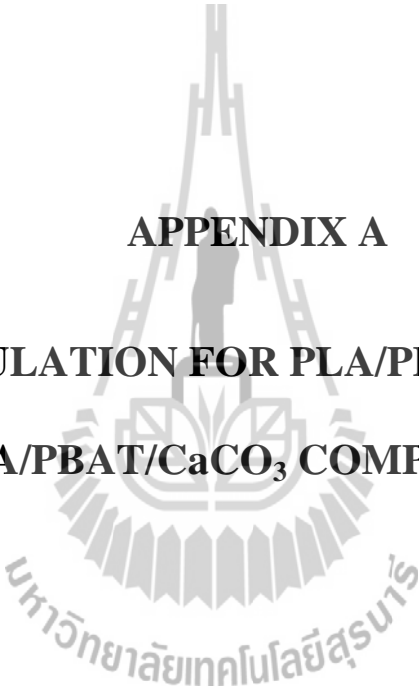
- Plackett, D. (2004). Maleated polylactide as an interfacial compatibilizer in biocomposites. **J. Polym. Environ.** 12 (3): 131-138.
- Rzayew, Z. M. O. (2011). Graft copolymers of maleic anhydride and its isostructural analogues : High performance engineering materials. **Int. Rev. Chem. Eng.** 3: 153-215.
- Sailaja, R. R. N., Reddy, A. P., and Chanda, M. (2001). Effect of epoxy functionalized compatibilizer on the mechanical properties of low-density polyethylene/plasticized tapioca starch blends. **Polym. Int.** 50 (12): 1352-1359.
- Sarasua, J.-R., Prud'homme, R. E., Wisniewski, M., Le Borgne, A., and Spassky, N. (1998). Crystallization and melting behavior of polylactides. **Macromolecules.** 31 (12): 3895-3905.
- Seung Woo, K., Rahul, K. G., Sati, N. B., and Hyoung Jin, C. (2010). Rheology and physical characteristics of synthetic biodegradable aliphatic polymer blends dispersed with MWNTs. **Macromol. Mater. Eng.** 295 (4): 320-328.
- Shahlari, M. and Lee, S. (2009). Effect of organically modified silicate layer on the morphology and mechanical properties of a poly (butylene adipate-*co*-terephthalate) and poly (lactic acid) blend. In **International Conference on Advanced Materials (ICAM2009)** Rio de Janeiro, Brazil.
- Shin, T. K., Kim, J., Choi, H. J., and Jhon, M. S. (2000). Miscibility of biodegradable aliphatic polyester and poly (vinyl acetate) blends. **J. Appl. Polym. Sci.** 77 (6): 1348-1352.

- Signori, F., Coltelli, M.-B., and Bronco, S. (2009). Thermal degradation of poly (lactic acid) (PLA) and poly (butylene adipate-*co*-terephthalate) (PBAT) and their blends upon melt processing. **Polym. Degrad. Stab.** 94 (1): 74-82.
- Stelescu, M. D., Manaila, E., and Niculescuaron, I.-G. (2007). Study on the improvement of physical-mechanical characteristics in the EPDM-HDPE blends. **U.P.B. Sci. Bull.** 69 (3): 51-58.
- Umamaheswara Rao, R., Suman, K. N. S., Kesava Rao, V. V. S., and Bhanukiran, K. (2011). Study of rheological and mechanical properties of biodegradable polylactide and polycaprolactone blends. **Int. J. Eng. Sci. Technol.** 3 (8): 6259-6265.
- Victor, H. O., Witold, B., Wunpen, C., and Betty, L. L. (2009). Preparation and characterization of poly (lactic acid)-*g*-maleic anhydride and starch blends. **Macromol. Symp.** 277 (1): 69-80.
- Wootthikanokkhan, J., Wongta, N., Sombatsompop, N., Kositchaiyong, A., Wong-On, J., Isarankura na Ayutthaya, S., et al. (2012). Effect of blending conditions on mechanical, thermal, and rheological properties of plasticized poly (lactic acid)/maleated thermoplastic starch blends. **J. Appl. Polym. Sci.** 124 (2): 1012-1019.
- Wu, C.-S. (2003). Physical properties and biodegradability of maleated-polycaprolactone/starch composite. **Polym. Degrad. Stab.** 80 (1): 127-134.
- Xiao, H., Lu, W., and Yeh, J.-T. (2009). Crystallization behavior of fully biodegradable poly (lactic acid)/poly (butylene adipate-*co*-terephthalate) blends. **J. Appl. Polym. Sci.** 112 (6): 3754-3763.

- Yang, L., Zhang, F., Endo, T., and Hirotsu, T. (2003). Microstructure of maleic anhydride grafted polyethylene by high-resolution solution-state NMR and FTIR spectroscopy. **Macromolecules**. 36 (13): 4709-4718.
- Yeh, J. T., Huang, C. Y., Chai, W. L., and Chen, K. N. (2009). Plasticized properties of poly (lactic acid) and triacetine blends. **J. Appl. Polym. Sci.** 112 (5): 2757-2763.
- Yeh, J. T., Tsou, C. H., Huang, C. Y., Chen, K. N., Wu, C. S., and Chai, W. L. (2010). Compatible and crystallization properties of poly (lactic acid)/poly (butylene adipate-*co*-terephthalate) blends. **J. Appl. Polym. Sci.** 116 (2): 680-687.
- Yokohara, T. and Yamaguchi, M. (2008). Structure and properties for biomass-based polyester blends of PLA and PBS. **Eur. Polym. J.** 44 (3): 677-685.
- Yuan, H., Liu, Z., and Ren, J. (2009). Preparation, characterization, and foaming behavior of poly (lactic acid)/poly (butylene adipate-*co*-butylene terephthalate) blend. **Polym. Eng. Sci.** 49 (5): 1004-1012.
- Zhang, J.-F. and Sun, X. (2004). Mechanical and thermal properties of poly (lactic acid)/starch blends with dioctyl maleate. **J. Appl. Polym. Sci.** 94 (4): 1697-1704.
- Zhang, J. and He, J. (2002). Interfacial compatibilization for PSF/TLCP blends by a modified polysulfone. **Polymer**. 43 (4): 1437-1446.
- Zhang, L., Goh, S. H., and Lee, S. Y. (1998). Miscibility and crystallization behaviour of poly (l-lactide)/poly (p-vinylphenol) blends. **Polymer**. 39 (20): 4841-4847.

- Zhang, N., Wang, Q., Ren, J., and Wang, L. (2009). Preparation and properties of biodegradable poly (lactic acid)/poly (butylene adipate-*co*-terephthalate) blend with glycidyl methacrylate as reactive processing agent. **J. Mater. Sci.** 44 (1): 250-256.
- Zhao, P., Liu, W., Wu, Q., and Ren, J. (2010). Preparation, mechanical, and thermal properties of biodegradable polyesters/poly (lactic acid) blends. **J. Nanomater.** 2010. doi:10.1155/2010/287082.
- Zuiderduin, W. C. J., Westzaan, C., Huétink, J., and Gaymans, R. J. (2003). Toughening of polypropylene with calcium carbonate particles. **Polymer.** 44 (1): 261-275.





**APPENDIX A**

**COST CALCULATION FOR PLA/PBAT BLENDS AND  
PLA/PBAT/CaCO<sub>3</sub> COMPOSITES**

## Cost analysis of PLA/PBAT blends and PLA/PBAT/CaCO<sub>3</sub> composite

### 1. Cost of materials for preparing PLA/PBAT blends

Total cost of materials for preparing PLA/PBAT blends based on 1 kg of the blends is shown in Table A.1

**Table A.1** Cost of materials for preparing PLA/PBAT blends based on 1 kg of the blends.

Sample	Component	Content (kg)	Price/Unit (bath/kg)	Total Price (bath/kg)
PLA	PLA	1.00	120.00	120.00
PLA/PBAT 90/10	PLA	0.90	120.00	135.00
	PBAT	0.10	270.00	
PLA/PBAT 80/20	PLA	0.80	120.00	150.00
	PBAT	0.20	270.00	
PLA/PBAT 70/30	PLA	0.70	120.00	165.00
	PBAT	0.30	270.00	
PBAT	PBAT	1.00	270.00	270.00

## 2. Cost of materials for preparing PLA-g-MA and compatibilized PLA/PBAT blends

PLA-g-MA was used as a compatibilizer for PLA/PBAT blend. Total cost of materials for preparing PLA-g-MA based on 1 kg of the compatibilizer is shown in Table A.2.

**Table A.2** Cost of materials for preparing PLA-g-MA based on 1 kg of the compatibilizer.

Sample	Component	Content (kg)	Price/Unit (bath/kg)	Total Price (bath/kg)
PLA-g-MA	PLA	0.94	120.00	202.80
	MA	0.05	1,800.00	
	Luperox101	0.10	35,381.00*	

\*Calculated form price of Luperox101 = 3,103.00 bath/100ml (Density 0.877 g/cm<sup>3</sup>)

Total cost of materials for preparing compatibilized PLA/PBAT blends based on 1 kg of the blends is shown in Table A.3.

**Table A.3** Cost of materials for preparing compatibilized PLA/PBAT blends based on 1 kg of the blends.

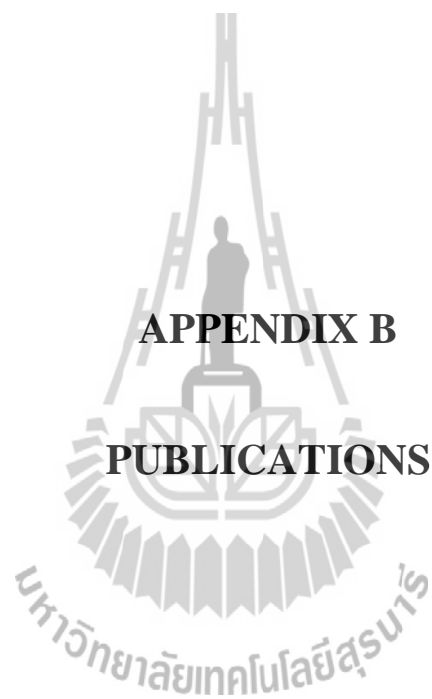
Sample	Component	Content (kg)	Price/Unit (bath/kg)	Total Price (bath/kg)
PLA/PBAT/PLA-g-MA 90/10/2 phr	PLA	0.90	120.00	136.33
	PBAT	0.10	270.00	
	PLA-g-MA	0.02	202.80	
PLA/PBAT/PLA-g-MA 90/10/4 phr	PLA	0.90	120.00	137.61
	PBAT	0.10	270.00	
	PLA-g-MA	0.04	202.80	
PLA/PBAT/PLA-g-MA 90/10/6 phr	PLA	0.90	120.00	138.84
	PBAT	0.10	270.00	
	PLA-g-MA	0.06	202.80	
PLA/PBAT/PLA-g-MA 90/10/8 phr	PLA	0.90	120.00	140.02
	PBAT	0.10	270.00	
	PLA-g-MA	0.08	202.80	
PLA/PBAT/PLA-g-MA 90/10/10 phr	PLA	0.90	120.00	141.16
	PBAT	0.10	270.00	
	PLA-g-MA	0.10	202.80	

### 3. Cost of materials for preparing PLA/PBAT/CaCO<sub>3</sub> composites

CaCO<sub>3</sub> was used as a filler for PLA/PBAT blend. Total cost of materials for preparing PLA/PBAT/CaCO<sub>3</sub> composite based on 1 kg of the composites is shown in Table A.4.

**Table A.4** Cost of materials for preparing PLA/PBAT/CaCO<sub>3</sub> composites based on 1 kg of the composites.

Sample	Component	Content (kg)	Price/Unit (bath/kg)	Total Price (bath/kg)
PLA/PBAT/PLA-g-MA/CaCO <sub>3</sub> 90/10/2 phr/5	PLA	0.90	120.00	129.76
	PBAT	0.10	270.00	
	PLA-g-MA	0.02	202.80	
	CaCO <sub>3</sub>	0.05	5.00	
PLA/PBAT/PLA-g-MA/CaCO <sub>3</sub> 90/10/2phr/10	PLA	0.90	120.00	123.20
	PBAT	0.10	270.00	
	PLA-g-MA	0.02	202.80	
	PLA	0.10	5.00	
PLA/PBAT/PLA-g-MA/CaCO <sub>3</sub> 90/10/2 phr/15	PLA	0.90	120.00	116.63
	PBAT	0.10	270.00	
	PLA-g-MA	0.02	202.80	
	PLA	0.15	5.00	
PLA/PBAT/PLA-g-MA/CaCO <sub>3</sub> 90/10/2 phr/30	PLA	0.90	120.00	96.93
	PBAT	0.10	270.00	
	PLA-g-MA	0.02	202.80	
	PLA	0.30	5.00	



**APPENDIX B**

**PUBLICATIONS**

## List of publications

- Teamsinsungvon, A., Ruksakulpiwat, Y., and Jarukumjorn, K. (2010). Preparation and characterization of melt free-radical grafting of maleic anhydride onto poly (lactic acid). In **Proceeding of Pure and Applied Chemistry International Conference 2010 (PACCON 2010)** (pp 257-259). Ubon Ratchathani, Thailand.
- Teamsinsungvon, A., Ruksakulpiwat, Y., and Jarukumjorn, K. (2010). Compatibilization and properties of poly (lactic acid)/poly (butylene adipate-*co*-terephthalate) blends. In **Abstract of The 1<sup>st</sup> National Research Symposium on Petroleum, Petrochemicals, and Advanced Materials and The 16<sup>th</sup> PCC Symposium on Petroleum, Petrochemicals, and Polymers** (pp. 82). Bangkok, Thailand.
- Teamsinsungvon, A., Ruksakulpiwat, Y., and Jarukumjorn, K. (2010). Properties of biodegradable poly(lactic acid)/poly (butylene adipate-*co*-terephthalate)/calcium carbonate composites. **Adv. Mater. Res.** 123-125: 193-196.
- Teamsinsungvon, A., Ruksakulpiwat, Y., and Jarukumjorn, K. (2010). Mechanical properties of polylactic acid/ poly (butylene adipate-*co*-terephthalate)/calcium carbonate composites. In **Abstract of The 2<sup>nd</sup> Thai-Japan Bioplastics and Biobased Materials Symposium (AIST-NIA Joint Symposium)**, Bangkok, Thailand.

- Teamsinsungvon, A., Ruksakulpiwat, Y., and Jarukumjorn, K. (2011). Mechanical and morphological properties of poly (lactic acid)/poly (butylene adipate-*co*-terephthalate)/calcium carbonate composite. **In Proceeding of The 18<sup>th</sup> International Conference on Composite Materials**, Jeju Island, Korea.
- Teamsinsungvon, A., Ruksakulpiwat, Y., and Jarukumjorn, K. (2011). Mechanical and morphological properties of poly (lactic acid)/poly (butylene adipate-*co*-terephthalate) blend and its composite. **In Abstract of The 3<sup>rd</sup> International Conference on Biodegradable and Biobased Polymers (BIOPOL-2011)**, Strasbourg, France.
- Teamsinsungvon, A., Ruksakulpiwat, Y., and Jarukumjorn, K. (2011). Poly (lactic acid)/poly (butylene adipate-*co*-terephthalate) blend and its composite: Effect of maleic anhydride grafted poly (lactic acid) as a compatibilizer. **In proceeding of the Twentieth International Symposium on Processing and Fabrication of Advanced Materials (PFAM XX)**, Hong Kong, Republic of China.
- Teamsinsungvon, A., Ruksakulpiwat, Y., and Jarukumjorn, K. (2012). Poly (lactic acid)/poly (butylene adipate-*co*-terephthalate) blend and its composite: Effect of maleic anhydride grafted poly (lactic acid) as a compatibilizer. **Adv. Mater. Res.** 410: 51-54.

## Preparation and characterization of melt free-radical grafting of maleic anhydride onto poly (lactic acid)

A.Teamsinsungvon<sup>1,2</sup>, Y. Ruksakulpiwat<sup>1,2</sup>, K. Jarukumjorn<sup>1,2\*</sup>

<sup>1</sup> School of Polymer Engineering, Institute of Engineering, Suranaree University of Technology, Nakhon Ratchasima, Thailand 30000

<sup>2</sup> Center of Excellence for Petroleum, Petrochemicals and Advanced materials, Chulalongkorn University, Bangkok, Thailand 10330

\*E-mail: kasama@sut.ac.th

**Abstract:** Poly (lactic acid) (PLA), a biodegradable polyester, derived from renewable resources has been widely used in biomedical and packaging applications. However, the shortcomings for using PLA include its processing instability, low melt viscosity and low flexibility. The free-radical grafting of PLA has been reported to enhance physical and chemical properties and/or improve the processability of PLA. Moreover, PLA grafted with monomers containing functional groups such as anhydride, carboxylic acid is used to improve compatibility between PLA and other biodegradable polymers or PLA and natural fibers. In this study, maleic anhydride monomer (MA) was grafted onto PLA in the presence of dicumyl peroxide (DCP) in an internal mixer. The effects of initiator and monomer concentration on the grafting level were investigated. The quantity of grafted anhydride was determined by the titration method. In addition, Fourier transform infrared spectrometer (FTIR) and melt flow index (MFI) measurement were used to characterize the grafted PLA. Increasing monomer and initiator concentrations resulted in an increase in the grafting level and MFI.

### Introduction

Poly (lactic acid) (PLA) is known as a biodegradable thermoplastic polymer with widely potential applications [1, 2]. PLA has a number of interesting properties including biodegradability, biocompatibility, high strength and high modulus [3-5]. For this reasons, PLA is an interesting candidate for producing package materials. However, its high brittleness, low toughness and high cost limit its application [6].

To overcome these limitations, combining PLA with nature materials and synthetic polymers provides ways of cost reduction and combined properties. Unfortunately, simple PLA composites with natural materials and polymer blends have poor mechanical properties because of the lack of interfacial adhesion [7].

PLA grafted with monomers e.g. anhydride, carboxylic acid has been used to improve the interfacial adhesion between PLA and other polymers [8, 9] or PLA and fillers [10]. It is common to use maleic anhydride (MA) monomer to graft onto PLA

because of its good reactivity and controllability in free radical polymerization [11, 12].

The objective of this work was to investigate the effects of DCP as an initiator and MA monomer concentration on the grafting level of maleic anhydride-grafted-PLA (PLA-g-MA).

### Materials and Methods

The materials used in this study were poly (lactic acid) (PLA Grade 4042, NatureWorks LLC), Maleic anhydride (MA, Sigma-Aldrich) and dicumyl peroxide (DCP, Aldrich Chemicals, 98%) as a free radical initiator.

The grafting reaction was carried out in an internal mixer (Haake Rheomix, 3000P). PLA pellets were dried at 70°C for 4 hrs before mixing. The mixer temperature was kept at 170°C. A rotor speed was 50 rpm and mixing time was 10 min. The MA contents were 0.5, 1.0, 1.5, 2.0 wt% and DCP contents were 0, 0.1, 0.25, 0.5 wt%.

The quantity of maleic anhydride content on PLA was determined by titration of acid groups derived from anhydride functions using phenolphthalein as an indicator. Samples were dissolved in chloroform and precipitated with methanol to remove residual MA and initiator. Then, the grafted PLA was accurately weighed and heated in xylene for 2 hrs and the hot solution was then titrated immediately with KOH (alcohol solution). The acid number and the grafting level (%G) were calculated using Eq. (1) and Eq. (2), respectively. Pure PLA without MA was also titrated under the same conditions to obtain blank values [13].

Acid number (mg KOH/g)

$$= \frac{V_{\text{KOH}}(\text{ml}) \times N_{\text{KOH}}(\text{N})}{\text{sample}(\text{g})} \times 56.1 \quad (1)$$

$$\text{G\%} = \frac{\text{Acid number} - M_0}{2 \times 561} \times 98.06 \quad (2)$$

Where N is the normality (mol/l), V is the volume (ml),  $M_0$  is the blank titration value of pure PLA and 98.06 is the molecular weight of MA.

The extracted samples were made into thin films by compression molding at 170°C. The grafting

identification of MA onto PLA was determined by FTIR (BRUKER, TENSOR 27). The spectra were recorded in the 400-4000  $\text{cm}^{-1}$  region with 4  $\text{cm}^{-1}$  resolution.

Melt flow index (MFI) of grafted polymers were measured at 170°C with a load of 2.16 kgs.

### Results and Discussion

The FTIR spectra of PLA, MA and PLA-g-MA with various DCP and MA contents are shown in Figure 1 and 2, respectively. The characteristic transitions of PLA at 3300-3700, 1700-1760, and 500-1500  $\text{cm}^{-1}$  appeared in the spectra of all PLA samples, while two extra shoulders at 1791 and 1851  $\text{cm}^{-1}$  were observed in maleic anhydride spectrum [13, 14]. These features are characteristic of anhydride carboxyl groups [13, 15]. From Figure 1, the peaks of anhydride carbonyl group were found only in the grafted PLA with 0.25 wt% DCP (at 2.0 wt% MA). In addition, it can be observed these peaks in the grafted PLA with 1.5 and 2.0 wt% MA (at 0.5 wt% DCP) as shown in Figure 2. This confirmed that the discernible shoulder in the grafted PLA at 1791 and 1851  $\text{cm}^{-1}$  demonstrated grafting of MA onto PLA.

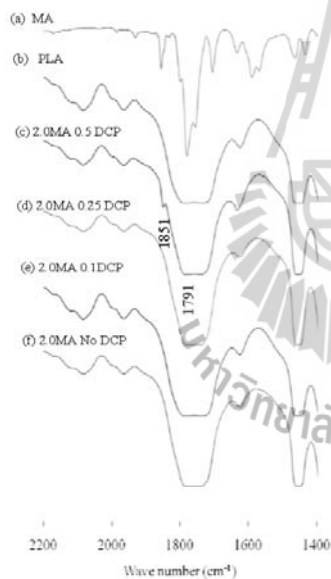


Figure 1. FTIR spectra of PLA, MA and PLA-g-MA with different DCP contents.

The grafting levels of PLA-g-MA are shown in Table 1. No grafting level was found in the grafted PLA samples containing 0, 0.1 wt% DCP with 2.0 wt% MA and 0.5, 1.0 wt% MA with 0.5 wt% DCP. The result agreed with FTIR observation. Incorporating DCP into PLA generated more radical sites on PLA backbone for the grafting reaction [16]. With increasing the MA concentration, the probability of PLA macroradicals reacting with the MA is higher leading to increasing grafting level. The variation of

MFI with the concentration of MA and DCP was illustrated in Table 1. MFI data showed that all the grafted samples had higher MFI (i.e. lower viscosity) than that of pure PLA (23.70 g/10 min). In addition, MFI of PLA-g-MA increased with increasing DCP and MA concentration. With the same amount of MA (2 wt%), the MFI of grafted PLA with adding DCP was higher than the grafted PLA without DCP because increasing DCP content might reduce chain of PLA macroradicals by chain scission [7]. Similarly, in the case of the modification of polypropylene (PP), the incorporation of peroxide caused chain scission of PP and the presence of MA also caused further chain scission of the PP chain [17]. On the other hand, this result was different from what was found in the modification of polyethylene (PE). The addition of peroxide caused branching and gelation and the presence of MA further promoted branching and gelation [18].

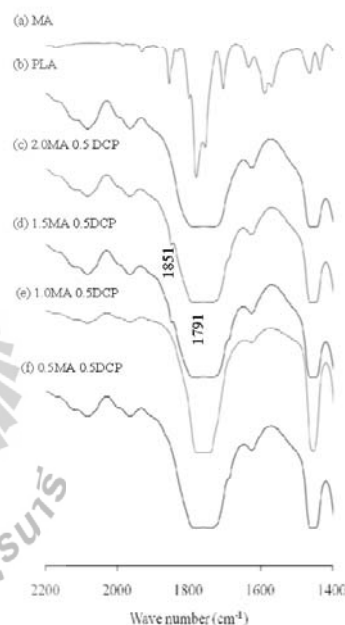


Figure 2. FTIR spectra of PLA, MA and PLA-g-MA with different MA contents.

Table 1: MFI of PLA and PLA-g-MA and grafting level PLA-g-MA.

ID No.	PLA sample		MFI (g/10 min)	%G
	Wt% MA	Wt% DCP		
1	Pure PLA		23.70	-
2	2.0	-	107.04	-
3	2.0	0.10	165.25	-
4	2.0	0.25	179.65	0.10
6	0.5	0.50	113.95	-
7	1.0	0.50	116.46	-
8	1.5	0.50	127.86	0.06
9	2.0	0.50	173.36	0.12

### Conclusions

The grafting level was influenced by initiator and monomer concentrations. An increase in monomer concentration resulted in an increase in the grafting level of PLA-g-MA. MFI of the grafted PLA increased with increasing DCP and MA concentrations which indicated a decrease in viscosity by the chain scission of PLA molecules.

### Acknowledgements

The authors wish to acknowledge for financial support granted by Suranaree University of Technology and Center of Excellence for Petroleum, Petrochemicals and Advanced Materials and Dr. Wanwisa Pateanasiriwisawa (National Synchrotron Research Center, NSRC) for assistance with FTIR measurements.

### References

- [1] M. Baiardo, G. Frisoni, M. Scandola, M. Rimelen, D. Lips and K. Ruffieux, *J. Appl. Polym. Sci.* 90 (2003), pp. 1731-1738.
- [2] K. Arakawa, T. Madaa, S. Parka, and M. Todoa, *Polym. Test.* 25 (2006), pp. 628-634.
- [3] N. Ljungberg, and B. Wesslen, *Polymer.* 44 (2003), pp. 7679-7688.
- [4] N. Ljungberg and B. Wesslen, *Biomacromolecules.* 6 (2005), pp. 1789-1796.
- [5] R. Auras, B. Harte and S. Selke, *Macromol. Biosci.* 4 (2004), pp. 835-864.
- [6] J. Yeh, C. Huang, W. Chai and K. Chen, *J. Appl. Polym. Sci.* 112 (2009), pp. 2757-2763.
- [7] D. Carlson, L. Nie, R. Narayan and P. Dubois, *J. Appl. Polym. Sci.* 72 (1999), pp. 477-485.
- [8] W. Jang, B. Shin, T. Lee and R. Narayan, *J. Ind. Eng. Chem.* 13 (2007), pp. 457-464.
- [9] H. Yuan, Z. Liu and J. Ren, *Polym. Eng. Sci.* 49 (2009), pp. 1004-1012.
- [10] L. Jiang, B. Liu and J. Zhang, *Ind. Eng. Chem. Res.* 48 (2009), pp. 7594-7602.
- [11] C. Jiang, S. Filippi and P. Magagnoli, *Polymer.* 44 (2003), pp. 2411-2422.
- [12] C. Chen, S. Peng, B. Fei, Y. Zhuang, L. Dong, Z. Feng, S. Chen and H. Xia, *J. Appl. Polym. Sci.* 88 (2003), pp. 659-668.
- [13] C. Wu, *Polym. Degrad. Stab.* 80 (2003), 127-134.
- [14] F. Yao, W. Chen, H. Wang, H. Lin, K. Yao and P. Sun, *Polymer.* 44 (2003), pp. 6435-6441.
- [15] J. John, J. Tang, Z. Yang and M. Bhattacharya, *J. Polym. Sci. Part A Polym. Chem.* 35 (1997), pp. 1139-1148.
- [16] R. Maliger, S. McGlashan, P. Halley and L. Matthew, *Polym. Eng. Sci.* 46 (2006), pp. 248-263.
- [17] P. Callais and R. Kazmierczak *ANTEC* 90 (1990), pp. 1921-1923.
- [18] A. Hogt, *ANTEC* 88 (1988), pp. 1478-1480.



The 1<sup>st</sup> National Research Symposium on Petroleum, Petrochemicals, and Advanced Materials and The 16<sup>th</sup> PPC Symposium on Petroleum, Petrochemicals, and Polymers  
April 22, 2010, Rajmontien Grand Ballroom, Motien Hotel, Bangkok, Thailand

## Poster Sessions

### SUT-PE

#### **PA-P(9)-13** Compatibilization and Properties of Poly (lactic acid)/Poly (butylene adipate-co-terephthalate) Blends

**Arpaporn Teamsinsungvon<sup>a,b</sup>, Yupaporn Ruksakulpiwat<sup>a,b</sup>, Kasama Jarukumjorn<sup>a,b</sup>**

<sup>a)</sup>School of Polymer Engineering, Institute of Engineering, Suranaree University of Technology

<sup>b)</sup>Center for Petroleum, Petrochemicals, and Advanced Materials

Poly (lactic acid) (PLA), a biodegradable polyester derived from renewable resources, has been used in packaging applications. However its high brittleness limited its applications. In order to improve ductility of PLA, poly (butylene adipate-co-terephthalate) (PBAT) was blended with PLA. Unfortunately, the compatibility between PLA and PBAT is poor. This results in the blends with poor mechanical properties. To solve this problem, compatibility of these blends could be improved by adding maleic anhydride grafted PLA (PLA-g-MA) as a compatibilizer leading to improve the interfacial adhesion between PLA and PBAT. In this study, PLA/PBAT blends were prepared by an internal mixer. Mechanical and morphological properties of all blends were investigated. In addition, the effect of compatibilizer contents on the properties of the PLA/PBAT blends was investigated.



*Advanced Materials Research Vols. 123-125 (2010) pp 193-196*  
 Online available since 2010/Aug/11 at [www.scientific.net](http://www.scientific.net)  
 © (2010) Trans Tech Publications, Switzerland  
 doi:10.4028/www.scientific.net/AMR.123-125.193

## Properties of Biodegradable Poly (lactic acid)/Poly (butylene adipate-co-terephthalate)/Calcium Carbonate Composites

Arpaporn Teamsinsungvon<sup>1,2,a</sup>, Yupaporn Ruksakulpiwat<sup>1,2,b</sup>  
 and Kasama Jarukumjorn<sup>1,2,c</sup>

Corresponding to; Kasama Jarukumjorn ([kasama@sut.ac.th](mailto:kasama@sut.ac.th))

<sup>1</sup>School of Polymer Engineering, Institute of Engineering, Suranaree University of Technology,  
 Nakhon Ratchasima 30000, Thailand

<sup>2</sup>Center of Excellence for Petroleum, Petrochemicals, and Advanced Materials,  
 Chulalongkorn University, Bangkok 10330, Thailand

<sup>a</sup>[jeabb.na@gmail.com](mailto:jeabb.na@gmail.com), <sup>b</sup>[yupa@sut.ac.th](mailto:yupa@sut.ac.th), <sup>c</sup>[kasama@sut.ac.th](mailto:kasama@sut.ac.th)

**Keywords:** Poly (lactic acid), Poly (butylene adipate-co-terephthalate), Maleic anhydride grafted PLA, Calcium carbonate

**Abstract.** Poly (lactic acid) (PLA), a biodegradable polyester, derived from renewable resources has been widely used in biomedical and packaging applications. However, the shortcomings for using PLA including its processing instability, low melt viscosity and low flexibility limited its applications. To overcome these shortcomings, poly (butylene adipate-co-terephthalate) (PBAT) was blended with PLA to improve ductility of PLA. However, PLA and PBAT are incompatible. Maleic anhydride grafted PLA (PLA-g-MA) was used to enhance the compatibility of the blends. Moreover, the blend of PLA and PBAT exhibited higher elongation at break but lower tensile strength and Young's modulus than the pure PLA due to the addition of a ductile phase. Therefore, the addition of calcium carbonate (CaCO<sub>3</sub>) to PLA/PBAT blends led to achieve balanced properties of the blends. In this study, PLA/PBAT blends and PLA/PBAT/CaCO<sub>3</sub> composites were prepared by an internal mixer. PLA-g-MA was as a compatibilizer. Mechanical properties and rheological properties of the blend and composites were investigated. In addition, morphologies of PLA/PBAT blend and their composites were observed by a scanning electron microscope (SEM). The incorporation of PBAT gave rise to remarkable improvement in elongation at break and impact strength of PLA. Tensile strength of PLA/PBAT blend was enhanced by adding PLA-g-MA. With increasing CaCO<sub>3</sub> content, Young's modulus of the composites increased while tensile strength and elongation at break decreased.

### Introduction

Poly (lactic acid) (PLA) is known as a biodegradable thermoplastic polymer with widely potential applications [1, 2]. PLA has a number of interesting properties including biodegradability, biocompatibility, high strength and high modulus [3]. However, its high brittleness and low toughness limit its application [4]. To overcome these limitations, blending PLA with flexible polymers is a practical and economical way to obtain toughened PLA. Poly (butylene adipate-co-terephthalate) (PBAT), an aliphatic-aromatic copolyester, is considered a good candidate for the toughening of PLA due to its high toughness and biodegradability. Generally, the binary blends of PLA and PBAT exhibited higher elongation at break but lower tensile strength and modulus than the pure PLA due to the addition of a ductile phase. Therefore, the addition of filler to PLA/PBAT blends led to a modulus approaching that of the pure PLA. Unfortunately, PLA composites with natural materials e.g. natural fiber, CaCO<sub>3</sub> have poor mechanical properties because of the lack of

interfacial adhesion. PLA grafted with maleic anhydride (PLA-g-MA) has been used to improve the interfacial adhesion between PLA and other polymers [5, 6] or PLA and fillers [7]. The objective of this work was to investigate the effects of PLA-g-MA and CaCO<sub>3</sub> content on mechanical, rheological and morphological properties of PLA/PBAT/CaCO<sub>3</sub> composites.

### Materials and Method

**Materials.** PLA used in this study was Natureworks PLA 4042D. PBAT was BASF Ecoflex FBX 7011. Precipitated calcium carbonate with an average particle size of 1.20-1.40  $\mu\text{m}$  (HICOAT 810) was supplied from Sand and Soil Co., Ltd. 2,5-bis(*tert*-butylperoxy)-2,5 dimethylhexane (L101) and maleic anhydride (MA) were purchased from Aldrich. PLA-g-MA was used as a compatibilizer more detail in PLA-g-MA preparation was reported in Teamsinsungvon et.al [8].

**Sample Preparation.** All blends and composites were prepared using an internal mixer (Haake Rheomix, 3000P). The rotor speed was 50 rpm and the mixing temperature was 170°C. The total mixing time was 10 min. PLA and PBAT pellets were dried at 70°C for 4 hrs before mixing. The designation and composition of the blends and composites are shown in Table 1. Test specimens were molded by a compression molding machine (GOTECH) at 170°C.

**Properties Measurement.** Tensile properties were tested using an universal testing machine (UTM, INSTRON: 5565). Impact strength was examined using an impact testing machine (Atlas: BPI). Viscosity at various shear rates (shear rate ranges of 10-10000 s<sup>-1</sup>) were obtained using a capillary rheometer (Kayeness: D5052m) at 170°C. Fracture surfaces from tensile test of the blends and composites were examined using a scanning electron microscope (SEM, JEOL: JSM-6400). All samples were coated with gold prior to examination.

Table 1: Designation and composition of PLA, PLA/PBAT blends and PLA/PBAT/CaCO<sub>3</sub> composites

Designation	PLA [%wt.]	PBAT [%wt.]	CaCO <sub>3</sub> [%wt.]	PLA-g-MA [phr]
PLA	100	-	-	-
PLA/PBAT	80	20	-	-
cPLA/PBAT	80	20	-	2
cPLA/PBAT/5 CaCO <sub>3</sub>	80	20	5	2
cPLA/PBAT/10 CaCO <sub>3</sub>	80	20	10	2
cPLA/PBAT/20 CaCO <sub>3</sub>	80	20	20	2
cPLA/PBAT/30 CaCO <sub>3</sub>	80	20	30	2

### Results and Discussion

**Mechanical properties.** Tensile properties and impact strength of PLA, PLA/PBAT and PLA/PBAT/CaCO<sub>3</sub> composites are shown in Table 2. The addition of PBAT to PLA resulted in a remarkable improvement of PLA ductility. This was expected since PBAT has a lower modulus and tensile strength than PLA [9]. Moreover, adding PLA-g-MA into PLA/PBAT blend exhibited a significant enhancement in the tensile strength of the blend due to improved interfacial adhesion between PLA and PBAT through the formation of miscible blends between PLA parts of PLA-g-MA and PLA [7]. As CaCO<sub>3</sub> content was increased, Young's modulus of the composites increased while tensile strength, elongation at break and impact strength decreased. This was attributed to the agglomeration of CaCO<sub>3</sub>, especially at high CaCO<sub>3</sub> content as shown in Fig. 3.

**Rheological properties.** Shear viscosities of PLA, PBAT and their blends are shown in Fig. 1. No significant difference in the viscosities of PLA, PBAT and PLA/PBAT blends was observed. However, at low shear rate, the addition of PLA-g-MA into the blend resulted in lower viscosity. This was probably due to the addition of PLA-g-MA which has lower viscosity than PLA and

PBAT into the blend. Viscosities of PLA/PBAT blend with various  $\text{CaCO}_3$  contents are shown in Fig. 2. At low shear rate, the viscosities of the composites slightly increased with increasing  $\text{CaCO}_3$  content since  $\text{CaCO}_3$  perturbed the flow of the polymer and hindered the mobility of chain segments in the melt flow. On the other hand, at high shear rate, incorporating  $\text{CaCO}_3$  into the blend had less effect on the viscosities.

Table 2: Mechanical properties of PLA, PLA/PBAT and PLA/PBAT/ $\text{CaCO}_3$  composites

Designation	Tensile strength [MPa]	Elongation at break [%]	Young's modulus [MPa]	Impact strength [ $\text{kJ/m}^2$ ]
PLA	60.89±0.77	1.68±0.13	541.71±25.96	3.34±1.01
PLA/PBAT	33.20±2.25	35.55±0.62	401.46±10.27	6.12±0.67
cPLA/PBAT	47.79±1.68	33.82±3.67	442.77±6.65	5.42±0.39
cPLA/PBAT/5 $\text{CaCO}_3$	43.61±1.03	8.74±0.46	456.42±26.45	6.59±0.22
cPLA/PBAT/10 $\text{CaCO}_3$	43.06±1.31	4.34±1.48	492.42±31.09	6.26±0.46
cPLA/PBAT/20 $\text{CaCO}_3$	40.55±1.27	3.00±0.60	525.90±30.75	4.67±0.22
cPLA/PBAT/30 $\text{CaCO}_3$	34.40±1.54	1.58±0.82	533.42±72.44	3.18±0.37

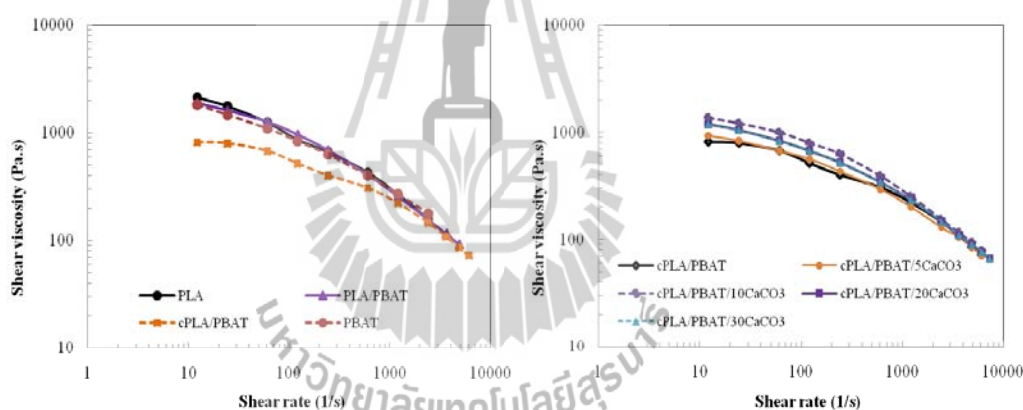


Figure 1. Shear viscosities of PLA, PBAT and PLA/PBAT blends

Figure 2. Shear viscosities of PLA/PBAT blend and PLA/PBAT/ $\text{CaCO}_3$  composites

**Morphological properties.** PLA and its blends and composites exhibited very different post-tension morphology due to the toughening effect of PBAT and the addition of  $\text{CaCO}_3$ . As shown in Fig. 3(a), PLA showed little sign of plastic deformation under tensile loading. In contrast, PLA matrix in PLA/PBAT blend demonstrated a fibrillation due to the release of strain constraints initiated by interfacial debonding between the PLA and PBAT phase (Fig. 3(b)). In case of compatibilized blend, the dispersed phase was finely dispersed in the matrix as shown in Fig. 3(c) due to improved interfacial adhesion between the matrix and dispersed phase. From Fig. 3(d) and 3(e), the micrograph showed agglomerates of  $\text{CaCO}_3$ . This caused high stress concentration and led to large voids during the tension process. These large voids could develop into cracks resulting in significant reduction in the elongation of the composites [7].

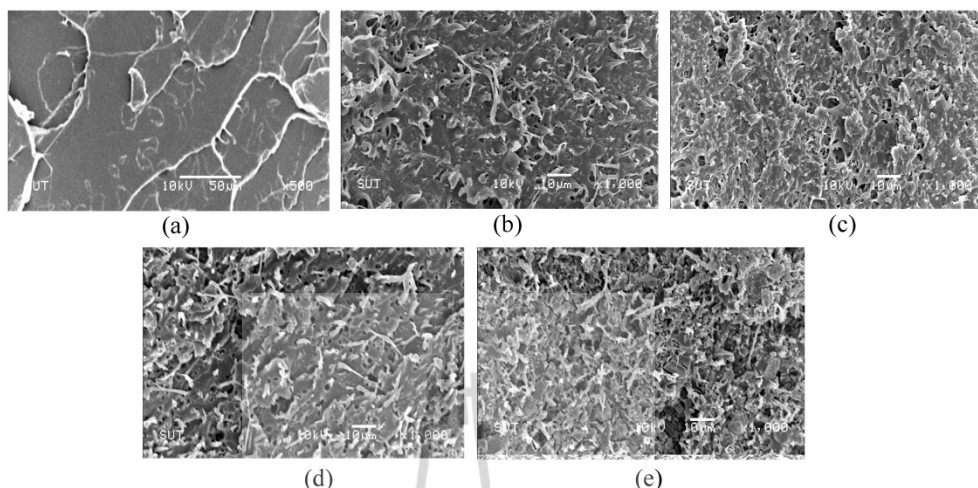


Figure 3. SEM micrographs (a) PLA, (b) PLA/PBAT, (c) cPLA/PBAT, (d) cPLA/PBAT/5 CaCO<sub>3</sub> and (e) cPLA/PBAT/30 CaCO<sub>3</sub>

### Conclusions

The addition of PBAT significantly improved elongation at break and impact strength of PLA but reduced tensile strength and Young's modulus. The adhesion between PLA and PBAT was enhanced with adding PLA-g-MA leading to an improvement of tensile properties of the blend. With increasing CaCO<sub>3</sub> contents, tensile strength and elongation at break of the composites decreased while Young's modulus increased.

### Acknowledgements

The authors wish to acknowledge Suranaree University of Technology and Center of Excellence for Petroleum, Petrochemicals and Advanced Materials for financial support and Sand and Soil Co., Ltd. for supplying CaCO<sub>3</sub>.

### References

- [1] M. Baiardo, G. Frisoni, M. Scandola, M. Rimelen, D. Lips and K. Ruffieux: *J. Appl. Polym. Sci.* Vol. 90 (2003), p. 1731
- [2] K. Arakawa, T. Madaa, S. Parka and M. Todoa: *Polym. Test.* Vol. 25 (2006), p. 628
- [3] N. Ljungberg and B. Wesslen: *Polymer.* Vol. 44 (2003), p. 7679
- [4] J. Yeh, C. Huang, W. Chai and K. Chen: *J. Appl. Polym. Sci.* Vol. 112 (2009), p. 2757
- [5] W. Jang, B. Shin, T. Lee and R. Narayan: *J. Ind. Eng. Chem.* Vol. 13 (2007), p. 457
- [6] H. Yuan, Z. Liu and J. Ren: *Polym. Eng. Sci.* Vol. 49 (2009), p. 1004
- [7] L. Jiang, B. Liu and J. Zhang: *Ind. Eng. Chem. Res.* Vol. 48 (2009), p. 7594
- [8] A. Teamsinsungvon, Y. Ruksakulpiwat and K. Jarukumjorn, in: *Pure and Applied Chemistry International Conference 2010, Ubonratchathani, Thailand* (2010).
- [9] L. Jiang, M. P. Wolcott and J. Zhang: *Biomacromolecules.* Vol.7 (2005), p.199

**Multi-Functional Materials and Structures III**

10.4028/www.scientific.net/AMR.123-125

**Properties of Biodegradable Poly(lactic acid)/Poly(butylene adipate-co-terephthalate)/Calcium Carbonate Composites**

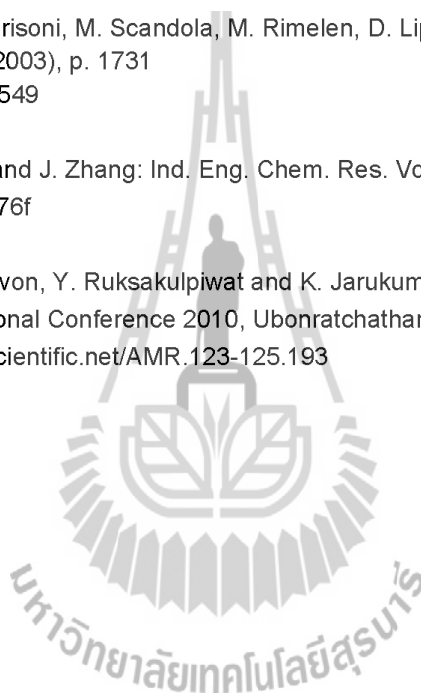
10.4028/www.scientific.net/AMR.123-125.193

**DOI References**

[1] M. Baiardo, G. Frisoni, M. Scandola, M. Rimelen, D. Lips and K. Ruffieux: J. Appl. Polym. ci. Vol. 90 (2003), p. 1731  
doi:10.1002/app.12549

[7] L. Jiang, B. Liu and J. Zhang: Ind. Eng. Chem. Res. Vol. 48 (2009), p. 7594  
doi:10.1021/ie900576f

[8] A. Teamsinsungvon, Y. Ruksakulpiwat and K. Jarukumjorn, in: Pure and Applied Chemistry International Conference 2010, Ubonratchathani, Thailand (2010).  
doi:10.4028/www.scientific.net/AMR.123-125.193





## The Second Thai-Japan Bioplastics and Biobased Materials Symposium (AIST - NIA Joint Symposium)

**10 September 2010**

### Organized by

National Institute of Advanced Industrial Science and Technology (AIST, Japan)  
National Innovation Agency (NIA, Thailand)  
Kasetsart University (KU, Thailand)

### Supported by

[JENESYS Program 2010]  
JSPS Exchange Program for East Asian Young Researchers (Japan)  
National Institute of Advanced Industrial Science and Technology (AIST, Japan)  
National Innovation Agency (NIA, Thailand)

### Scope

To create a sustainable society, biobased plastics produced from renewable resources (biomass) and biodegradable plastics should be the critical materials in 21st century. The purpose of this symposium is to overview the current research activities and global trends on bioplastics (biobased and biodegradable plastics) and biobased materials and to promote these activities in both countries. In addition researcher exchange between Thailand and Japan will be expected.

### Topics

- Biobased polymers and biodegradable polymers
- Production of biomass-containing materials; adhesive, composite, and resin
- Conversion of biomass-related materials to monomers and polymers
- Biosyntheses of polymers; in vitro and in vivo
- Polymerization of biobased monomers
- Functional biobased polymers
- High performance bioplastics
- Processing of biobased polymers; blend, molding, and spinning
- Biodegradation evaluation
- Application

C-5

**Mechanical Properties of Poly(lactic acid)/Poly(butylene adipate-co-terephthalate)/Calcium Carbonate Composites***Arpaporn Teamsinsungvon<sup>1,2</sup>, Yupaporn Ruksakulpiwat<sup>1,2</sup>, and Kasama Jarukumjorn<sup>1,2</sup>*

<sup>1</sup> School of Polymer Engineering, Institute of Engineering, Suranaree University of Technology, Nakhon Ratchasima, Thailand (E-mail: kasama@sut.ac.th)

<sup>2</sup> Center of Excellence for Petroleum, Petrochemicals and Advanced Materials, Chulalongkorn University, Bangkok, Thailand

**Abstract**

Poly(lactic acid) (PLA)/poly (butylene adipate-co-terephthalate) (PBAT) blend and its composites were prepared using melt mixing process. The blend of PLA and PBAT exhibited higher elongation at break but lower tensile strength and Young's modulus than the pure PLA. Therefore, calcium carbonate ( $\text{CaCO}_3$ ) was incorporated into PLA/PBAT blends at 5, 10, 20 and 30 wt% to balance properties of the blend. In addition, PLA grafted with maleic anhydride (PLA-g-MA) was added as a compatibilizer into the composites. With increasing  $\text{CaCO}_3$  loading, Young's modulus of the composites increased while tensile strength and elongation at break decreased. It was revealed from SEM micrographs of the composites that texture of fracture surfaces had been changed with the presence of  $\text{CaCO}_3$ .

**Keywords:** Poly(lactic acid), Poly (butylene adipate-co-terephthalate), Calcium carbonate, Poly(lactic acid) grafted with maleic anhydride

## MECHANICAL AND MORPHOLOGICAL PROPERTIES OF POLY (LACTIC ACID)/POLY (BUTYLENE ADIPATE-CO-TEREPHTHALATE)/CALCIUM CARBONATE COMPOSITE

A. Teamsinsungvon<sup>1,2</sup>, Y. Ruksakulpiwat<sup>1,2</sup>, K. Jarukumjorn<sup>1,2\*</sup>

<sup>1</sup> School of Polymer Engineering, Suranaree University of Technology, Nakhon Ratchasima, Thailand,

<sup>2</sup> Center for Petroleum, Petrochemical and Advanced materials, Chulalongkorn University, Bangkok, Thailand

\* Corresponding author ([kasama@sut.ac.th](mailto:kasama@sut.ac.th))

**Keywords:** PLA, PBAT, Maleic anhydride grafted PLA, Calcium carbonate

### 1 General Introduction

Poly (lactic acid) (PLA), a linear aliphatic polymer, is known as a biodegradable thermoplastic polymer with widely potential applications [1, 2]. PLA has a number of interesting properties including biodegradability, biocompatibility, high strength, and high modulus [3]. For this reasons, PLA is a candidate for producing package materials. However, its high brittleness and low toughness limit its application [4]. To overcome these limitations, blending PLA with flexible polymers is a practical and economical way to obtain toughened PLA. Poly (butylene adipate-co-terephthalate) (PBAT), an aliphatic-aromatic copolyester, is considered a good candidate for the toughening of PLA due to its high toughness and biodegradability [5]. Binary blends of PLA and PBAT exhibited higher elongation at break but lower tensile strength and modulus than the pure PLA due to the addition of a ductile phase. Therefore, the addition of filler to PLA/PBAT blends led to a modulus approaching that of the pure PLA. Unfortunately, PLA blends and PLA filled with natural materials e.g. natural fiber, calcium carbonate (CaCO<sub>3</sub>) have poor mechanical properties due to the poor interfacial adhesion. Maleic anhydride grafted PLA (PLA-g-MA) has been used to improve the interfacial adhesion between PLA and other polymers [6, 7, 8] or PLA and fillers [9, 10, 11]. CaCO<sub>3</sub> is selected in this study since it yields a cost reduction in polymer and can influence mechanical properties. The objective of this work was to investigate the effects of PLA-g-MA and CaCO<sub>3</sub> on mechanical, morphological, and thermal properties of PLA/PBAT blend.

### 2 Experimental

#### 2.1 Materials

PLA used in this study was Natureworks PLA 4042D. PBAT was BASF Ecoflex FBX 7011. Calcium carbonate (CaCO<sub>3</sub>) with an average particle size of 1.20-1.40 μm (HICOAT 810) was supplied from Sand and Soil Co., Ltd. PLA-g-MA prepared in-house was used as a compatibilizer. The grafting level (%G) of the PLA-g-MA was 0.41% [12].

#### 2.2 Preparation of blend and composite

PLA and PBAT pellets were dried at 70°C for 4 hrs before mixing. All blends and composite were prepared using a co-rotating intermeshing twin screw extruder (Brabender DSE 35/17D). A temperature profile was 160/165/170/165/160°C. Screw speed was 25 rpm. After exiting die, the extrudates were cooled in air before being granulated by a pelletizer. The test specimens were prepared by a compression molding machine (LabTech, LP20-B). The compression condition was processed at the temperature of 170°C and pressure of 100 MPa. The designation and composition of the blends and composite are shown in Table 1.

Table 1. Designation and composition of blend and composite

Designation	PLA [%wt.]	PBAT [%wt.]	CaCO <sub>3</sub> [%wt.]	PLA-g-MA [phr]
PLA	100	-	-	-
PBAT10	90	10	-	-
cPBAT10	90	10	-	2
30CaCO <sub>3</sub>	90	10	30	2

### 2.3 Characterization of blend and composite

#### 2.3.1 Mechanical properties

Tensile properties were obtained according to ASTM D638 using an Instron universal testing machine (UTM, model 5565) with a load cell of 5 kN.

Impact test was performed according to ASTM D256 using an Atlas testing machine (model BPI).

#### 2.3.2 Morphological properties

Morphologies of all blends and composite were examined by a scanning electron microscope (JEOL, model JSM-6400). Acceleration voltage of 10 kV was used to collect SEM images of sample. The samples were freeze-fractured in liquid nitrogen and coated with gold before analysis.

#### 2.3.3 Thermal properties

Thermal properties of PLA, PLA/PBAT blends, and PLA/PBAT/CaCO<sub>3</sub> composite were investigated using a differential scanning calorimeter (Perkin Elmer, DSC7). All samples were heated from 25°C to 200°C with a heating rate of 5°C/min (heating scan) and kept isothermal for 2 min under a nitrogen atmosphere to erase previous thermal history. Then, the sample was cooled to 25°C with a cooling rate of 20°C/min and heated again to 200°C with a heating rate of 5°C/min (2<sup>nd</sup> heating scan).

Thermogravimetric analysis of PLA, PLA/PBAT blends and PLA/PBAT/CaCO<sub>3</sub> composite were examined using a thermogravimetric analyzer (Perkin Elmer, SDT 2960). Thermal decomposition temperature of each sample was examined under nitrogen atmosphere. The sample with a weight between 10 to 20 mg was used for each run. Each sample was heat from room temperature to 600°C at a heating rate of 10°C/min. The weight change was recorded as a function of temperature.

## 3 Results and discussion

### 3.1 Mechanical properties

Mechanical properties of PLA, PLA/PBAT blends, and PLA/PBAT/CaCO<sub>3</sub> composite are listed in Table 2. Young's modulus, tensile strength, elongation at break, and impact strength values were normalized against those of pure PLA (643.95 MPa, 55.49 MPa, 11.89%, and 1.58 kJ/m<sup>2</sup> for Young's modulus, tensile strength, elongation at break, and impact strength, respectively) are shown in Fig. 1.

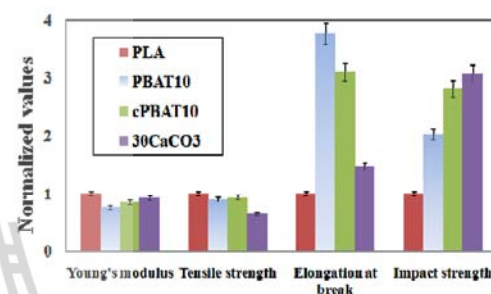


Fig.1. Mechanical properties of PLA, PLA/PBAT blend, compatibilized PLA/PBAT blend, and PLA/PBAT/CaCO<sub>3</sub> composite (values normalized against the Young's modulus, tensile strength, elongation at break, and impact strength of pure PLA)

The addition of PBAT into PLA resulted in a noticeable improvement of PLA ductility. Moreover, adding PLA-g-MA increased tensile strength and impact strength of the PLA/PBAT blend due to improved interfacial adhesion between PLA and PBAT through the formation of miscible blends between PLA parts of PLA-g-MA and PLA [9]. When CaCO<sub>3</sub> was incorporated into the compatibilized blend Young's modulus increased but tensile strength and elongation at break

Table 2. Tensile properties and impact strength of PLA, PLA/PBAT blends, and PLA/PBAT/CaCO<sub>3</sub> composite.

Designation	Tensile strength [MPa]	Elongation at break [%]	Young's modulus [MPa]	Impact strength [kJ/m <sup>2</sup> ]
PLA	55.49±1.22	11.89±1.92	643.95±83.13	1.58±0.16
PBAT10	49.40±1.37	44.72±8.51	487.10±36.77	3.21±0.18
cPBAT10	51.67±1.85	36.85±1.74	543.65±24.19	4.45±0.33
30CaCO <sub>3</sub>	35.58±2.02	17.56±2.91	593.34±40.77	4.85±0.61

decreased. The reduction of tensile strength of the compatibilized blend may be due to the agglomeration of  $\text{CaCO}_3$  as shown in Fig.2 (e and f).

### 3.2 Morphological properties

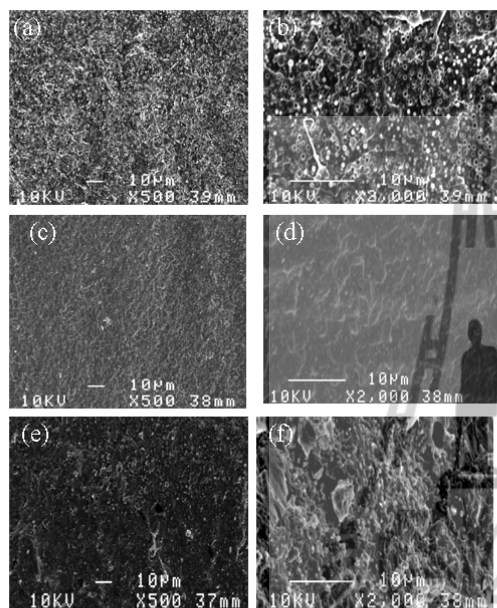


Fig.2. SEM micrographs of (a) PLA/PBAT blend (x500), (b) PLA/PBAT blend (x2000), (c) cPLA/PBAT blend (x500), (d) cPLA/PBAT blend (x2000) (e) 30 $\text{CaCO}_3$  composite (x500), and (f) 30 $\text{CaCO}_3$  composite (x2000)

SEM micrographs of the fracture surface of PLA/PBAT blend, compatibilized PLA/PBAT blend, and PLA/PBAT/ $\text{CaCO}_3$  composite are shown in Fig. 2. Fig. 2(a) and (b) present PLA/PBAT blend

without PLA-g-MA. Large PBAT phase domains were found. In a case of the compatibilized PLA/PBAT blend, the dispersed phase was finely dispersed in the matrix as shown in Fig. 2(c and d) due to improved interfacial adhesion between matrix and dispersed phase. This resulted in the improvement of the mechanical properties of the PLA/PBAT blend. With the addition of  $\text{CaCO}_3$  to compatibilized blend, agglomerates of  $\text{CaCO}_3$  were observed as shown in Fig. 2(e) and (f). This may be because PLA-g-MA content was not enough to improve both the interfacial adhesion between PLA and PBAT in the blend and the distribution of  $\text{CaCO}_3$  in the blend resulted in PLA/PBAT/ $\text{CaCO}_3$  composite with poor tensile strength, elongation at break.

### 3.3 Thermal properties

DSC thermograms of PLA, PLA/PBAT blends and PLA/PBAT/ $\text{CaCO}_3$  composite are shown in Fig.3. DSC data of PLA, PLA/PBAT blends, and PLA/PBAT/ $\text{CaCO}_3$  composite are listed in Table 3. Neat PLA displayed a glass transition temperature ( $T_g$ ) at 57.63°C, cold crystallization temperature ( $T_c$ ) at 112.20°C, and melting temperature ( $T_m$ ) at 148.67°C accompanied with shoulder-melting peak at 155.17°C. The incorporation of PBAT decreased  $T_c$  of PLA by approximate 5°C and narrowed the peak width, indicating enhancement of crystalline ability of PLA [5]. However,  $T_g$  and  $T_m$  of PLA/PBAT blend did not change when compared with PLA. With incorporation of PLA-g-MA,  $T_g$ ,  $T_c$ , and  $T_m$  of PLA/PBAT blend did not change while heat of melting ( $\Delta H_m$ ) increased. This result suggested that PLA-g-MA improved compatibility of PLA/PBAT blend [14]. Adding  $\text{CaCO}_3$  resulted in a decrease in heat of crystallization ( $\Delta H_c$ ) of the compatibilized PLA/PBAT blend. The observed

Table 3. DSC data of PLA, PLA/PBAT blends, and PLA/PBAT/ $\text{CaCO}_3$  composite.

Designation	$T_g$ [°C]	$T_c$ [°C]	$\Delta H_c$ [ $\text{Jg}^{-1}$ ]	$T_{m1}$ [°C]	$T_{m2}$ [°C]	$\Delta H_m$ [ $\text{Jg}^{-1}$ ]
PLA	57.63	112.20	27.02	148.67	155.17	24.65
PBAT10	57.70	107.61	23.32	148.08	154.91	19.29
cPBAT10	57.44	107.19	23.22	148.11	154.35	21.05
30 $\text{CaCO}_3$	57.05	107.19	15.66	147.33	154.33	15.91

$T_g$ : glass transition temperature,  $T_c$ : cold crystallization temperature,  $\Delta H_c$ : heat of crystallization,  $T_m$ : melting temperature,  $\Delta H_m$ : Heat of melting.

reduction in the  $\Delta H_c$  was probably attributed to the lesser polymer content in the composite available for crystallization [15].

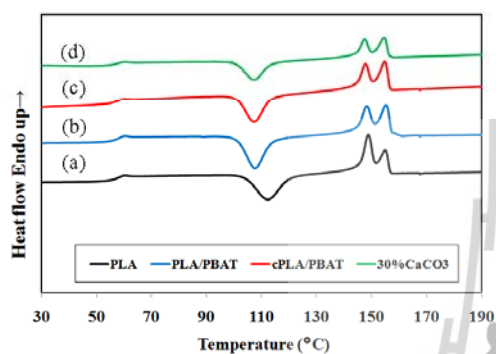


Fig.3 DSC thermograms of (a) PLA, (b) PLA/PBAT blend, (c) compatibilized PLA/PBAT blend, and (d) PLA/PBAT/CaCO<sub>3</sub> composite (the second heating, heating rate 5°C/min)

Table 4. Degradation temperature of PLA, PLA/PBAT blends and PLA/PBAT/CaCO<sub>3</sub> composite as determine from TGA results.

Designation	T <sub>5</sub> [°C]	T <sub>50</sub> [°C]	T <sub>f</sub> [°C]
PLA	333.70	362.01	387.96
PBAT10	333.71	363.30	428.80
cPBAT10	340.76	363.72	434.18
30CaCO <sub>3</sub>	287.97	324.77	434.81

TGA thermograms of PLA, PLA/PBAT blends, and PLA/PBAT/CaCO<sub>3</sub> composite are presented in Fig.4. Thermal degradation at 5% weight loss (T<sub>5</sub>), thermal degradation at 50% weight loss (T<sub>50</sub>) and final degradation temperature (T<sub>f</sub>) of PLA, PLA/PBAT blends and PLA/PBAT/CaCO<sub>3</sub> composite are listed in Table 4. T<sub>5</sub>, T<sub>50</sub>, and T<sub>f</sub> of neat PLA were at 333.70°C, 362.01°C, and 387.96°C, respectively. The addition of PBAT into PLA increased T<sub>f</sub> of PLA indicating the improvement of thermal stability of PLA. Furthermore, the compatibilized PLA/PBAT blend

showed higher T<sub>5</sub>, T<sub>50</sub>, and T<sub>f</sub> than PLA/PBAT blend. This suggested that thermal stability of the blend was enhanced with addition of PLA-g-MA. PLA and PLA/PBAT blends left no char residue at 600°C. For the PLA/PBAT/CaCO<sub>3</sub> composite, T<sub>5</sub> and T<sub>50</sub> was lower than that of the blend. This indicated that thermal stability of PLA/PBAT blend significantly decreased with the compounding with CaCO<sub>3</sub>. Because the basic nature of CaCO<sub>3</sub> had catalyzed the depolymerization of the ester bonds of PLA, thus it was responsible for the reduced thermal stability [16]. Moreover, the composite left the char residual at 30.22%.

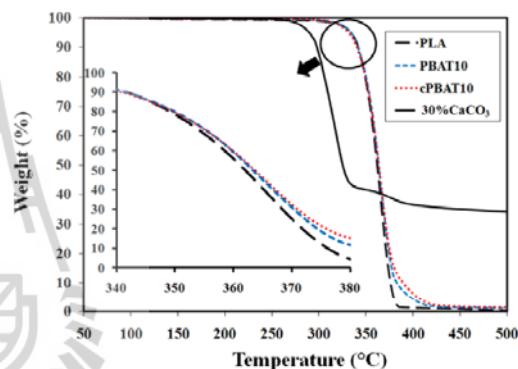


Fig.4 TGA thermograms of PLA, PLA/PBAT blend, and PLA/PBAT/CaCO<sub>3</sub> composite

#### Conclusions

PLA/PBAT blend exhibited higher elongation at break and impact strength but lower tensile strength and Young's modulus than PLA. PLA-g-MA enhanced the adhesion between PLA and PBAT leading to the improvement of the mechanical properties of PLA/PBAT blend. With the addition of CaCO<sub>3</sub>, tensile strength and elongation at break of the PLA/PBAT blend decreased while Young's modulus and impact strength increased. The incorporation of PBAT decreased T<sub>c</sub> of PLA indicating enhancement of crystalline ability of PLA. With presence of PLA-g-MA, T<sub>g</sub>, T<sub>c</sub>, and T<sub>m</sub> of the PLA/PBAT blend did not change while  $\Delta H_m$  increased. The incorporation of CaCO<sub>3</sub> resulted in a decrease in  $\Delta H_c$  of the compatibilized PLA/PBAT blend. The thermal stability of PLA/PBAT blend improved with adding PLA-g-MA. However, CaCO<sub>3</sub>

resulted in a reduction of thermal stability of compatibilized PLA/PBAT blend.

#### Acknowledgement

The authors wish to acknowledge National Innovation Agency, Suranaree University of Technology, and Center for Petroleum, Petrochemicals, and Advanced Materials for financial support and Sand and Soil Co., Ltd. for supplying CaCO<sub>3</sub>.

#### References

- [1] M. Baiardo, G. Frisoni, M. Scandola, M. Rimelen, D. Lips and K. Ruffieux. "Thermal and mechanical properties of plasticized poly (L-lactic acid)". *J. Appl. Polym. Sci.*, Vol. 90, pp 1731-1738, 2003.
- [2] K. Arakawa, T. Madaa, S. Parka and M. Todoa. "Tensile fracture behavior of a biodegradable polymer, poly (lactic acid)". *Polym. Test*, Vol. 25, pp 628-634, 2006.
- [3] N. Ljungberg and B. Wesslen. "Tributyl citrate oligomers as plasticizers for poly (lactic acid): thermo-mechanical film properties and aging". *Polymer*, Vol. 44, pp 7679-7688, 2003.
- [4] J. Yeh, C. Huang, W. Chai and K. Chen. "Plasticized properties of poly (lactic acid) and triacetin blends". *J. Appl. Polym. Sci.*, Vol. 112, pp 2757- 2763, 2009.
- [5] L. Jiang, M. P. Wolcott and J. Zhang. "Study of biodegradable poly (lactide)/poly (butylene adipate-co-terephthalate) blends". *Biomacromolecules*, Vol.7, pp 199-207, 2005.
- [6] W. Jang, B. Shin, T. Lee and R. Narayan. "Thermal properties and morphology of biodegradable PLA/starch compatibilized blends". *J. Ind. Eng. Chem.*, Vol. 13, pp 457-464, 2007.
- [7] H. O. Victor, B. Witold, C. Wunpen and L. L. Betty. "Preparation and characterization of poly (lactic acid)-g-maleic anhydride and starch blends". *Macromol. Symp.*, Vol. 277, pp 69-80, 2009.
- [8] Y. Hua, L. Zhiyong and R. Jie. "Preparation, characterization, and foaming behavior of poly (lactic acid)/poly (butylenes adipate-co-butylene terephthalate) blend". *Polym. Eng. Sci.*, Vol. 49, pp 1004-1012, 2009.
- [9] L. Jiang, B. Liu and J. Zhang. "Properties of poly (lactic acid)/poly (butylene adipate-co-terephthalate)/nanoparticle ternary composites". *Ind. Eng. Chem. Res.*, Vol. 48, pp 7594-7602, 2009.
- [10] S. Jae Hun, K. Eung Soo, J. Jung Hiuk and Y. Jin San. "Properties and morphology of poly (L-lactide)/clay composites according to the clay modification". *J. Appl. Polym. Sci.*, Vol. 102, pp 4983-4988, 2006.
- [11] S. Ko, M. Hong, B. Park, R. Gupta, H. Choi and S. Bhattacharya. "Morphological and rheological characterization of multi-walled carbon nanotube/PLA/PBAT blend nanocomposites". *Polym. Bull.*, Vol. 63, pp 125-134, 2009.
- [12] A. Teamsinsungvon, Y. Ruksakulpiwat and K. Jarukumjorn. "Preparation and characterization of melt free-radical grafting of maleic anhydride onto poly (lactic acid)". Proceeding of *Pure and Applied Chemistry International Conference 2010*, Ubon Ratchathani, Thailand. pp 527-529, 2010.
- [13] C. -S. Wu. "Physical properties and biodegradability of maleated polycaprolactone/starch composite". *Polym. Degrad. Stab.*, Vol. 80, pp 127-134, 2003.
- [14] N. Zhang, Q. Wang, J. Ren and L. Wang. "Preparation and properties of biodegradable poly (lactic acid)/poly (butylene adipate-co-terephthalate) blend with glycidyl methacrylate as reactive processing agent". *J. Mater. Sci.*, Vol. 44, pp 250-256, 2009.
- [15] H. Hanim, R. Zarina1, M. Y. Ahmad Fuad, Z. A. Mohd. Ishak and A. Hassan. "The effect of calcium carbonate nanofiller on the mechanical properties and crystallisation behaviour of polypropylene". *Malaysian Polym. J.*, Vol. 3, pp 38-49, 2008.
- [16] H. -S. Kim, B. H. Park, J. H. Choi and J. -S. Yoon. "Mechanical properties and thermal stability of poly (L-lactide)/calcium carbonate composites". *J. Appl. Polym. Sci.*, Vol. 109, pp 3087-3092, 2008.

## MECHANICAL AND MORPHOLOGICAL PROPERTIES OF POLY (LACTIC ACID)/POLY (BUTYLENE ADIPATE-*CO*-TEREPHTHALATE) BLEND AND ITS COMPOSITE

A. Teamsinsungvon<sup>1,2</sup>, Y. Ruksakulpiwat<sup>1,2</sup>, K. Jarukumjorn<sup>1,2</sup>

<sup>1</sup> School of Polymer Engineering, Institute of Engineering, Suranaree University of Technology,  
Nakhon Ratchasima 30000, Thailand

<sup>2</sup> Center for Petroleum, Petrochemical, and Advanced materials, Chulalongkorn University, Bangkok 10330,  
Thailand - E-mail: [kasama@sut.ac.th](mailto:kasama@sut.ac.th)

### Introduction

Poly (lactic acid) (PLA), a biodegradable thermoplastic polymer, has been used to produce packaging due to its high modulus and strength. However, its high brittleness and low toughness limit its application. To overcome these limitations, blending PLA with flexible polymers is a practical and economical way to obtain toughened PLA. Poly (butylene adipate-*co*-terephthalate) (PBAT) is a good candidate for the toughening of PLA due to its high toughness and biodegradability. Binary blends of PLA and PBAT exhibited higher elongation at break but lower tensile strength and modulus than the pure PLA. Therefore, the addition of filler led to the composite having a modulus approaching that of the pure PLA. Unfortunately, PLA blend and PLA composite with natural materials e.g. natural fiber, CaCO<sub>3</sub> have poor mechanical properties due to the lack of interfacial adhesion. Maleic anhydride grafted PLA (PLA-*g*-MA) has been used to improve the interfacial adhesion between PLA and other polymers [1] or PLA and fillers [2]. In this study, CaCO<sub>3</sub> is used as filler since it yields a cost reduction in polymer and affects on mechanical properties. The objective of this work was to investigate the effects of PLA-*g*-MA and CaCO<sub>3</sub> on mechanical and morphological properties of PLA/PBAT blends. In addition, tensile properties of blown film of the blend and the composite were determined.

### Experimental

#### Materials

PLA used in this study was Natureworks PLA 4042D. PBAT was BASF Ecoflex FBX 7011. CaCO<sub>3</sub> with an average particle size of 1.20-1.40 μm (HICOAT 810) was supplied from Sand and Soil Co., Ltd. PLA-*g*-MA prepared in house was used as a compatibilizer [3].

#### Preparation and testing of materials

PLA and PBAT pellets were dried at 70°C for 4 hrs before mixing. All blends and composites were prepared using a co-rotating intermeshing twin screw extruder (Brabender DSE35/17D). A temperature profile was 160/165/170/165/160°C. Screw speed was 25 rpm. Blend and composite composition are shown in Table 1. Test specimens were prepared by a compression molding machine (LabTech LP20-B). The compression condition was processed at the temperature of 170 °C. Blown films of the compatibilized blend and the compatibilized composite were prepared.

Tensile properties of the blends and composites were obtained according to ASTM D638 using a universal testing machine (Instron model 5565) with a load cell of 5 kN. Impact test was performed according to ASTM D256 using an Atlas testing machine (model BPI). Morphologies of all blends and composites were examined by a scanning electron microscope (JEOL, model JSM-6400). Acceleration voltage of 10 kV was used to collect SEM images of sample. The samples were freeze-fractured in liquid nitrogen and coated with gold before analysis. Tensile properties of the blown films were determined according to ASTM D882-02 using a universal testing machine (Instron model 5565) with a load cell of 5 kN.

Table 1 Blend and composite composition

Designation	PLA (%wt.)	PBAT (%wt.)	CaCO <sub>3</sub> (%wt.)	PLA- <i>g</i> -MA (phr)
PLA	100	-	-	-
PBAT10	90	10	-	-
cPBAT10	90	10	-	2
5CaCO <sub>3</sub>	90	10	5	2

### Results and discussion

Tensile and impact properties of PLA, PLA/PBAT blends, and PLA/PBAT/CaCO<sub>3</sub> composite are shown in Table 2. The addition of PBAT into PLA resulted in an improvement of PLA ductility. Moreover, adding PLA-*g*-MA increased tensile and impact strength of the blend due to improved interfacial adhesion between PLA and PBAT through the formation of miscible blends between PLA parts of PLA-*g*-MA and PLA [2]. When CaCO<sub>3</sub> was added into the compatibilized blend Young's modulus increased but tensile strength and elongation at break decreased. Tensile properties in machine direction (MD) and transverse direction (TD) of the composite were lower than that of the blend as listed in Table 2.

**Table 2** Mechanical properties of PLA, PLA/PBAT blends, PLA/PBAT/CaCO<sub>3</sub> composite, and blown film of PLA/PBAT blend and PLA/PBAT/CaCO<sub>3</sub> composite

Designation	Tensile strength (MPa)	Elongation at break (%)	Young's modulus (MPa)	Impact strength (kJ/m <sup>2</sup> )
PLA	55.49±1.22	11.89±1.92	643.95±83.13	1.58±0.16
PBAT10	49.40±1.37	44.72±8.51	487.10±36.77	3.21±0.18
cPBAT10	51.67±1.85	36.85±1.74	543.65±24.19	4.45±0.33
5CaCO <sub>3</sub>	50.38±1.04	27.26±2.46	518.36±10.26	3.21±0.61
BFcPBAT10(MD)	49.61±22.49	106.36±6.86	2450.71±147.82	-
BFcPBAT10(TD)	22.94±2.95	36.57±10.74	1698.61±80.94	-
BF5CaCO <sub>3</sub> (MD)	30.50±14.11	37.42±4.71	1666.67±117.85	-
BF5CaCO <sub>3</sub> (TD)	19.91±1.22	32.53±22.19	1319.05±74.69	-

BF: blown film

SEM micrographs of the fracture surface of PLA/PBAT blend, cPLA/PBAT blend, and PLA/PBAT/CaCO<sub>3</sub> composite are shown in Figure 1. Reduction in dispersed phase size with adding the compatibilizer was observed as shown in Figure 1 (b) due to enhanced interfacial adhesion between matrix and dispersed phase. This resulted in improved mechanical properties of PLA/PBAT blend. The good dispersion of CaCO<sub>3</sub> in the blend was found as shown in Figure 3(c-d).

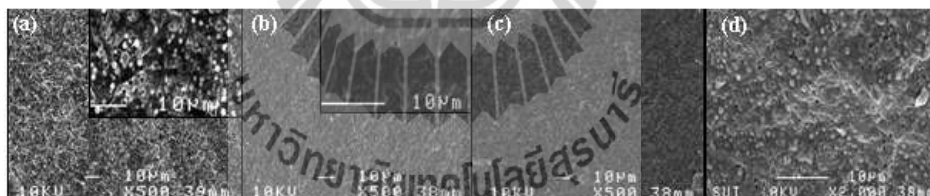


**Figure 1** SEM micrographs of (a) PLA/PBAT blend, (b) cPLA/PBAT blend, (c) 5CaCO<sub>3</sub> composite (x500), (d) 5CaCO<sub>3</sub> composite (x2000)

### Conclusions

PLA/PBAT blend exhibited higher elongation at break and impact strength but lower tensile strength and Young's modulus than PLA. PLA-*g*-MA enhanced the adhesion between PLA and PBAT leading to the improvement of the mechanical properties. With the addition of CaCO<sub>3</sub>, tensile strength and elongation at break of the PLA/PBAT blend decreased while Young's modulus and impact strength increased. Incorporating CaCO<sub>3</sub> resulted in decreased tensile properties of film of PLA/PBAT blend.

### References

1. W. Jang, B. Shin, T. Lee, R. Narayan J. Ind. Eng. Chem. 2007, 13, 457.
2. L. Jiang, B. Liu, J. Zhang Ind. Eng. Chem. Res. 2009, 48, 7594.
3. A. Teamsinsungvon, Y. Ruksakulpiwat, K. Jarukumjorn, Pure and Applied Chemistry International Conference, 2010, Ubon Ratchathani, Thailand, Book of Abstracts, p. 527.

### Acknowledgements

The authors wish to acknowledge National Innovation Agency, Suranaree University of Technology, and Center of Excellence for Petroleum, Petrochemicals, and Advanced Materials for financial support, Sand and Soil Co., Ltd. for supplying CaCO<sub>3</sub>, and Bags and Gloves Co., Ltd for preparing blown films.

*Advanced Materials Research Vol. 410 (2012) pp 51-54*  
 Online available since 2011/Nov/29 at [www.scientific.net](http://www.scientific.net)  
 © (2012) Trans Tech Publications, Switzerland  
 doi:10.4028/www.scientific.net/AMR.410.51

## Poly (lactic acid)/Poly (butylene adipate-co-terephthalate) Blend and Its Composite: Effect of Maleic Anhydride Grafted Poly (lactic acid) as a Compatibilizer

Arpaporn Teamsinsungvon<sup>1, 2, a</sup>, Yupaporn Ruksakulpiwat<sup>1, 2, b</sup>  
 and Kasama Jarukumjorn<sup>1, 2, c\*</sup>

<sup>1</sup>School of Polymer Engineering, Institute of Engineering, Suranaree University of Technology, Nakhon Ratchasima 30000, Thailand

<sup>2</sup>Center for Petroleum, Petrochemicals, and Advanced Materials, Chulalongkorn University, Bangkok 10330, Thailand

<sup>a</sup>jeabb.na@gmail.com, <sup>b</sup>yupa@sut.ac.th, <sup>c</sup>kasama@sut.ac.th

**Keywords:** Poly (lactic acid), Poly (butylene adipate-co-terephthalate), Maleic anhydride grafted PLA, Calcium carbonate.

**Abstract.** Poly (lactic acid) (PLA)/poly (butylene adipate-co-terephthalate) (PBAT) blend and its composite were prepared by melt blending method. Maleic anhydride grafted PLA (PLA-g-MA) prepared in-house was used as a compatibilizer to enhance the interfacial adhesion between PLA and PBAT and also to improve the dispersion of calcium carbonate (CaCO<sub>3</sub>) in polymer matrices. Increasing PBAT content (10-30 wt%) resulted in the improvement of elongation at break and impact strength of PLA. Tensile strength, Young's modulus, and impact strength of PLA/PBAT blend improved with the presence of PLA-g-MA due to enhanced interfacial adhesion between PLA and PBAT. As CaCO<sub>3</sub> (5 wt%) was incorporated into the compatibilized blend, tensile strength, Young's modulus, and impact strength insignificantly changed while elongation at break decreased.

### Introduction

In recent years, environmental pollution has become a great concern due to the high impact of plastic waste in daily use. One of the possible solutions to this problem is to replace the commodity synthetic polymers with the biodegradable polymers which are readily susceptible to microbial action. Poly (lactic acid) (PLA) is known as a biodegradable thermoplastic polymer with widely potential applications [1, 2]. PLA has a number of interesting properties including biodegradability, biocompatibility, high strength, and high modulus [3]. For this reasons, PLA is a candidate for producing packaging materials. However, its high brittleness and low toughness limit its application [4]. To overcome these limitations, blending PLA with flexible polymers is a practical and economical way to obtain toughened PLA. Poly (butylene adipate-co-terephthalate) (PBAT), an aliphatic-aromatic copolyester, is considered a good candidate for the toughening of PLA due to its high toughness and biodegradability [5]. Binary blends of PLA and PBAT exhibited higher elongation at break but lower tensile strength and modulus than the pure PLA due to the addition of a ductile phase. Therefore, the addition of filler to PLA/PBAT blends led to a modulus approaching that of the pure PLA. Unfortunately, PLA blends and PLA filled with natural materials e.g. natural fiber, calcium carbonate (CaCO<sub>3</sub>) have poor mechanical properties due to the poor interfacial adhesion. Maleic anhydride grafted PLA (PLA-g-MA) has been used to improve the interfacial adhesion between PLA and other polymers [6, 7] or PLA and fillers [8, 9, 10]. CaCO<sub>3</sub> is selected in this study since it yields a cost reduction in polymer and can influence mechanical properties. The objective of this work was to investigate the effects of PLA-g-MA and CaCO<sub>3</sub> on mechanical and morphological properties of PLA/PBAT blend.

### Materials and Method

**Materials.** PLA used in this study was Natureworks PLA 4042D. PBAT was BASF Ecoflex FBX 7011. Precipitated calcium carbonate with an average particle size of 1.20-1.40  $\mu\text{m}$  (HICOAT 810) was supplied from Sand and Soil Co., Ltd. 2, 5-bis (*tert*-butylperoxy)-2, 5 dimethylhexane (L101) and maleic anhydride (MA) were purchased from Aldrich. PLA-*g*-MA prepared in-house was used as a compatibilizer. The grafting level (%G) of the PLA-*g*-MA was 0.41% [11].

**Preparation of Blend and Composite.** PLA and PBAT pellets were dried at 70°C for 4 hrs before mixing. All blends and composite were prepared using a co-rotating intermeshing twin screw extruder (Brabender DSE 35/17D). A temperature profile was 160/165/170/165/160°C. Screw speed was 25 rpm. After exiting die, the extrudates were cooled in air before being granulated by a pelletizer. The test specimens were prepared by a compression molding machine (LabTech, LP20-B). The compression condition was processed at the temperature of 170°C and pressure of 100 MPa. The designation and composition of the blends and composite are shown in Table 1.

**Characterization of Blend and Composite.** Tensile properties were obtained according to ASTM D638 using a universal testing machine (Instron, 5565) with a load cell of 5 kN. Impact test was performed according to ASTM D256 using an impact testing machine (Atlas, BPI). Morphologies of all blends and composite were examined by a scanning electron microscope (JEOL, JSM-6400). Acceleration voltage of 10 kV was used to collect SEM images of sample. The samples were freeze-fractured in liquid nitrogen and coated with gold before analysis.

Table 1 Designation and composition of PLA, PLA/PBAT blends, and PLA/PBAT/CaCO<sub>3</sub> composite

Designation	PLA [wt%]	PBAT [wt%]	PLA- <i>g</i> -MA [phr]	CaCO <sub>3</sub> [wt%]
PLA	100	-	-	-
PLA/PBAT10	90	10	-	-
PLA/PBAT20	80	20	-	-
PLA/PBAT30	70	30	-	-
cPLA/PBAT	90	10	2	-
cPLA/PBAT/5CaCO <sub>3</sub>	90	10	2	5

### Results and Discussion

**Mechanical Properties.** Mechanical properties of PLA, PLA/PBAT blends, and PLA/PBAT/CaCO<sub>3</sub> composite are listed in Table 2. The addition of PBAT into PLA resulted in a noticeable improvement of PLA ductility. In addition, adding PLA-*g*-MA increased tensile strength, Young's modulus, and impact strength of the PLA/PBAT blend due to improved interfacial adhesion between PLA and PBAT through the formation of miscible blends between PLA parts of PLA-*g*-MA and PLA [8]. When CaCO<sub>3</sub> was incorporated into the compatibilized blend, tensile strength, Young's modulus, and impact strength insignificantly changed while elongation at break decreased. This was attributed to the agglomeration of CaCO<sub>3</sub> as shown in Fig. 3(f).

Young's modulus, tensile strength, elongation at break, and impact strength values of PLA/PBAT blend with difference PBAT contents and PLA/PBAT/CaCO<sub>3</sub> composite were normalized against those of pure PLA (643.95 MPa, 55.49 MPa, 11.89 %, and 1.58 kJ/m<sup>2</sup> for Young's modulus, tensile strength, elongation at break, and impact strength, respectively) are shown in Fig. 1 and 2, respectively.

Table 2 Tensile strength, Young's modulus, elongation at break, and impact strength of PLA, PLA/PBAT blends, and PLA/PBAT/CaCO<sub>3</sub> composite.

Designation	Tensile strength [MPa]	Elongation at break [%]	Young's modulus [MPa]	Impact strength [kJ/m <sup>2</sup> ]
PLA	55.49±1.22	11.89±1.92	643.95±83.13	1.58±0.16
PLA/PBAT10	49.40±1.37	44.72±8.51	487.10±36.77	3.21±0.18
PLA/PBAT20	40.98±1.76	58.42±11.62	395.13±17.15	3.46±0.35
PLA/PBAT30	34.77±0.63	73.02±10.72	283.66±30.15	4.47±0.34
cPLA/PBAT	51.67±1.85	36.85±1.74	543.65±24.19	4.45±0.33
cPLA/PBAT/5CaCO <sub>3</sub>	50.38±1.04	27.26±2.46	518.36±10.26	3.21±0.12

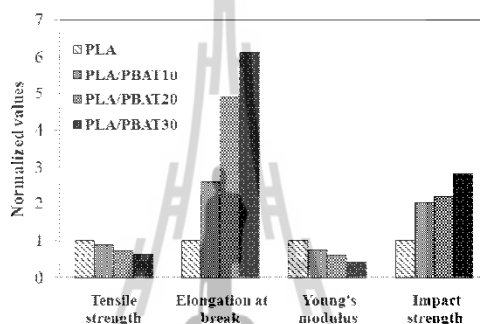


Fig. 1 Mechanical properties of PLA and PLA/PBAT blend with difference PBAT contents (values normalized against the Young's modulus, tensile strength, elongation at break, and impact strength of pure PLA)

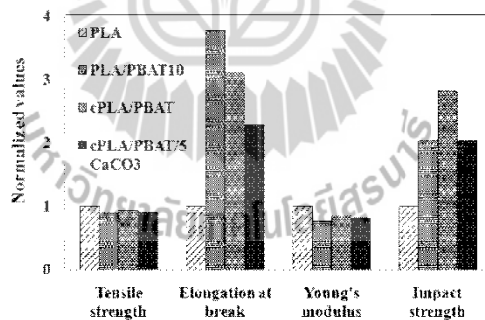


Fig. 2 Mechanical properties of PLA and PLA/PBAT blend, compatibilized PLA/PBAT blend, and PLA/PBAT/CaCO<sub>3</sub> composite (values normalized against the Young's modulus, tensile strength, elongation at break, and impact strength of pure PLA)

**Morphological Properties.** SEM micrographs of the fracture surface of the PLA/PBAT blends and compatibilized PLA/PBAT blend are shown in Fig. 3(b-d). Dispersed phase of PBAT was observed in PLA matrix indicating that PLA/PBAT blend was immiscible. Moreover, the size of PBAT domain increased with increasing PBAT content due to coalescence of PBAT droplets in the blends [12]. In a case of compatibilized PLA/PBAT blend, the dispersed phase was finely dispersed in the matrix as shown in Fig. 3(e) resulting in the improvement of tensile strength, Young's modulus, and impact strength of PLA/PBAT blend. With the addition of CaCO<sub>3</sub> into compatibilized blend, the agglomerates of CaCO<sub>3</sub> were observed in Fig. 3(f). This led to PLA/PBAT/CaCO<sub>3</sub> composite with poor mechanical properties.

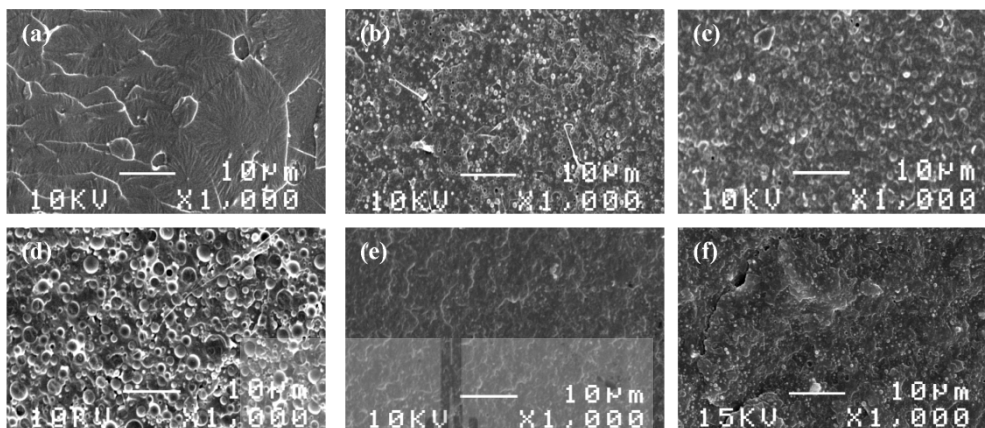


Fig. 3 SEM micrographs of (a) PLA, (b) PLA/PBAT10 blend, (c) PLA/PBAT20 blend, (d) PLA/PBAT30 blend, (e) cPLA/PBAT10 blend, and (f) cPLA/PBAT/5CaCO<sub>3</sub> composite

### Summary

PLA/PBAT blend exhibited higher elongation at break and impact strength but lower tensile strength and Young's modulus than PLA. PLA-g-MA enhanced the adhesion between PLA and PBAT leading to the improvement of tensile strength, Young's modulus, and impact strength of PLA/PBAT blend. With the addition of CaCO<sub>3</sub>, tensile strength, Young's modulus, and impact strength insignificantly changed while elongation at break of the compatibilized PLA/PBAT blend decreased.

### Acknowledgements

The authors wish to acknowledge National Innovation Agency, Suranaree University of Technology, and Center for Petroleum, Petrochemicals, and Advanced Materials for financial support and Sand and Soil Co., Ltd. for supplying CaCO<sub>3</sub>.

### References

- [1] M. Baiardo, G. Frisoni, M. Scandola, M. Rimelen, D. Lips and K. Ruffieux: *J. Appl. Polym. Sci.* Vol. 90 (2003), p 1731.
- [2] K. Arakawa, T. Madaa, S. Parka and M. Todoa: *Polym. Test.* Vol. 25 (2006), p 628.
- [3] N. Ljungberg and B. Wesslen: *Polymer.* Vol. 44 (2003), p 7679.
- [4] J. Yeh, C. Huang, W. Chai and K. Chen: *J. Appl. Polym. Sci.* Vol. 112 (2009), p 2757.
- [5] L. Jiang, M. P. Wolcott and J. Zhang: *Biomacromolecules.* Vol.7 (2005), p 199.
- [6] W. Jang, B. Shin, T. Lee and R. Narayan: *J. Ind. Eng. Chem.* Vol. 13 (2007), p 457.
- [7] Y. Hua, L. Zhiyong and R. Jie: *Polym. Eng. Sci.* Vol. 49 (2009), p 1004.
- [8] L. Jiang, B. Liu and J. Zhang: *Ind. Eng. Chem. Res.* Vol. 48 (2009), p 7594.
- [9] S. Jae Hun, K. Eung Soo, J. Jung Hiuk and Y. Jin San: *J. Appl. Polym. Sci.* Vol. 102 (2006), p 4983.
- [10] S. Ko, M. Hong, B. Park, R. Gupta, H. Choi and S. Bhattacharya: *Polym. Bull.* Vol. 63 (2009), p 125.
- [11] A. Teamsinsungvon, Y. Ruksakulpiwat and K. Jarukumjorn, in: *Pure and Applied Chemistry International Conference 2010, Ubon Ratchathani, Thailand (2010).* p 527.
- [12] J. Hong, H. Namkung, K. Ahn, S. Lee and C. Kim: *Polymer.* Vol. 47 (2006), p 3967.

**Processing and Fabrication of Advanced Materials**

10.4028/www.scientific.net/AMR.410

**Poly(lactic acid)/Poly(butylene adipate-co-terephthalate) Blend and its Composite: Effect of Maleic Anhydride Grafted Poly(lactic acid) as a Compatibilizer**

10.4028/www.scientific.net/AMR.410.51



## **BIOGRAPHY**

Miss Arpaporn Teamsinsungvon was born on May 1, 1983 in Udonthani Province, Thailand. She finished high school from Satri Rachinuthit School in 2000. She attended Khon Kaen University (KKU) and graduated in 2004 with a Bachelor's degree of Science (Chemistry). Topic of senior project during her Bachelor's degree was "Physical and Chemical Properties of Polymer Blends of Natural rubber Cassava Starch and Glycerol". After graduation, she has been employed as a research analyst at Research and Development (R&D) department, Advance Agro Public Company limited for 3 years. She then pursued her Master's degree in Polymer Engineering at School of Polymer Engineering, Institute of Engineering, Suranaree University of Technology (SUT) in Nakhon Ratchasima Province. Her research was about poly (lactic acid)/poly (butylene adipate-*co*-terephthalate) blends and their composites. In the period of her Master's degree study, she presented seven poster presentations as shown in Appendix A. During her graduate study, she got a research assistant scholarship from Suranaree University of Technology, Center of Excellence on Petrochemical and Materials Technology, and National Innovation Agency (NIA).